



**AMPEROMETRIC BIOSENSOR FOR SULFITE DETERMINATION
IN BEVERAGES USING GLASSY CARBON MODIFIED WITH
HYBRID NANO-MATERIAL ELECTRODE IN SIMPLE FLOW
INJECTION SYSTEM**

WONGDUAN SROYSEE

**A THESIS SUBMITTED IN PARTIAL FULFILLMENT OF THE REQUIREMENTS
FOR THE DEGREE OF MASTER OF SCIENCE
MAJOR IN CHEMISTRY
FACULTY OF SCIENCE
UBON RATCHATHANI UNIVERSITY
YEAR 2013
COPYRIGHT OF UBON RATCHATHANI UNIVERSITY**



UBON RATCHATHANI UNIVERSITY

THESIS APPROVAL

MASTER OF SCIENCE

MAJOR IN CHEMISTRY FACULTY OF SCIENCE

TITLE AMPEROMETRIC BIOSENSOR FOR SULFITE DETERMINATION IN
BEVERAGES USING GLASSY CARBON MODIFIED WITH HYBRID NANO-
MATERIAL ELECTRODE IN SIMPLE FLOW INJECTION SYSTEM

AUTHOR MISS WONGDUAN SROYSEE

EXAMINATION COMMITTEE

DR. YUPAPORN SAMEENOI	CHAIRPERSON
ASST. PROF DR. MALIWAN AMATATONGCHAI	MEMBER
DR. SANOE CHAIRAM	MEMBER
DR. SUPARB TAMUANG	MEMBER

ADVISOR

M. Amatongchai

(ASST. PROF DR. MALIWAN AMATATONGCHAI)

Utith Inprasit

(ASSOC. PROF. DR. UTITH INPRASIT)

DEAN, FACULTY OF SCIENCE

H. Juthamas

(DR. JUTHAMAS HONGTHONG)

ACTING FOR VICE PRESIDENT

FOR ACADEMIC AFFAIRS

COPYRIGHT OF UBON RATCHATHANI UNIVERSITY

ACADEMIC YEAR 2013

ACKNOWLEDGEMENT

I would like to thank my advisor asst. prof. Dr. Maliwan Amatatongchai for her constant advice, guidance, insight, and for sharing her extensive chemistry knowledge. I wish to thank Dr. Suparb Tamuang, Dr. Sanoc Chairam for comments and suggestions and Dr. Yupaporn Sameenoi for her advice and criticism as the external examiner.

I would like to thank the Science Achievement Scholarship of Thailand (SAST) and Ubon Ratchathani University for financial support. My gratitude is extended to Department of Chemistry, Faculty of Science, Ubon Ratchathani University for providing all laboratory facilities.

Above all, my deepest gratitude is given to my beloved parents for their eternal love and care throughout my life.

N. Sroysee
(MissWongduan Sroysee)

Researcher

บทคัดย่อ

ชื่อเรื่อง : แอมเพอร์โรเมตริกไบโอเซนเซอร์สำหรับตรวจวัดปริมาณซัลไฟด์ในตัวอย่าง
เครื่องดื่มโดยใช้ขั้วไฟฟ้ากาสีคาร์บอนโมดิฟายด์ด้วยวัสดุลูกผสมขนาดนาโน
ในระบบโพลีเมอร์
โดย : วงเดือน ศรีอยล
ชื่อปริญญา : วิทยาศาสตรมหาบัณฑิต
สาขาวิชา : เคมี
ประธานกรรมการที่ปรึกษา : ผู้ช่วยศาสตราจารย์ ดร. นະลิวรรณ อมตขงไชย

ศัพท์สำคัญ : ซัลไฟด์ไบโอเซนเซอร์ โพลีเมอร์ วัสดุลูกผสมขนาดนาโน ซีเอนที-พีดีดีเอ

งานวิทยานิพนธ์นี้ได้พัฒนาซัลไฟด์ไบโอเซนเซอร์สำหรับวิเคราะห์ปริมาณซัลไฟด์ใน
เทคนิคโพลีเมอร์ไบโอเซนเซอร์พัฒนาโดยใช้วัสดุลูกผสมของท่อนาโนคาร์บอนแบบผนัง
หลายชั้นที่มีหมู่คาร์บอกซิลิก-พีดีดีเอ และอนุภาคทองคำนาโนเคลือบบนผิวหน้าของขั้วไฟฟ้ากาสี
คาร์บอน วัสดุลูกผสมสามารถนำมาใช้เป็นแมทริกซ์ในการตรึงเอนไซม์ได้อย่างมีประสิทธิภาพทำให้
เอนไซม์มีไบโอแอคติวิตีที่คงตัวและมีความเสถียร เอนไซม์ซัลไฟด์ออกซิเดสจะถูกตรึงในวัสดุ
ลูกผสมท่อนาโนคาร์บอน พีดีดีเอ อนุภาคทองคำนาโนและไซโตโครม ซี โดยอาศัยการเชื่อมไขว้
ด้วยกลูตาไรลดีไฮด์ ไบโอเซนเซอร์ที่พัฒนาขึ้นมา (GC/CNTs-PDDA-AuNPs/SOx) จะนำมา
ประยุกต์ใช้ในโพลีเมอร์อะนาไลซิส (FIA) จะศึกษาประสิทธิภาพของไบโอเซนเซอร์ในการ
วิเคราะห์ปริมาณซัลไฟด์ 2 วิธี คือ การวัดโดยตรงหรือวัดการเกิดปฏิกิริยาออกซิเดชันของซัลไฟด์ที่
ขั้วไบโอเซนเซอร์และ วิธีทางอ้อมหรือวัดการเกิดปฏิกิริยารีดักชันของไฮโดรเจนเปอร์ออกไซด์
ในการวัดจะใช้โพลีเมอร์เล็กโตรเคมีคัลเซลล์ที่มีขั้วไฟฟ้าใช้งานเป็น GC/CNTs-PDDA-AuNPs/SOx
ใช้ Ag/AgCl เป็นขั้วไฟฟ้าอ้างอิง และถาดแพลทินัมเป็นขั้วไฟฟ้าช่วย

สำหรับวิธีโดยตรง จะศึกษาการเกิดปฏิกิริยาออกซิเดชันของซัลไฟด์ โดยใช้ขั้วไฟฟ้า
GC/CNTs-PDDA-AuNPs/SOx ในสารละลายฟอสเฟตบัฟเฟอร์ ความเข้มข้น 0.1 โมลาร์ พีเอช 8.0
เป็นสารละลายตัวพา และให้ศักย์ไฟฟ้า 0.3 โวลต์ ผลการศึกษาพบว่าซัลไฟด์ไบโอเซนเซอร์ที่
พัฒนาขึ้นมีการตอบสนองแบบเป็นเส้นตรงในช่วง 2-200 มิลลิกรัมต่อลิตร ค่าความชันเท่ากับ
204.66 นาโนแอมแปร์ต่อมิลลิกรัมต่อลิตร ค่าสัมประสิทธิ์สหพันธ์ (r^2) เท่ากับ 0.9991 جيدจำกัดค่าสุดใน
การตรวจวัด (3σ) เท่ากับ 1.3 มิลลิกรัมต่อลิตร ค่ากระแสที่ได้จากการวัดความเที่ยง (%RSD) ของ

การวิเคราะห์ค่าไฟต์ความเข้มข้น 5 มิลลิกรัมต่อลิตรซ้ำ 20 ครั้ง มีค่าเท่ากับร้อยละ 3.8 และสามารถวิเคราะห์ได้รวดเร็วถึง 57 ตัวอย่างต่อชั่วโมง

วิธีทางอ้อม ศึกษากระแสมาจากปฏิกิริยารีดักชันของไฮโดรเจนเปอร์ออกไซด์ที่เกิดขึ้นจากการเร่งปฏิกิริยาของเอนไซม์ ในการศึกษาการเกิดปฏิกิริยารีดักชันของไฮโดรเจนเปอร์ออกไซด์ที่ขั้วไฟฟ้าไบโอเซนเซอร์ที่พัฒนาขึ้น (GC/CNTs-PDDA-AuNPs/SOx) โดยใช้เทคนิคโวลติกโวลแทมเมทรี (CV) และแอมเพอร์โรเมทรี ผลการศึกษาพบว่าศักย์ไฟฟ้าที่เหมาะสมสำหรับตรวจวัดแบบแอมเพอร์โรเมทรี มีค่าเท่ากับ -0.4 โวลต์ ในการตรวจวัดค่าไฟต์แบบแอมเพอร์โรเมทรีกในระบบโฟลอินเจกชันจะใช้สารละลายฟอสเฟตบัฟเฟอร์ความเข้มข้น 0.1 โมลาร์ พีเอช 8.0 เป็นสารละลายตัวพา และให้ศักย์ไฟฟ้าที่ -0.4 โวลต์ ช่วงความเป็นเส้นตรงอยู่ในช่วงระหว่าง 500 ถึง 1500 มิลลิกรัมต่อลิตร ค่าสมการคือ $y=7.61x-1792.30$ ($r^2=0.9697$) เมื่อ y และ x คือพื้นที่ใต้พีคของสัญญาณกระแส (นาโน-แอมแปร์) และความเข้มข้นค่าไฟต์ (มิลลิกรัมต่อลิตร) ขีดจำกัดต่ำสุดในการตรวจวัดเท่ากับ 44.25 มิลลิกรัมต่อลิตร ค่ากระแสที่ได้จากการวัดความเที่ยง (%RSD) เท่ากับร้อยละ 2.93 และสามารถวิเคราะห์ได้รวดเร็วถึง 65 ตัวอย่างต่อชั่วโมง ผลจากการทดลองแสดงให้เห็นว่าวิธีการตรวจวัดโดยตรงให้ค่าความว่องไวที่สูง และช่วงความเป็นเส้นตรงที่กว้างกว่าวิธีจากการตรวจวัดโดยอ้อม

ABSTRACT

TITLE : AMPEROMETRIC BIOSENSOR FOR SULFITE DETERMINATION IN BEVERAGES USING GLASSY CARBON MODIFIED WITH HYBRID NANO-MATERIAL. ELECTRODE IN SIMPLE FLOW INJECTION SYSTEM

BY : WONGDUAN SROYSEE

DEGREE : MASTER OF SCIENCE

MAJOR : CHEMISTRY

CHAIR : ASST. PROF. MALIWAN AMATATONGCHAI, Ph. D.

KEYWORDS : SULFITE BIOSENSOR / FLOW INJECTION / HYBRID-NANO MATERIAL / CNTs-PDDA

This work presented the development of sulfite biosensor for determination of sulfite in a simple flow injection system. The biosensor was developed based on the hybrid materials, composed of carboxylic functionalized carbon nanotubes, poly(diallyldimethylammoniumchloride) and gold nanoparticle (CNTs-PDDA-AuNPs) coated on a glassy carbon (GC) electrode, which constructed an effective immobilization matrix and made the immobilized components hold high stability and bioactivity. Sulfite oxidase (SOx) was immobilized to CNTs-PDDA-AuNPs and cytochrome C composites film by using glutaraldehyde (Glu). This developed biosensor (GC/CNTs-PDDA-AuNPs/SOx) was applied in flow injection analysis (FIA). Performances for determination of sulfite were investigated using two approaches including direct method or detection the oxidation of sulfite and indirect method or detection the reduction of hydrogen peroxide. Flow through electrochemical cell using GC/CNTs-PDDA-AuNPs/SOx as a working electrode, Ag/AgCl as a reference electrode and Pt wire as a counter electrode was applied for the detection.

In the direct method, oxidation of sulfite was studied at the GC/CNTs-PDDA-AuNPs/SOx using a solution of 0.1 M phosphate buffer (pH 8.0) as a carrier and applying a potential of 0.3 V. The proposed method exhibits linear calibration over the range of

2-200 mg L⁻¹ of sulfite with slope of 204.66 nA mg⁻¹ L and correlation coefficient of 0.9991. The detection limit (3σ) was 1.3 mg L⁻¹. The developed biosensor also provided good precision (RSD=3.8%) for sulfite signal (5 mg L⁻¹, n=20) with a rapid sample throughput (57 samples h⁻¹).

In the indirect method, response current is based on the reduction of hydrogen peroxide which produced during the enzyme-catalyzed reaction. Reduction of hydrogen peroxide was studied at the developed biosensor (GC/CNTs-PDDA-AuNPs/SOx) using cyclic voltammetry (CV) and amperometry. The optimization potential for the amperometric detection was -0.4 V. The amperometric detection of sulfite was performed in flow injection system using solution of 0.1 M phosphate buffer (pH 8.0) as a carrier and applying a potential of -0.4 V. Linear concentration dependence is observed in the range between 500 to 1500 mg L⁻¹. The regression equation is given by $y=7.61x-1792.3$ ($r^2=0.9697$), when y and x are the area of peak current (nA) and sulfite concentration (mg L⁻¹). The detection limit (3σ) was 44.25 mg L⁻¹, %RSD=2.93. Sample throughput was 65 samples h⁻¹. From experimental results, direct method offers higher sensitivity and wider dynamic range than indirect method.

CONTENTS

	PAGE
ACKNOWLEDGEMENTS	I
THAI ABSTRACT	II
ENGLISH ABSTRACT	IV
CONTENTS	VI
LIST OF TABLES	X
LIST OF FIGURES	XI
LIST OF ABBREVIATIONS	XVII
CHAPTER	
1 INTRODUCTION	
1.1 The importance and the source of the research	1
1.2 Objectives	2
1.3 Expected outcomes	3
1.4 Scope of research	3
2 LITERATURE REVIEWS	
2.1 Biosensor	5
2.2 Carbon nanotubes	6
2.3 Poly(diallyldimethylammonium chloride) (PDDA)	8
2.4 Gold nanoparticles (AuNPs)	9
2.5 Cytochrome C (Cyt C)	9
2.6 Sulfite oxidase (SOx)	9
2.7 Sulfite	11
2.8 Reaction	12
2.9 Cyclic voltametry (CV)	13
2.10 Amperometry	15
2.11 Related research	17

CONTENTS (CONTINUED)

	PAGE
3 EXPERIMENTAL	
3.1 Instrumentation	23
3.2 Reagents and Chemical	24
3.3 Chemical preparation	25
3.4 Electrode preparation	27
3.5 Measurement procedures	27
3.5.1 Detection in batch mode	27
3.5.2 Amperometric detection in flow system	28
3.6 Sample preparation	30
3.7 Procedure	31
3.7.1 Part I: Electrochemical detection of sulfite oxidation on sulfite based-biosensor	31
3.7.2 Part II: Indirect method for sulfite based-biosensor	34
3.7.3 Characterization of the nanocomposites	34
4 RESULTS AND DISCUSSION	
4.1 Part I: Electrochemical detection of sulfite oxidation on developed Sulfite biosensor	38
4.1.1 Cyclic voltammetric study of sulfite oxidation	38
4.1.2 Studied of parameters that effect the sensitivity of the developed biosensor	40
4.1.2.1 Effect of CNTs-PDDA loading	40
4.1.2.2 Effect of gold nanoparticles (AuNPs) loading	41
4.1.2.3 Effect of cytochrome C (Cyt C) loading	42
4.1.2.4 Effect of sulfite oxidase enzyme (SOx) loading	43
4.1.2.5 Effect of buffer pH (phosphate buffer solution), 0.1 M	44

CONTENTS (CONTINUED)

	PAGE
4.1.3 Cyclic voltammetry (CV) of the potential interferences	45
4.1.4 The apparent Michaelis-Menten constant (K_m^{app})	47
4.1.5 Scan rate dependence study	48
4.1.6 Stability study	49
4.1.7 Amperometric detection of sulfite in the developed FIA system	50
4.1.7.1 Optimum potential for amperometric detection	50
4.1.7.2 Optimum flow rate	51
4.1.7.3 Analytical feature	52
1) Linear concentration range	52
2) Limit of detection	53
3) Interference study	54
4) Method validation	55
4.2 Part II: Indirect method for detection of sulfite	57
4.2.1 Cyclic voltammetric study of H_2O_2 reduction	57
4.2.2 Optimization potential for amperometric detection of H_2O_2	59
4.2.3 Analytical feature	59
4.2.3.1 Linearity range	59
4.2.3.2 Limit of detection	61
4.3 Characterization of the nanocomposites	61
4.3.1 UV-Visible spectroscopy	61
4.3.2 IR spectroscopy	62
4.3.3 Scanning electron microscopy (SEM)	63
4.3.4 Atomic force microscopy (AFM)	65

CONTENTS (CONTINUED)

	PAGE
5 CONCLUSIONS	66
REFERENCES	69
APPENDICES	
A Electrochemical detection of sulfite oxidation on developed sulfite biosensor	79
B Indirect method for detection of sulfite	98
C Characterization of the nanocomposites	100
D COFERENCES	104
VITAE	111

LIST OF TABLE

TABLE	PAGE
3.1 Instrumentation used for cyclic voltammetric, FIA and nanocomposite characterized experimentals.	23
3.2 List of reagents, grade and their suppliers.	24
4.1 Effect of foreign ions on the alteration of FI amperometric signal obtained from replicate injections (n=3) of 10 mg L ⁻¹ standard sulfite.	55
4.2 Sulfite contents analyzed from the developed method (FI-sulfite sensor) and standard method (iodometric method). Each analysis sample was carried out in triplicate injections.	56

LIST OF FIGURE

FIGURE	PAGE
2.1 Major stages of measurements of analytes with a biosensor.	5
2.2 Diffusions of the analyte A from solution to enzyme layer and the product P via enzymatic reaction to the transducer.	6
2.3 Structure representation of a) a MWCNTs and b) a SWCNTs.	7
2.4 Schematic diagram showing how a hexagonal sheet of graphene is rolled to form a CNTs with different chiralities (A: armchair; B: zigzag; C: chiral).	8
2.5 Structure of PDDA	8
2.6 Representative wild-type protein structure of a) vertebrate (SOx), b) plants (SOx) and c) bacterial (SDH).	10
2.7 Molybdenum-protein complexes or protein cofactor.	10
2.8 Accepted reaction cycle of the molybdenum-containing enzyme sulfite oxidase.	11
2.9 Schematic diagram showing the various reactions occur during operation of the sulfite biosensor.	13
2.10 The waveform of the potential applied during a typical cyclic voltammetric experiment. In this case the initial potential, E_i is 0.5 V, the final potential, E_f is -0.5 V and the scan rate, ν is 0.1 V s ⁻¹ .	14
2.11 A typical cyclic voltammogram produced by the application of the potential waveform in Figure 2.10	15
2.12 The potential-time profile for the stepped or staircase voltage applied to the working electrode. T_{step} , time interval of the voltage step ($=t_o$), ΔE_{step} , voltage step of the applied staircase waveform	16
2.13 Schematic diagram of amperometric detection. WE- working electrode; AE- auxiliary electrode; RE-reference electrode.	17

LIST OF FIGURE (CONTINUED)

FIGURE	PAGE
3.1 Schematic diagram of modification steps for preparation of the developed sulfite biosensor (GC/CNTs-PDDA-AuNPs/SOx)	27
3.2 Photograph of the set up for cyclic voltammetric measurements; potentiationstat (e-DAQ) voltammetric cell; (vial 25 mL); working electrode (GC or modified GC), reference electrode (Ag/AgCl), auxiliary electrode (Pt wire).	28
3.3 Manifold of flow injection analysis (a) used in this work and photograph of the set up for amperometric detection in flow system (b) using a e-DAQ potentiationstat, IV: Injection valve. Injection valve was equipped with 20 μ L loop. Thin layer flow cell are the three electrode type, WE: working electrode, AE: stainless steel tube and RE: Ag/AgCl	29
3.4 sample of beers (Chang, Hienegen and Singha) and wines (French white wine, Mamaow wine, Mulberry, Berri estates bin 777, Sicilian, Berri estates bin 222, Marsol and South Africa).	30
3.5 UV-Vis spectrometer (Lamda 25, Perkin Elmer)	35
3.6 FT-IR spectrometer (Spectrum RX I, Perkin-Elmer)	36
3.7 Scanning electron microscope (JSM 5410-LV, JEOL).	36
3.8 Atomic force microscope (XE-100, Park System)	37
4.1 Solid lines are the cyclic voltammograms obtained for 4 mM sulfite on a) bare glassy carbon electrode (GC) and b) modified sulfite biosensor (GC/CNTs-PDDA-AuNPs/SOx). Background voltammograms (0.1 M phosphate buffer, pH 7.0) are also shown as dotted for both electrodes. The scan rate was fixed at 50 mV s^{-1} .	39
4.2 The effect of the concentration of CNTs-PDDA (mg mL^{-1}) on the amperometric response of oxidation current to 0.5 mM sulfite solution in 0.1 M phosphate buffer solution pH 8.0 at potential of 0.3 V.	40

LIST OF FIGURE (CONTINUED)

FIGURE	PAGE
4.3 Dependence of AuNPs concentration (%) on the oxidation current. The concentration of sulfite is 0.5 mM in 0.1 M phosphate buffer solution of pH 8.0 at potential of 0.3 V.	41
4.4 Dependence of cytochrome c concentration (mg mL^{-1}) on the oxidation current. The concentration of sulfite is 0.5 mM in 0.1 M phosphate buffer solution of pH 8.0 at potential of 0.3 V.	42
4.5 Dependence of sulfite oxidase enzyme concentration (U mL^{-1}) on the oxidation current. The concentration of sulfite is 0.5 mM in 0.1 M phosphate buffer solution of pH 8.0 at potential of 0.3 V.	43
4.6 a) Cyclic voltammetric responses of 4 mM sulfite at various buffer pHs and the dependence of buffer pH on the b) peak potential c) peak current obtained from the biosensor, scan rate 50 mV s^{-1} .	44
4.7 Cyclic voltammogram of substances a) fructose, b) glucose, c) NaNO_3 , d) Na_2SO_4 , e) sucrose, f) NaCl , g) NaCH_3COO , h) $\text{CH}_3\text{CH}_2\text{OH}$, i) ascorbic acid and j) KI concentration of 12 mM in 0.1 M phosphate buffer pH 8.0. The scan rate was fixed at 50 mV s^{-1} .	46
4.8 a) Amperometric response of modified sulfite biosensor toward sulfite in the concentration range 0.025–0.25 mM and b) Lineweaver-Bulk plot of sulfite immobilized on the sulfite biosensor.	48
4.9 a) Cyclic voltammograms, obtained at various scan rates for 4 mM sulfite in 0.1 M phosphate buffer (pH 8.0) at modified sulfite biosensor and b) the linear relationship between the oxidation currents and the square root of the scan rate.	49
4.10 The storage stability of the GC/CNTs-PDDA-AuNPs/SOx using 0.05 mM sulfite.	50

LIST OF FIGURE (CONTINUED)

FIGURE	PAGE
4.11 Influence of the applied potential on the biosensor response for 10 mg L^{-1} sulfite.	51
4.12 Effect of the flow rate on sulfite biosensor response and sample throughput.	52
4.13 FIA grams obtain from injections of sulfite standards. The inset shows the linear relationship between the signal of sulfite and the concentration.	53
4.14 FI amperometric response obtained from the developed sulfite biosensor for 20 repetitive injection of 5 mg L^{-1} sulfite. Carrier solution; 0.1 M phosphate buffer pH 8.0, applied potential at 0.3 V using 1.0 mL min^{-1} of flow rate.	54
4.15 Comparison of sulfite content found in wine and beer sample, which were analyzed by the developed method (FI-sulfite biosensor) and iodometric method. Determination by each method was carried out in triplicate for a sample.	57
4.16 Solid lines are the cyclic voltammograms obtained from $4 \text{ mM H}_2\text{O}_2$ analysis on a) bare glassy carbon (GC) electrode and b) GC/CNTs-PDDA-AuNPs/SOx. Background voltammograms (0.1 M phosphate buffer pH 8.0) are also shown as dotted for both electrodes. The scan rate was fixed at 50 mV s^{-1} .	58
4.17 Influence of the applied potential on the biosensor response for $0.5 \text{ mM H}_2\text{O}_2$.	59
4.18 FI amperometric responses obtained from the developed sulfite biosensor of a) FIA grams obtained from injection of the various sulfite concentration ($n=3$) using the amperometric detection on the developed biosensor and b) calibration curve.	60
4.19 FIA grams obtained from the developed sulfite biosensor for 20 times injections of 500 mg L^{-1} sulfite using 0.1 M phosphate buffer pH 8.0, applied potential -0.4 V at flow rate 1.0 mL min^{-1} .	61

LIST OF FIGURE (CONTINUED)

FIGURE	PAGE
4.20 UV-Vis spectra of a) PDDA solution, b) SOx enzyme solution, c) AuNPs solution, d) PDDA-AuNPs solution and e) PDDA-AuNPs-SOx solution.	62
4.21 FTIR spectra of a) CNTs-PDDA-AuNPs, b) CNT-COOH, c) CNT and d) CNTs-PDDA	63
4.22 SEM images of a) CNT-COOH, b) CNTs-PDDA, c) CNTs-PDDA-AuNPs, d) CNTs-PDDA-AuNPs-SOx	64
4.23 AFM images of a) CNT-COOH, b) CNTs-PDDA, c) CNTs-PDDA-AuNPs, d) CNTs-PDDA-AuNPs-SOx	65
A.1 Amperogram of concentration of CNTs-PDDA (mg mL^{-1})	80
A.2 Amperogram of concentration of AuNPs (%)	81
A.3 Amperogram of concentration of Cyt C (mg mL^{-1})	82
A.4 Amperogram of concentration of SOx (U mL^{-1})	83
A.5 Amperogram of concentration of sulfite in the rang 2 to 20 mg L^{-1}	84
A.6 Amperogram of stability using 0.5 mM sulfite	86
A.7 FIA grams of the applied potential on the sulfite biosensor response 10 mg L^{-1} sulfite	88
A.8 FIA grams of the flow rate on the sulfite biosensor response 10 mg L^{-1} sulfite	89
A.9 FIA grams of the interference on the sulfite biosensor	93
A.10 FIA grams of the sample on the sulfite biosensor	97
B.1 Amperogram of potential using 0.5 mM H_2O_2 at sulfite biosensor	99
C.1 SEM images of a) CNT-COOH, b) CNTs-PDDA, c) CNTs-PDDA-AuNPs, d) CNTs-PDDA-AuNPs-SOx at 5000x	101
C.2 AFM images of a) CNT-COOH, b) CNTs-PDDA, c) CNTs-PDDA-AuNPs, d) CNTs-PDDA-AuNPs-SOx at scan size 10 μm	102

LIST OF FIGURE (CONTINUED)

FIGURE	PAGE
C.3 AFM images of a) CNT-COOH, b) CNTs-PDDA, c) CNTs-PDDA-AuNPs, d) CNTs-PDDA-AuNPs-SOx using scan rate 0,3 Hz	103

LIST OF ABBREVIATION

CNTs	Carbon nanotubes
PDDA	Poly(diallyldimethylammonium chloride)
AuNPs	Gold nanoparticle
Glu	Glutaraldehyde
Cyt C	Cytochrome C
SOx	Sulfite oxidase
CV	Cyclic voltammetry
FIA	Flow injection analysis
M	Molar
G	Gram
mL	Mililiter
Mg	Miligram
Min	Minute
S	Second
H	Hour
SD	Standard deviation
μ L	Microliter
LOD	Limit of detection

CHAPTER 1

INTRODUCTION

1.1 The importance and the source of the research

Sulfiting agent in various forms (sulfite, sulfur dioxide, hydrogen sulfite, metabisulfite) are commonly used as preservatives in foods, beverages and several products such as dried fruits and vegetable to prevent microbiological growth, to control browning reaction and to assist in vitamin C preservation [1-3]. However, the level of sulfite in food has been the subject of legislation since it was discovered that is certain concentration level causes allergic reactions in some individuals [4, 5]. The United States Food and Drug Administration (FDA) have required labeling of products containing more than 10 mg L^{-1} of sulfite in food or beverages [6].

Sulfite-oxidizing enzymes can be separated into two classes based on their ability to transfer electron to molecular oxygen. The first class is sulfite oxidases (SOx) enzyme (animals and plants) and the second class is the sulfite dehydrogenases (SDH) enzyme (bacteria) [7]. SOx enzyme from animal is a mitochondrial enzyme which is used cytochrome C (Cyt C) as the physiological electron acceptor. This enzyme can be purified and characterized from bovine and chicken livers. SOx enzyme catalyzes $2e^-$ oxidation of sulfite to sulfate and the terminal reaction is the degradation of the sulfur-containing amino acid cysteine and methionine in mammals [8, 9].

The use of functional hybrid materials are composed of carbon nanotubes (CNTs) and conducting polymers for the preparation of chemical sensors and biosensors has attracted great attention. CNTs can display metallic, semiconducting and superconducting because of their electron transport properties that are able to promote electron or proton transfer reaction and high thermal capacity. The conductivity along with their small size made them can be used as molecular wires in molecular electronics and as smallest possible electrodes. Moreover, they are friendly to the environment [10].

Poly(diallyldimethylammonium chloride) or PDDA is a conducting polymer used widely in industrial applications and in fabrication of chemical or biological sensors [11-12]. It was also used as the dispersant for functional materials including CNTs [13]. PDPA is a water-

soluble that usually acts as a positively charged colloid when dissolved in aqueous solution [13]. Positively charged PDDA molecules are easily coated on the negatively charge surface of the CNTs by electrostatic interaction [13].

Gold nanoparticles (AuNPs) are well known biocompatible materials that possess many superb properties including specific surface area, strong adsorption ability as well as good conductivity, strongly interact with biomaterials and on combination with carbon nanotubes. These unique electrical properties make AuNPs widely used and applied for many biosensors and electrochemical sensors [14-16].

In this work, a simple flow injection system, which employs an amperometric detection on a novel sulfite biosensor, was proposed. The biosensor was fabricated using CNTs-PDDA-AuNPs composites as an effective matrix to immobilized SOx enzyme. The nanocomposite materials were formed by coating negatively charged carboxylated CNTs with positively charged PDDA followed by capping with negatively charged AuNPs via electrostatic interaction. The CNTs-PDDA-AuNPs nano-composite is used to construct a sulfite biosensor by drop coating on the surface of the glassy carbon (GC) electrode. The developed biosensor (GC/CNTs-PDDA-AuNPs/SOx) provides many good characteristics including high activity, excellent sensitivity and selectivity in detection of sulfite.

In this work, performances for determination of sulfite were investigated using two methods including direct method for the oxidation of sulfite biosensor and indirect method for reduction of sulfite biosensor.

1.2 Objectives

1.2.1 Direct method: detection of SO_3^{2-} oxidation on sulfite biosensor

1.2.1.1 To investigate the possibility of using CNTs-PDDA-AuNPs composite as an effective matrix to immobilize SOx enzyme and to construct a sulfite biosensor for sulfite determination via sulfite oxidation by cyclic voltammetric technique.

1.2.1.2 To optimize parameters affecting the sensitivity of sulfite biosensor for detection of sulfite by cyclic voltammetry and amperometry.

1.2.1.3 To implement the developed sulfite biosensor as an amperometric detector in a flow injection or FIA system for evaluation of sulfite contents in beverage samples.

1.2.2 Indirect method: detection of H_2O_2 reduction on the sulfite biosensor

1.2.2.1 To study the possibility of sulfite determination via determination of H_2O_2 reduction by cyclic voltammetric and amperometric techniques.

1.2.2.2 To study the analytical features of the biosensor on the quantitative analysis of sulfite.

1.3 Expected outcomes

1.3.1 A sensitive and selective biosensor was developed by immobilizing SOx enzyme to CNTs-PDDA-AuNPs composite. This hybrid composite (CNTs-PDDA-AuNPs) can be used as an effective matrix to make the immobilized components hold high stability and bioactivity.

1.3.2 A high throughput screening system for assessing sulfite content using sulfite biosensor coupled with flow injection analysis.

1.4 Scope of research

Development of sulfite biosensor based on CNTs-PDDA-AuNPs/SOx composite.

Development of a sulfite biosensor can be carried out by immobilizing SOx enzyme to CNTs-PDDA-AuNPs composite. This composite was prepared by coating negatively charged carboxylated CNTs with positively charged PDDA followed by capping with negatively charged AuNPs via electrostatic interaction. SOx enzyme was immobilized to CNTs-PDDA-AuNPs and Cyt C composites film by using glutaraldehyde (Glu). Electrochemical oxidation of sulfite was studied at the developed biosensor (GC/CNTs-PDDA-AuNPs/SOx) in 0.1 M phosphate buffer pH 7.0 using cyclic voltammetry. Then, the developed biosensor was applied in the flow injection system for amperometric detection of sulfite oxidation using solution of 0.1 M phosphate buffer (pH 8.0) as a carrier and applying a potential of +0.3 V at the working electrode.

1.4.1 Direct method for sulfite detection using the developed biosensor

1.4.1.1 Cyclic voltammetric study of sulfite oxidation.

1.4.1.2 Parameters that affect the sensitivity of the sulfite biosensor will be optimized using cyclic voltammetry and amperometry.

- 1) Effect of CNTs-PDDA loading
- 2) Effect of gold nanoparticles (AuNPs) loading
- 3) Effect of cytochrome C (Cyt C) loading
- 4) Effect of sulfite oxidase enzyme (SOx) loading
- 5) Effect of pH (phosphate buffer solution), 0.1 M

1.4.1.3 Cyclic voltammetry (CV) of potential interferences

1.4.1.4 The apparent Michaelis-Menten constant (K_{mapp})

1.4.1.5 Scan rate dependence study

1.4.1.6 Stability study

1.4.1.7 Parameters that affect the sensitivity of the amperometric detection of on the developed sulfite biosensor in a FIA system were optimized.

- 1) Optimum potential for amperometric detection
- 2) Optimum flow rate
- 3) Performance characteristic of the amperometric response from the

FIA system assessed in terms of linear concentration range and limit of detection will be evaluated.

4) Interferences study

5) Method validation

1.4.2 Indirect method for sulfite determination using the developed biosensor

1.4.2.1 Cyclic voltammetric study of H_2O_2 reduction

1.4.2.2 Optimization potential for amperometric detection of H_2O_2

1.4.2.3 Studies the analytical features of amperometric detection on the biosensor in a FIA system for evaluation of sulfite such as linearity and limit of detection (LOD)

1.4.3 Characterization of the nanocomposites

1.4.3.1 UV-Visible spectroscopy

1.4.3.2 Infrared spectroscopy (IR)

1.4.3.3 Atomic force microscopy (AFM)

1.4.3.4 Scanning electron microscopy (SEM)

CHAPTER 2

LITERATURE REVIEWS

2.1 Biosensor

A biosensor is an analytical device capable of specific quantitative analytical signal using a biological element. A main biosensor consists of two parts including a bioreceptor and the transducer. A bioreceptor is an immobilized elements specifically bind to an analyte such as enzyme, nucleic acid, microorganism, etc. The transducer is used to convert chemical signal from the interaction of the analyte with bioreceptor into an electronic signal. The intensity signal is directly proportional to the analyte concentration [18]. The stages of measurement using biosensor device is shown in Figure 2.1.

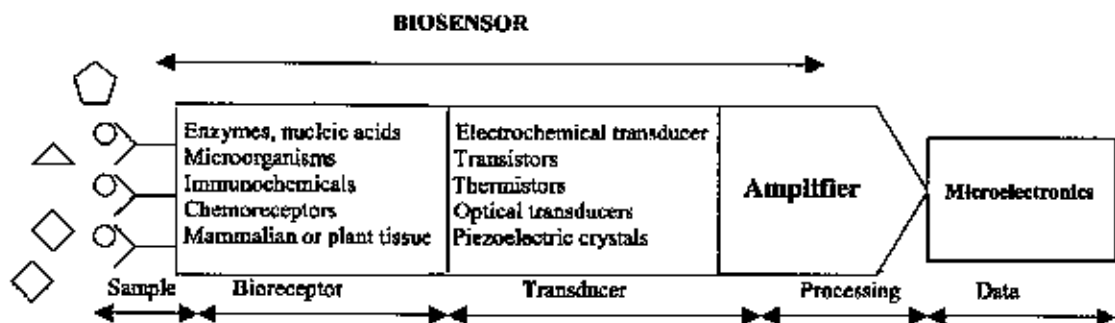


Figure 2.1 Major stages of measurements of analytes with a biosensor [17].

The enzymatic reaction transforms the substrate into a reaction detectable product by a transducer. A schematic representation of an enzyme sensor is illustrates in Figure 2.2. The sensitive surface of the transducer remains in contact with an enzymatic layer and it is assumed that there is no mass transfer across this interface. The external surface of the enzymatic layer is immersed in a solution containing the substrate migrates towards the interior of the layer and is converted into reaction product when it reacts with the immobilized enzyme [17].

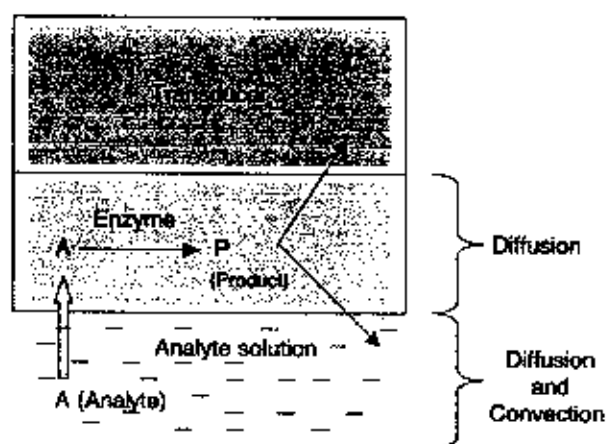


Figure 2.2 Diffusions of the analyte A from solution to enzyme layer and the product P via enzymatic reaction to the transducer [17].

Application of biosensors area are clinical, diagnostic, medical applications, process control, bioreactors, quality control, agriculture and veterinary medicine, bacterial and viral diagnostic, drug production, control of industrial waste water, mining, military defense industry, etc. The reason of biosensor has been widely used because of its ability to measure nonpolar molecules, specific, rapid, short of response time and practical. Biosensor, however, has some disadvantages including the heat sterilization which is not possible because denaturization of biological material and stability of biological material depends on the nature properties of the molecule (pH, temperature, ions) and the cell in the biosensor can become intoxicated by other molecules that are able to diffuse through the membrane [18].

2.2 Carbon nanotubes

A carbon nanotubes (CNTs) is a tube-shaped material, made of carbon, having a diameter measuring on the nanometer scale. CNTs can be divided into two types including multiwalled carbon nanotubes (MWCNTs) and single walled carbon nanotubes (SWCNTs). CNTs was discovered in 1991 by Iijima et al. [19]. The structure of SWCNTs include a single graphene layer rolled up into a seamless while MWCNTs have multi rolled layer (concentric tubes) of graphene sheets as shown in Figure 2.3 [20]. The interlayer distance in MWCNTs is close to the distance between graphene layers in graphite, approximately 0.34 nm, diameters of ~ 1 nm and large/diameter ratio.

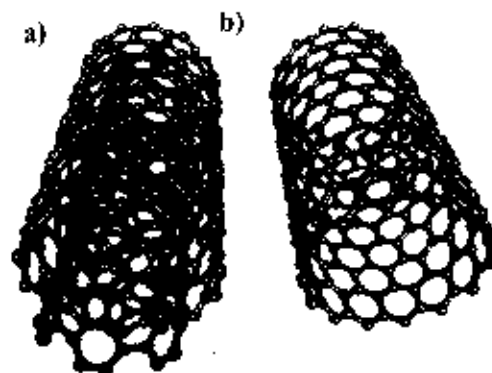


Figure 2.3 Structure representation of a) a MWCNTs and b) a SWCNTs [20].

The atom structure of CNTs is described in terms of the tube chirality which is defined by the chiral vector (C_h). The chiral vector can be described by the following equation:

$$C_h = na_1 + ma_2 \quad (2.1)$$

Where the integers (n, m) are the number of steps along the unit vectors (a_1, a_2) of hexagonal lattice. If $n = m$, the nanotubes are called armchair, and if $m = 0$, the nanotubes are called zigzag. Otherwise, they are called chiral. Schematic diagram of different chiralities CNTs is shown in figure 2.4 [21].

The CNTs are employed in many fields such as biosensor, modified chemical electrodes and field-effect transistors. In addition, CNTs can display conductivity, flexibility and mechanical stability because CNTs have a large specific surface area and they possess excellent absorption ability [22, 23].

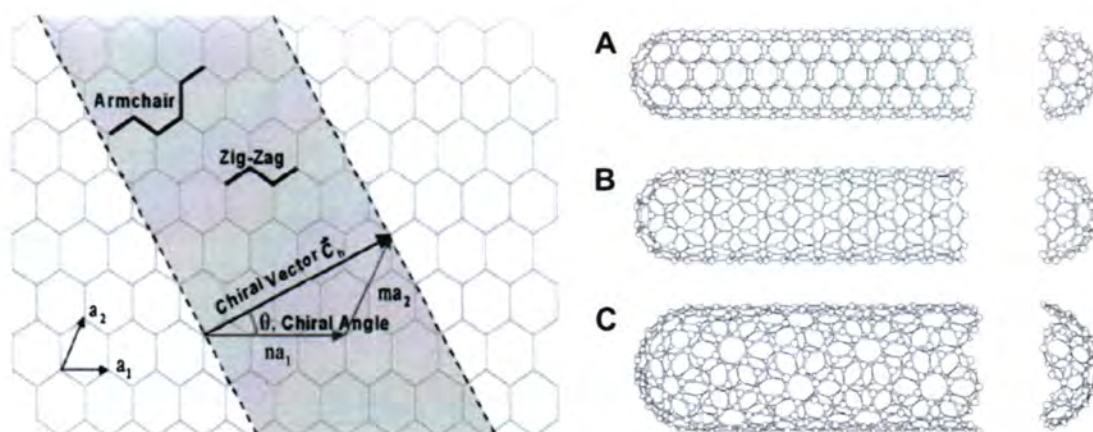


Figure 2.4 Schematic diagram showing how a hexagonal sheet of graphene is rolled to form a CNTs with different chiralities (A: armchair; B: zigzag; C: chiral) [21].

2.3 Poly(diallyldimethylammonium chloride) (PDDA)

Poly(diallyldimethylammonium chloride) (PDDA) is a water soluble cationic polyelectrolyte which has been widely used in industrial and various fields such as biology, medicine, cosmetic-care, membrane technology and water treatment [24-25]. The structure of PDDA is shown in Figure 2.5.

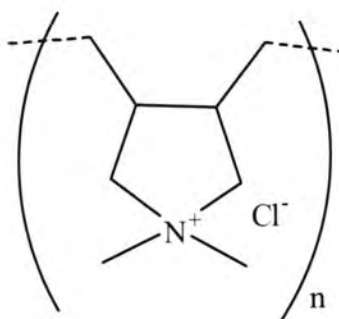


Figure 2.5 Structure of PDDA (adopt from [26]).

2.4 Gold nanoparticles (AuNPs)

Gold nanoparticles have been widely applied in various field including drug-delivery, tissue/tumor imaging, photothermal therapy, catalysis, water purification, surface-enhanced raman-scattering detection and optoelectronics [27]. The unique properties of AuNPs have been explored including nanoparticle size, shape-dependent optical, catalytic, magnetic and electronic properties [28]. These properties of gold nanoparticles made them widely used in the biosensor field because they can enhance the ability to decrease proteins-metal particles distance, high conductivity and electron transfer [29].

2.5 Cytochrome C (Cyt C)

The cytochrome C (Cyt C) is a basic redox heme protein with a spherical shape of 3.4 Å in diameter [30, 31]. Cyt C has been used extensively as a test system for direct electron transfer (DET) of redox proteins and communication in a protein matrix. It plays an important role in the biological respiratory chain in both plants and animals as its redox transition between ferrous and ferric states within cells makes it an efficient biological electrotransporter. But it is usually difficult to transfer to a conventional electrode. To avoid the disruption of a biological material in these bio-interphases to the electron transfer, multiprotein co-assembly technique developed, for example, mediator-free electron transfer of the enzymes within the bio-interphase was achieved, through layer-by-layer assembly of the redox protein Cyt C with sulfite oxidase, by taking advantage of direct interactions between the two functional biocomponents.

2.6 Sulfite oxidase (SOx)

Sulfite oxidizing enzymes have two classes including sulfite oxidase (SOx) and sulfite dehydrogenases (SDH). SOx found in animals and plants are in EC 1.8.3.1 class whereas SDH found in bacteria is in EC 1.8.2.1, respectively. The different between two type enzymes are able to transfer electron to oxygen. For the SOx is transferred electron to oxygen, ferricyanide and Cyt C. However, the SDH is not transferred electron to oxygen but it is used both of the later two electron acceptor [32]. The different protein structure of SOx and SDH is shown in Figure 2.6.

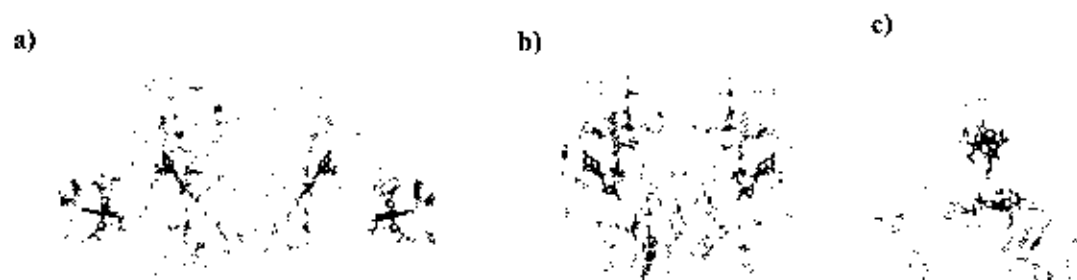


Figure 2.6 Representative wild-type protein structure of a) vertebrate (SOx), b) plants (SOx) and c) bacterial (SDII) [33].

SOx is an enzyme containing molybdenum cofactors. The active site of Molybdenum is transferred to the metabolism of sulfur compounds. It is available to biological systems because of the solubility of its high valence oxides in water. The molybdenum cofactors have been identified as molybdenum-protein complexes (Figure 2.7).

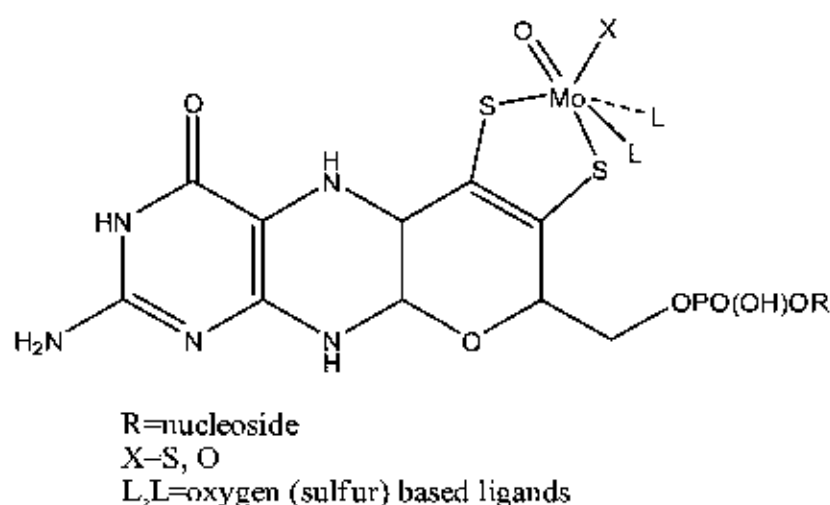


Figure 2.7 Molybdenum-protein complexes or protein cofactor [34].

The Mo center in these complexes couples electron-transfer to atom-transfer chemistry. Sulfite oxidase catalyzes the physiologically vital oxidation of sulfite to sulfate, the terminal reaction in the oxidative degradation of the sulfur containing amino acids such as cysteine and methionine. In this enzyme, molybdenum is coordinated by five ligands with approximately square pyramidal coordination geometry. The equatorial plane is occupied by three

sulfur ligands and one water/hydroxo ligand whereas an oxo group occupies the axial position. According to the postulated mechanism for sulfite oxidase, in the reductive half-cycle the sulfate is released and an oxygen-containing ligand from the solvent is then coordinated to the Mo(IV) center (step 1, Figure 2.8). The oxidative half-cycle consists of two one-electron intramolecular transfers to obtain first Mo(V) and then Mo(VI) (steps 2 and 4, Figure 2.8) and two one-electron transfers from the heme Fe(II) to the terminal electron acceptor, cytochrome c (ox) (steps 3 and 5, Figure 2.8).

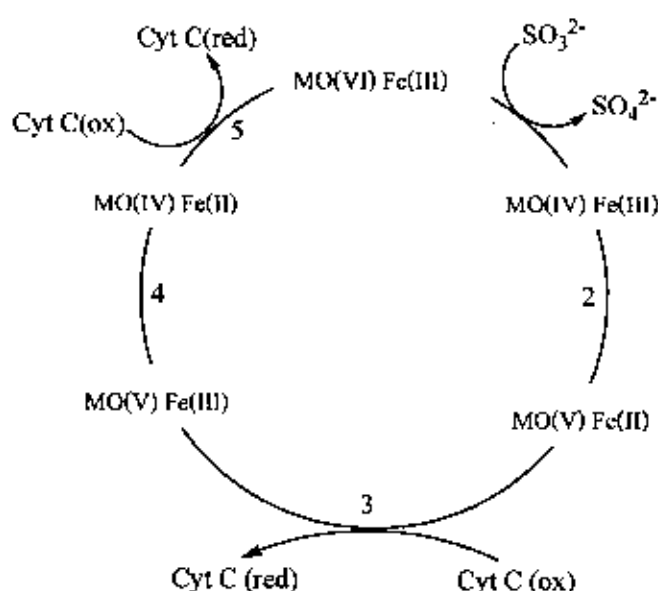


Figure 2.8 Accepted reaction cycle of the molybdenum-containing enzyme sulfite oxidase [34].

2.7 Sulfite

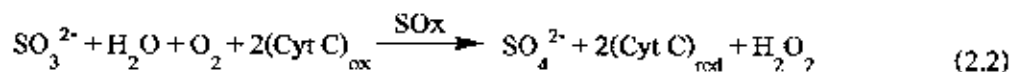
Sulfites or sulfiting agent in various forms (sulfur dioxide, sodium and potassium metabisulfite, sodium and potassium bisulfite and sodium sulfite) are widely used as additive in food and beverages. It was added to prevent oxidation, enzymatic and non-enzymatic browning, yeast and bacterial growth. The sulfite is the allergen. Its affect on hypersensitive individuals such as asthmatics, gastric irritation, nausea, diarrheal and nettle rash or swelling, may have difficulty breathing within minutes of eating a food containing sulfites [35]. Since 1986, the United States Food and Drug Administration (FAD) have required labeling of products containing

more than 10 mg L^{-1} ($156 \text{ }\mu\text{M}$) of sulfite in food and beverages. In 2002, the Australian Food Standard Code (AFSC) has regulated that any wine containing added sulfites in concentration of 10 mg L^{-1} or more sold in Australia must be labeled as such. Therefore a sensitive, easy to applied and accurate analytical method for the determination of sulfite is required for control the quality of manufactured products [36].

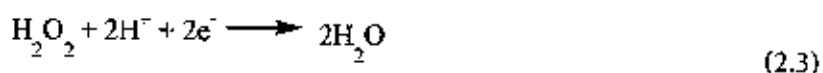
2.8 Reaction

In the previous reports, determination of sulfite using amperometric detections have been performed using a working electrode such as platinum [37], glassy carbon [38] and gold electrode [39]. However, these traditional electrodes somehow have some drawbacks. For example, problems associated with the electrode fouling were found since high positive potential must be applied for the oxidation of sulfite ($0.8\text{--}1.2 \text{ V Vs. Ag/AgCl}$). As a result, many substances can be interfere the measurement. Therefore, this work developed the sulfite biosensor (GC/CNTs-PDDA-AuNPs/SOx) to achieve high sensitivity and selectivity. Performances of the sulfite biosensor for determination of sulfite were examined. Biosensor responses were resulted from 2 approaches (i) SO_3^{2-} oxidation reaction and (ii) H_2O_2 reduction.

In the first part, SOx enzyme catalyzes the oxidation of sulfite to sulfate with the concomitant reduction of two equivalents of cytochrome C (Cyt C_{ox}) as described in Eq.2.2 [40]. In this reaction, sulfite oxidation can be monitored amperometrically at the developed biosensor (0.3 V) used in this work. The oxidation current is related to sulfite concentration in the sample.



In the second part, determination of the response current is based on the reduction of hydrogen peroxide which produced during the enzyme-catalyzed reaction. The reduction of hydrogen peroxide is detected by the amperometric current method (-0.4 V) during reaction at the enzyme electrode as shown in Eq. 2.3.



From the reaction above, operation of the sulfite biosensor can be schematically is shown in Figure 2.9. Initiation, the enzyme (SOx) catalytic oxidizes sulfite to sulfate, and simultaneously undergoes reduction at the active sites involving Cyt C-cofactor. The reduced form of SOx then reacts with the oxidized form of Cyt C. This process produces the oxidized form of the enzyme and simultaneously generates the reduced form of Cyt C. The reduced form of Cyt C is re-oxidised at the developed electrode which constitutes the analytical signal.

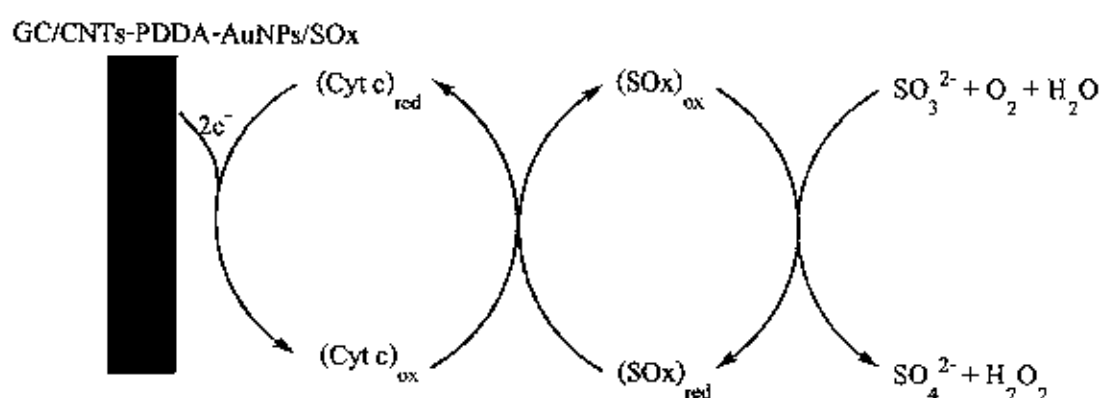


Figure 2.9 Schematic diagram showing the various reactions occur during operation of the sulfite biosensor.

2.9 Cyclic voltametry (CV)

Cyclic voltametry (CV) is used mainly for acquiring qualitative information about electrochemical reaction. The power of CV results from its ability to rapidly provide considerable information on the thermodynamics of redox processes and the kinetics of heterogeneous electron transfer reactions and on coupled chemical reactions or absorption processes. The CV is often the first experiment performed in an electroanalytical study [42]. The CV consists of scanning linearly the potential of a stationary working electrode using a triangular potential wave form is shown in Figure 2.10.

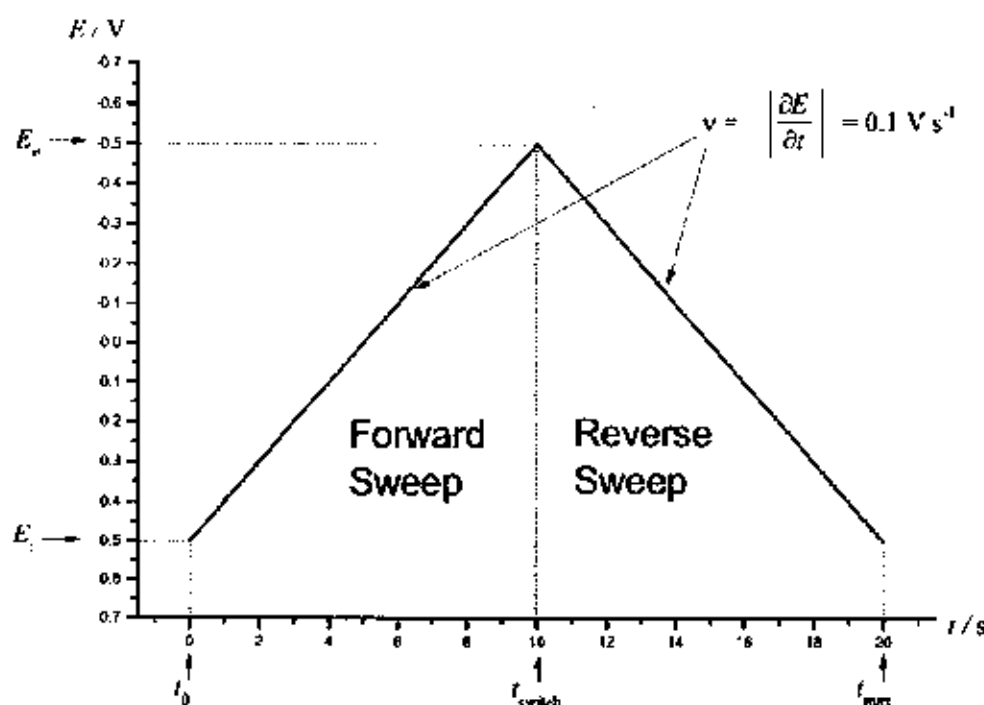


Figure 2.10 The waveform of the potential applied during a typical cyclic voltammetric experiment. In this case the initial potential, E_i , is 0.5 V, the final potential, E_p , is -0.5 V and the scan rate, v is 0.1 V s^{-1} [43].

The information based on sought, single or multiple cycles. During the potential sweep, the potentiostat measures the current resulting from the applied potential. The resulting plot of current versus potential was called cyclic voltammogram. A typical cyclic voltammogram is shown in Figure 2.11. Figure 2.11 illustrates the expected response of a reversible redox couple during a single potential cycle.

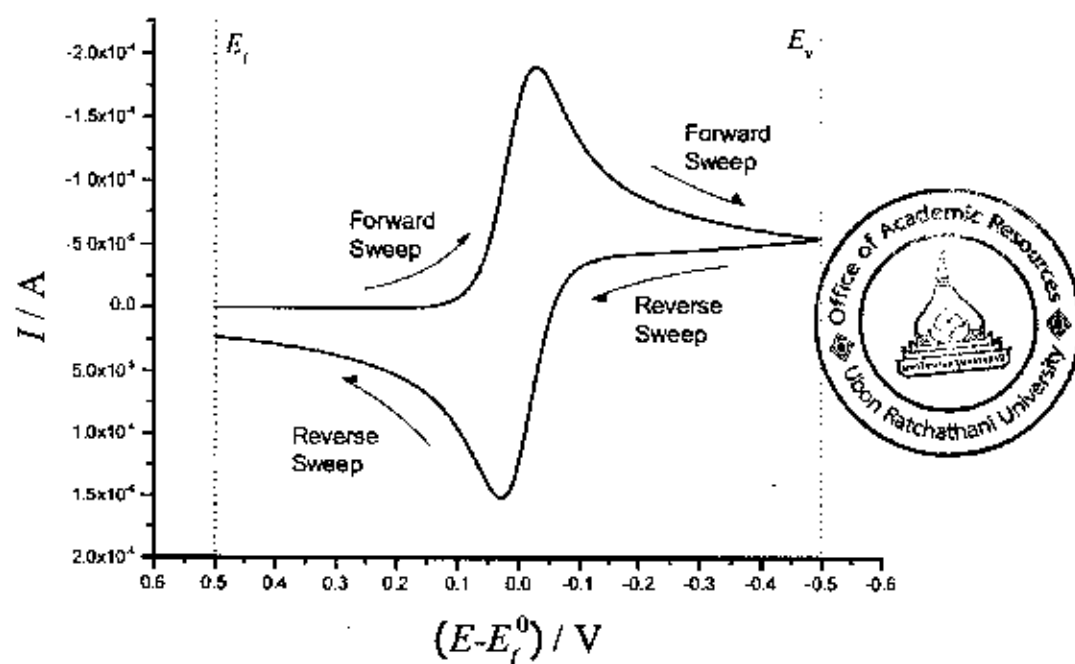


Figure 2.11 A typical cyclic voltammogram produced by the application of the potential waveform in Figure 2.10 [43].

This technique is widely used to the as the experimental, the resulting peak-shaped signal provides a direct of the feature of the reduction and oxidation processes. Analysis of the position and shape of the peaks give important information about the nature of the electrochemical process taking place and about the chemical species themselves.

2.10 Amperometry

Amperometry involves the controlled-potential techniques which it is measured the current response to an applied potential. It is a method of electrochemical analysis in which the signal of interest, current, is linearly dependent upon the concentration of the analyte [44]. Oxidation or reduction of species is generally proformed by working electrodes and electrons are transferred from the analyte to the working electrode. Flow direction of electrons depends upon the properties of the analyte and can be controlled by the electric potential applied to the working electrode. To maintain charge neutrality within the sample, a counter-reaction occurs at a second electrode, the counter electrode. The third electrode acts as a reference. During electrolysis, the

working electrode may act as an anode or a cathode, according to the nature of analyte. The amperogram shows in Figure 2.12.

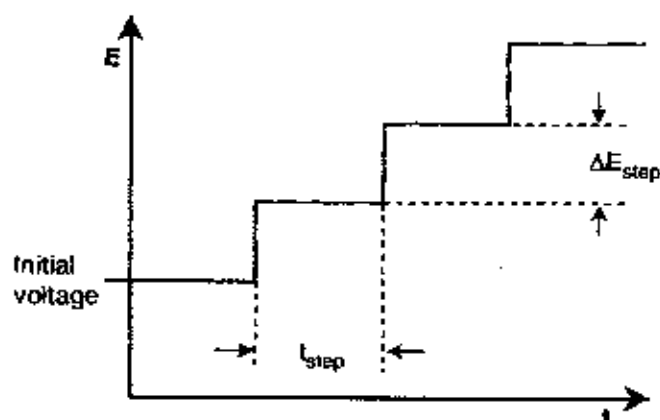


Figure 2.12 The potential- time profile for the stepped or staircase voltage applied to the working electrode. T_{step} , time interval of the voltage step ($=t_{\text{step}}$), ΔE_{step} , voltage step of the applied staircase waveform (adopt from [45])

Amperometric flow-through detection

Amperometric detectors, which are the most commonly used, are of the three-electrode type [45]. The potential of working electrode is set relative to the reference electrode, the iR drop between the working and auxiliary electrode is compensated by the potentiostat and the current flowing through the working electrode is the measured signal. The current, which is in the pA to μA range, is amplified and recorded as a function of the time flow of the mobile phase. This gives the concentration-time profile or chromatogram of the analyte in the effluent. The principle of amperometric detection is outlined in Figure 2.13.

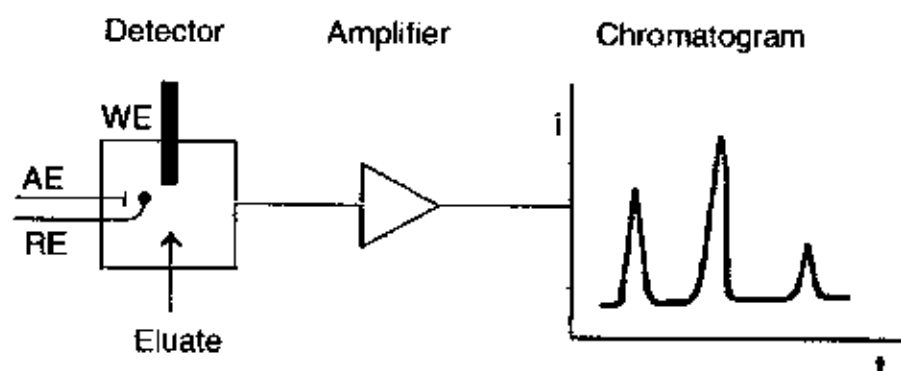


Figure 2.13 Schematic diagram of amperometric detection. WE–working electrode; AE–auxiliary electrode; RE–reference electrode [45].

2.11 Related research

In 2000, A. K. Abass, et al. [41] developed the amperometric sulfite biosensor based on SOx enzyme with Cyt C as electron acceptor and a screen-printed transducer. The screen-printed electrodes was deposited onto poly(vinylchloride) (PVC). The working electrode area was constructed using an insulating tape. The amperometric response of sulfite was measured at 0.3 V in 0.05 M phosphate buffer pH 7.4. The linearity was ranged from 4 to 750 mg L⁻¹.

In 2002, J. P. Hart, et al. [46] presented the development of disposable amperometric sulfur dioxide biosensors based on screen printed electrodes. The sulfite biosensor was fabricated by immobilizing the SOx enzyme and Cyt C on the screen printed carbon electrodes (SPCE). The biosensor was prepared by incorporating 1-2 mg of Cyt C and 1.0-0.45 U of SOx enzyme with an aliquot of buffer and depositing onto the polycarbonate membrane. Two methods of integrating the enzyme and Cyt C with the SPCE, b-type and s-type biosensors, were investigated. The developed biosensors were measured at the potential of 0.3 V versus Ag/AgCl electrode. Both devices gave linear response over the range 4-500 mg L⁻¹ but the sensitivity of the s-type was higher than the b-type biosensor.

In 2005, S. B. Adeloju, et al. [47] developed the electro-synthesis and characterization of polypyrrole (PPy)-Dextran (Dex)-SOx composite films by using galvanostatic polymerization. The composite of PPy-Dex-SOx film was prepared at the platinum or gold electrode immersed in the mixture of 0.5 M pyrrole, 0.02 g L⁻¹ Dex and 2 U mL⁻¹ SOx enzyme. After that, the solution was purged with nitrogen and accomplished galvanostatically by applying a current density of

0.5 mA cm⁻² to the working electrode for 30 seconds. The electrochemical detection was performed in 0.1 M phosphate buffer solution containing 0.05 M KCl pH 7.2 and fixed scan rate of 50 mV s⁻¹. The composite PPy-Dex-SOx electrode shows the mechanical stability of the composite film.

In 2007, E. Dinçkaya, et al. [48] presented the sulfite oxidase biosensor based on GC electrode coated with thin mercury film. The sulfite biosensor was fabricated by immersing GC electrodes in a voltammetric cell containing 10 mL of distilled water and 10 mL of mercury plating solution (200 mg L⁻¹ HgCl₂ in 2 M HCl). Nitrogen gas was bubbled through the cell for 5 min and then the potential between -0.1 and 1.2 V was applied to electrode for several times. Then apply a potential of -0.8 V was maintained for 90 s to deposit mercury onto the electrode under stirring at 1800 rpm. Then, 50 µL of the modified solution (0.5 U of SOx enzyme containing 1 mg 50 mL⁻¹ gelatin in 0.05 M phosphate buffer pH 7.0) was spread onto the GC surface and dried at 4 °C for 1 h. Finally, the modified electrode was immersed in 2.5% glutaraldehyde (Glu) solution in 0.05 M phosphate buffer for 5 min. The modified electrode was used as the working electrode, platinum as auxiliary electrode and Ag/AgCl electrode as reference electrode. The results from electrochemical behaviors demonstrate that the fast response, long time stability and a good detection range were obtained.

J. D. Qui, et al. [49] presented the synthesis, characterization and immobilization of Prussian blue-modified AuNPs nanoparticles application to electrocatalytic reduction of H₂O₂ in 2007. The synthesis of PB@AuNPs nanoparticles was prepared by 10 mL of a mixed aqueous solution of 1 mM FeCl₃, 1 mM K₃Fe(CN)₆, 0.1 M KCl and 0.025 M HCl was slowly added to the 10 mL of AuNPs suspension at room temperature with stirring. After that, stirring for 30 min give PB@AuNPs hybrid composite particles. Then, the dark-blue colloidal solution was centrifuged and washed with water. Finally, the particles were redispersed in ca. 10 mL of water. For the preparation of the multilayer films was fabricated by layer by layer self-assembly. The tin-doped indium oxide on glass (ITO) were treated with the 0.5 mg mL⁻¹ poly(allylamine hydrochloride) (PAH) aqueous solution for 5 min. After that washing with water and drying with N₂, the electrode was dipped in PB@AuNPs aqueous solution for 5 min. Then, the electrode was taken out washed with water and dried with N₂. This was defined as one bilayer. Further assemble of the PAH/PB@AuNPs bilayer was repeated to obtain the desired number of layer. The layer-by-

layer assembly was prepared by mixing a 1.5 mL of PAH and 2 mL of PB@AuNPs particles using ultrasonicate. After that this solution was dropped onto the ITO electrode. The electrocatalytic behavior of the {PAH/PB@AuNPs}_n multi layer films toward H₂O₂ was measured at -0.1 mV. The linearity was range from 0.01 to 6.0 mM.

In 2008, R. Cui. et al. [50] developed a novel amperometric immunosensor based on AuNPs/CNTs hybrids modified glass carbon electrode. In this work, CNTs was chemically shortened and carboxylated using acid treatment (mixture of H₂SO₄:HNO₃ 3:1) for 3 h. After that, the suspension was separated and washed repeatedly with distilled water by centrifugation until pH was ~7. The CNTs were functionalized with PDDA by using 0.5 mg mL⁻¹ of CNTs dispersed into 0.25% PDDA aqueous solution containing 0.5 M NaCl and sonicated for 30 min. Then, the suspension was centrifuged and rinsed with water for at least three times. Finally, the collected complex was redispersed in water and the resulting solution was sonicated for 5 min before preparing the films. The sensor was prepared by coating 5 μ L of 5 mg mL⁻¹ PDCNTs solution on well-polished GC electrode and drying in silica gel desiccators. Then, the modified electrode was immersed in the AuNPs solution for 30 min and washed with water. The electrode was stored at 4 °C when not in use. The last step was antibody immobilization and immune reaction procedure by spreading 5 μ L of 0.5 mg mL⁻¹ Ab₁ solution onto the AuNPs/PDCNTs/GC and incubating at 4 °C. The modified electrode was rinsed with phosphate buffer and 0.05% tween (PBST), respectively. The electrodes was blocked with 2% bovine serum albumin (BSA)+0.05% Tween-20 solution for 1 h at room temperature and washed with PBST. After that, the modified electrode was immersed into 60 μ L of HRP-Ab₂ or Ab₂-AuNPs-HRP bio conjugate, solution for an incubation of 50 min and washed with water. The resulting electrode provided a linear range between 0.125-80 ng mL⁻¹ and LOD of 40 pg mL⁻¹.

In 2010, B. Bahmani. et al. [51] presented the development of an electrochemical sulfite biosensor on conducting polyaniline film. The SOx enzyme was immobilized into the polyaniline film between the electrochemical polymerization of aniline in a solution of HCl NaH₂PO₄ (pH 8.5) containing 0.1 M aniline and 2.5 mg mL⁻¹ of SOx enzyme. The electro-polymerization was performed by cyclic voltammetry using potential scan between 1.2 and -0.5 V versus saturated calomel electrode (SCE) for 30 min. Then, the modified electrode was rinsed

with buffer and stored at 5 °C in phosphate buffer (pH 8.5) when not in use. The linear range was 0.006-5 mM for sulfite and LOD of 0.002 mM (S/N = 3).

In 2011, R. Rawal, [52] developed the amperometric sulfite biosensor based on a AuNPs/chitosan (CHIT)/CNTs/Polyaniline (PANI) modified gold electrode. The CNTs suspension was prepared by dispersing 1 g of CNTs in 1 mL of $\text{H}_2\text{SO}_4\text{:HNO}_3$ 3:1 and ultrasonication for 24 h. Then, 50 mL of PANI was added to 10 mL of 1 M HCl and mixed with 1 mL of CNTs suspension. This solution was called CNTs/PANI. Then the CNT/PANI was electrodeposited onto the Au electrode through CV at 0-1.5 V, by immersing the electrode into a solution (20 mL) containing 15 mL of electrolyte (0.1 N KCl) and 5 mL of 0.1 M tris-HCl buffer (pH 8.5). After that, the modified electrode was washed thoroughly with distilled water. Then, 2 mL of AuNPs were then dissolved into 2 mL of 0.5% chitosan solution. Next, the AuNPs/CHIT was adsorbed onto the electrode by dipping into the solution for 3 h and drying in air. Finally, the 100 mL SOx enzyme was immobilized onto the modified electrode at 4 °C overnight and washed with distilled water. Then, the SOx/AuNPs/CHIT/CNTs/PANI/Au electrode was dried and stored in refrigerator at 4 °C when not in use. Then the modified electrode was characterized by CV. The sensor produced its optimum response within 3 s when operated at 50 mV S^{-1} in 0.1 M phosphate buffer pH 7.0. The linear range and LOD of the sensor were 0.75-400 μM and 0.5 μM (S/N = 3).

M. Eguilaz, et al. [53] developed a cholesterol biosensor using a transduction platform constituted of a GC electrode modified with AuNPs/PDDA-CNTs nanocomposite in 2011. The CNTs were chemically shorten and carboxylated by acid treatment (mixture of $\text{H}_2\text{SO}_4\text{:HNO}_3$ 3:1) under ultrasonic stirring for 5 h. After that, the suspension was centrifuged at 14,000 rpm and washed repeatedly with DI water until the pH of water was 7. The CNTs-COOH was then functionalized with PDDA (CNTs-PDDA) by dispersing 10 mg of CNTs-COOH in 20 mL of a 0.25% PDDA aqueous solution containing 0.5 M NaCl and ultrasonic stirring for 30 min. The resulting dispersion was centrifuged and washed with water for three times to remove residual PDDA. Finally, 4 mg of the collected product was dispersed in 5 mL water and the resulting solution was sonicated for 5 min before use. Then, the 10 μL of PDDA-CNTs was dropped onto the glassy carbon electrode surface and dried under IR radiation. Next, 10 μL of AuNPs was dropped onto the modified electrode surface and stand for 30 min at 4 °C. Furthermore, the

enzyme was immobilized by dropping 5 μL of 200 U mL^{-1} ChOx onto the modified electrode and then dropping 5 μL of 0.5% Nafion. The developed cholesterol biosensor (ChOx/AuNPs/PDDA/CNTs/GC) gave linear response for cholesterol in the 0.02–1.2 mM range with the slope of 2.23 $\mu\text{A mM}^{-1}$ and LOD 4.4 μM . Moreover, the possibility of preparing bienzyme ChOx-HRP biosensors using the same electrode platform was explored. The HRP-ChOx/AuNPs/PDDA/CNTs/GC electrode was prepared by dropping a 5 μL of 940 U mL^{-1} HRP and 200 U mL^{-1} ChOx solution. Both biosensors designed in this work were used for determination of cholesterol in human serum samples.

In 2011, A. Salimi, et al. [54] presented a novel non-enzymatic hydrogen peroxide sensor based on single walled carbon nanotubes-manganese complex modified glassy carbon electrode. The preparation of electrode by 25 μL of 0.5 mg mL^{-1} DMSO-CNTs solution was cast on the surface of GC electrode and dried in air. After that, the modified electrode was immersed in DMF solution containing 5 mM Mn-complex for 20–100 s, after rinsing with water. For adsorption of Mn-complex on the surface of reactivate GC electrode, the process was carried out in two steps. First the GC electrode was held under a constant potential of 1.8 V for 5 min in 1 M H_2SO_4 solution. Second, the preanodized GC electrode was immersed in DMSO solution containing 5mM of Mn-complex for 1 h. The resulting electrode provided a linear range of 1 μM –1.5 mM and LOD of 0.2 μM for H_2O_2 . The developed electrode presented remarkable catalytic activity, good reproducibility, easy to prepare and long term stability.

J. Ping, et al. [55] developed an amperometric sensor based on Prussian blue and poly (o-phenylenediamine) (POPD) modified glassy carbon electrode for the determination of hydrogen peroxide in beverages in 2011. The electrode was deposited in a solution containing 2.5 mM FeCl_3 , 2.5 mM $\text{K}_3\text{Fe}(\text{CN})_6$, 0.1 M KCl and 0.1 M HCl at 0.4 V for 40 s. After that, the electrode was dipped into a solution containing 0.1 M KCl and 0.1 M HCl and electrochemically cycle for 20 times between 0.35 and -0.05 V at scan rate 0.05 V s^{-1} . Then, the electrode was washed with water and dried for 1 h at 100 $^\circ\text{C}$ in an oven. Next, the electropolymerization of POPD layer by cycling the applied potential from -0.05 to 0.8 V for 15 cycles at 0.01 V s^{-1} of scan rate in a phosphate buffer containing 5.0 mM OPD monomer. Finally, the developed electrode was placed into the phosphate buffer for 20 min to achieve equilibrium of the films. The developed electrode shows the linear range from 1.0 μM –0.12 mM and LOD of 0.05 μM for H_2O_2 .

In 2014, H. M. Moghaddam. et al. [56] developed nanostructure-based electrochemical sensor for determination of sulfite. The electrode was prepared by mixing 0.01 g of benzoylferrocene (BF) with 0.59 g graphite powder and 0.1 g CNTs with a mortar and pestle. Then, ~ 0.7 mL of paraffin was added to the mixture and mixed until a uniformly-wetted paste was obtained. The paste was packed into the end of a glassy tube. Then, the copper wire inserted into the carbon paste provided the electrical contact. After that, the modified electrode was characterized by CV, chronoamperometry and square wave voltammeter. The linear range exhibits from 1.0×10^{-7} to 4.0×10^{-4} M and LOD of 90 nM for sulfite.

CHAPTER 3

EXPERIMENTAL

3.1 Instrumentation

Equipments used in this work were list in table 3.1

Table 3.1 Instrumentation used for cyclic voltammetric, FIA and nanocomposite characterized experimentals.

Instrument	Model	Company
<i>Cyclic voltammetry</i>		
Potentiostat	EA 161	eDAQ, Australia
e-Corder	210	eDAQ, Australia
Data System	e-Chem (v2. 0. 13)	eDAQ, Australia
Working electrode	Glassy carbon electrode (3 mm)	CH Instruments, USA
Auxiliary electrode	Pt wire	CH Instruments, USA
Reference electrode	Ag/AgCl electrode (3 M KCl)	CH Instruments, USA
Stirrer	COLOR SQUID	Prodigy Science Instruments
<i>FIA experiments</i>		
Injection	20 μ L injection loop	Rheodyne, USA
Pump	LC-10AD	Shimadzu
Detector		
Potentiostat	EA 161	eDAQ, Australia
e-Corder	210	eDAQ, Australia
Data system	e-DAQ-chart (v. 5.5.15)	eDAQ, Australia

Table 3.1 Instrumentation used for cyclic voltammetric, FIA and nanocomposite characterized experimentals (Continued).

Instrument	Model	Company
Thin layer flow cell	MF-1048	BASi
Working electrode	Glassy carbon electrode (3 mm)	CHI Instruments, USA
Auxiliary electrode	Stainless steel tube	CH Instruments, USA
Reference electrode	Ag/AgCl electrode (3 M KCl)	CH Instruments, USA
<i>Nanocomposite characterization</i>		
UV-vis	Lamda 25	Perkin Elmer
AFM	XE-100	Park systems
IR	Spectrum RX I	Perkin Elmer
SEM	JSM 5410-LV	JEOL

3.2 Reagents and Chemical

All chemicals used in this work were summarized in Table 3.2

Table 3.2 List of reagents, grade and their suppliers.

Chemical and reagent	Grade	Supplier
Sulfite oxidase (SOx) from chicken liver (30-70 U mg ⁻¹)	High purity	ProNique Scientifics Inc. (Castle Rock, USA)
Cytochrome C (Cyt C) from horse heart	Laboratory	Acros Organic
Sodium sulfite (Na ₂ SO ₃)	Reagent	Sigma-Aldrich
Hydrogen tetrachloroaurate (HAuCl ₄ ·3 H ₂ O)	Laboratory	Acros Organic
Poly(diallyldimethylamonium chloride) (PDDA)	Low molecular weight, 20 wt. % in water	Sigma-Aldrich
Sodium hydrogen phosphate (NaH ₂ PO ₄)	Analysis	Carlo Erba

Table 3.2 List of reagents, grade and their suppliers. (Continued)

Chemical and reagent	Grade	Supplier
di-Sodium hydrogen phosphate anhydrous ($\text{Na}_2\text{HPO}_4 \cdot \text{H}_2\text{O}$)	Analysis	Carlo Erba
Glucose ($\text{C}_6\text{H}_{12}\text{O}_6$)	ACS	Sigma-Aldrich
Fructose ($\text{C}_6\text{H}_{12}\text{O}_6$)	AR	Sigma-Aldrich
Sucrose ($\text{C}_{12}\text{H}_{22}\text{O}_{11}$)	AR	Sigma-Aldrich
Ascorbic acid ($\text{C}_6\text{H}_8\text{O}_6$)	AR	Sigma-Aldrich
Sodium chloride (NaCl)	ACS	Carlo Erba
Sodium sulfate (Na_2SO_4)	ACS	Carlo Erba
Sodium acetate (NaCH_3COO)	ACS	Carlo Erba
Potassium iodide (KI)	ACS	Carlo Erba
Sodium nitrate (NaNO_3)	AR	Sigma-Aldrich
Ethanol ($\text{CH}_3\text{CH}_2\text{OH}$)	ACS	Carlo Erba

3.3 Chemical preparation

The followings include the preparation procedures of solutions and synthesis of AuNPs and other solutions used in this work.

0.5 M sulfite solution

Solution of 0.5 M sulfite solution was prepared by dissolving 6.300 ± 0.005 g in 0.1 M phosphate buffer pH 7.0 and diluted to 100 mL in volumetric flask with the buffer.

0.1 M Disodium hydrogen phosphate ($\text{Na}_2\text{HPO}_4 \cdot \text{H}_2\text{O}$) solution

11.87 g of Na_2HPO_4 was dissolved and diluted with deionized water to 1 L volumetric flask to give a 0.1 M Na_2HPO_4 solution.

0.1 M Sodium dihydrogen phosphate (NaH_2PO_4) solution

9.07 g of NaH_2PO_4 was dissolved and diluted with deionized water to 1 L volumetric flask to give a 0.1 M NaH_2PO_4 solution.

0.1 M Phosphate buffer pH 8.0

0.1 M Phosphate buffer pH 8.0 was prepared by mixing 96.3 mL of 0.1 M Na_2HPO_4 and 3.7 mL of 0.1 M NaH_2PO_4 then the mixture was adjusted to pH 8.0.

0.01% Glutaraldehyde (Glu) solution

0.01% Glu solution was prepared by pipette 400 μL from 0.25% Glu stock solution then diluted with deionized water to 10 mL volumetric flask.

6 mg mL⁻¹ Cytochrome C (Cyt C)

Solution of 6 mg mL⁻¹ Cyt C was prepared by dissolving 6 mg Cyt C in 1 mL of 0.05 M phosphate buffer pH 7.0.

0.3 U mL⁻¹ sulfite oxidase enzyme (SOx)

0.3 U mL⁻¹ SOx enzyme was prepared by diluting 100 μL of 3 U mg⁻¹ with 900 μL of 3.2 M ammonium sulfate ($(\text{NH}_4)_2\text{SO}_4$) of pH 7.5.

0.02 % AuNPs

0.02% AuNPs was synthesized according to the method developed by Y.Zhou. et al. [57]. Briefly, 10 mL of 0.02% HAuCl_4 solution was boiled thoroughly. Then, 2 mL of 38.8 mM sodium citrate was added under stirring. After that, the color of solution was changed from yellow to red, the solution was further boiled for 5 min. Then the solution was cooled to room temperature and stored in 4°C.

CNTs-PDDA

CNTs was chemically shorten and carboxylated by acid treatment (mixture of $\text{H}_2\text{SO}_4\text{:HNO}_3$ 3:1) under ultrasonic stirring for 5 h. After that, the suspension was centrifuged at 10,000 rpm and washed repeatedly with deionization water until the pH of water was 7.0. The resulting product was then dried at 110 °C. The CNTs-COOH was then functionalized with PDDA (CNTs-PDDA) using the method adopted from Cui. et al. [46]. Briefly, 10 mg of CNTs-COOH were dispersed in 20 mL of a 0.25% PDDA aqueous solution containing 0.5 M NaCl and ultrasonic stirring for 30 min. The resulting dispersion was centrifuged and washed with water for three times to remove residual PDDA. Finally, 4 mg of the collected product was dispersed in 1 mL water and the resulting solution was sonicated for 30 min before use.

3.4 Electrode preparation

Preparation of GC/CNTs-PDDA-AuNPs/SOx

40 μL of the 4 mg mL^{-1} CNTs-PDDA solution was casted on the surface of the well-polished glassy carbon (GC) electrode, and then dried at ambient temperature. The surface of the electrode was further coated with 40 μL of 0.02% AuNPs solution. After that, immobilization of SOx was carried out by dropping 15 μL of solution containing of SOx (0.1 U mg^{-1}) and Cyt C (4 mg mL^{-1}) onto the modified electrode. Finally, 15 μL of 0.01% glutaraldehyde was dropped on the modified electrode and dried at room temperature. Figure 3.1 is shown diagram for preparation of GC/CNTs-PDDA-AuNPs/SOx.

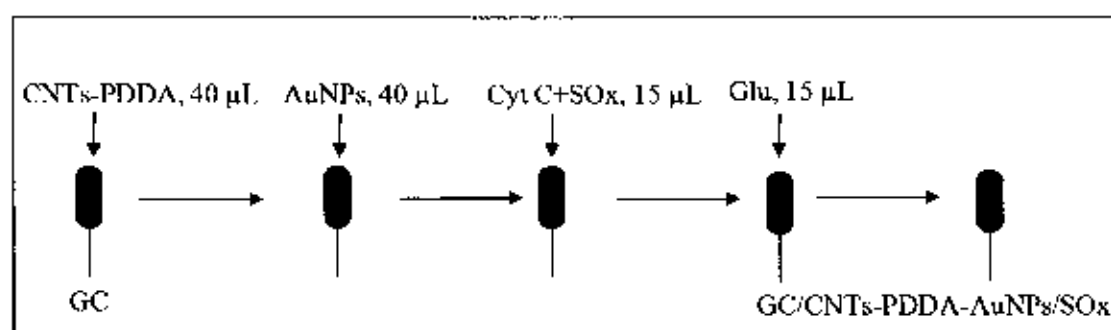


Figure 3.1 Schematic diagram of modification steps for preparation of the developed sulfite biosensor (GC/CNTs-PDDA-AuNPs/SOx).

3.5 Measurement procedures

3.5.1 Detection in batch mode

An eDAQ potentiostat (model EA 161) equipped with e-Corder (model 210) with three electrode system was used for all the cyclic voltammetric studies. Electrochemical oxidation of sulfite was studied at the developed biosensor using cyclic voltammetry and amperometry. The modified electrode was used as a working electrode, Ag/AgCl as a reference electrode and Pt wire as a counter electrode. 0.1 M phosphate buffer pH 8 was used as a supporting electrolyte. Figure 3.2 is shown the set up of the system used for all the studies.

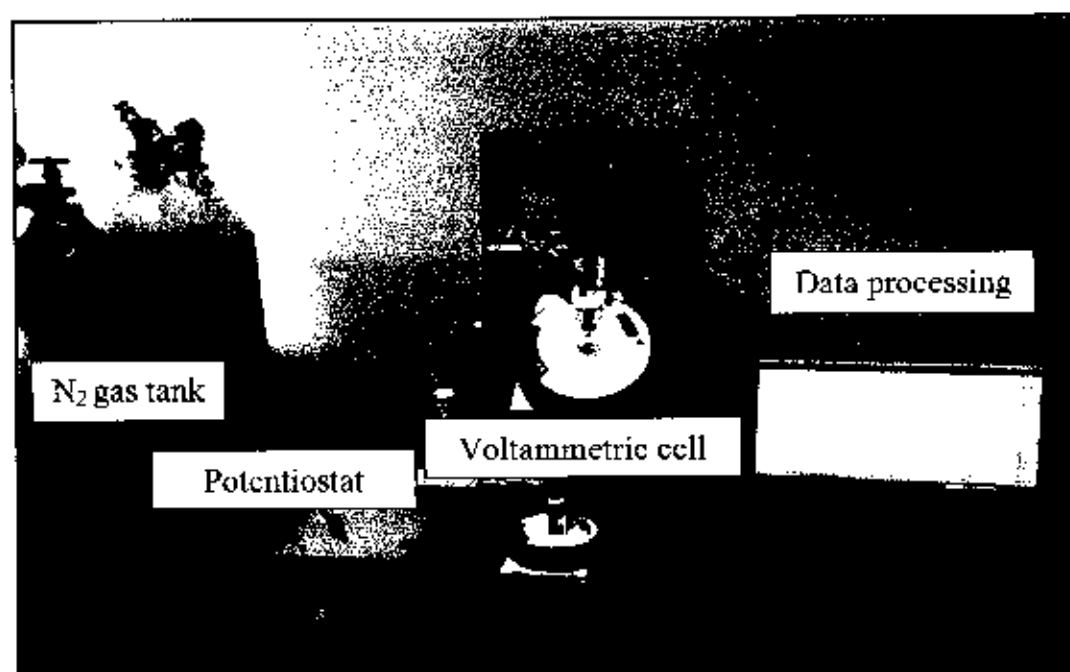


Figure 3.2 Photograph of the set up for cyclic voltammetric measurements; potentiostat (c-DAQ) voltammetric cell; (vial 25 mL); working electrode (GC or modified GC); reference electrode (Ag/AgCl); auxiliary electrode (Pt wire).

3.5.2 Amperometric detection in flow system

The flow injection analysis system used for the amperometric measurements, was comprised of a pump (model LC-10AD), injection valve equipped with 20 μ L injection loop, an cDAQ potentiostat (model EA161), c-Corder (model 210) and flow cell (model LF 018) with three electrode system. The modified electrode was used as a working electrode, Ag/AgCl as a reference electrode and a stainless steel tube as an auxiliary electrode. 0.1 M phosphate buffer pH 8.0 was used as a carrier solution. Figure 3.3 shows the set up of the system used for amperometric detection in flow system.

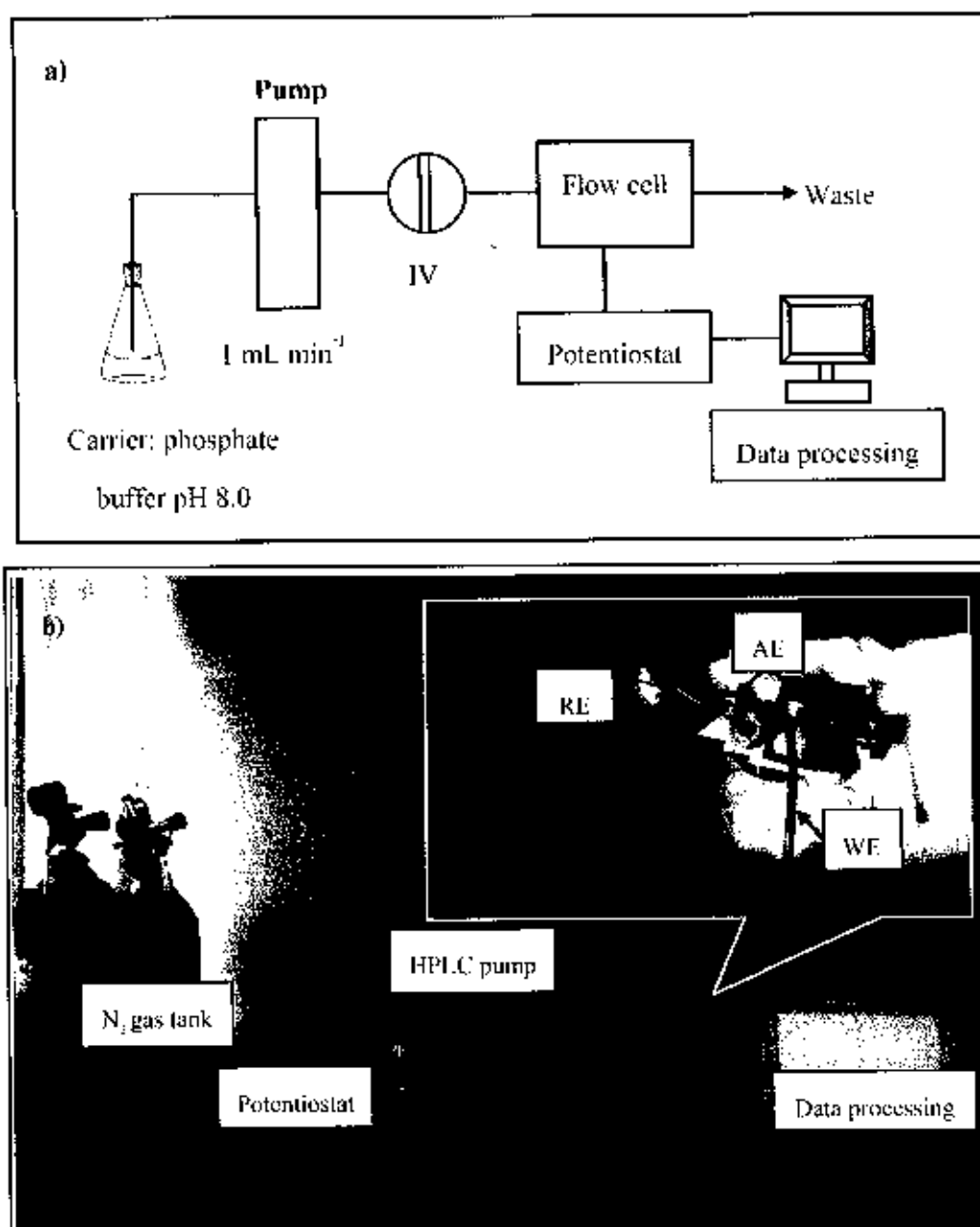


Figure 3.3 Manifold of flow injection analysis (a) used in this work and photograph of the set up for amperometric detection in flow system (b) using a e-DAQ potentiostat, IV: Injection valve, Injection valve was equipped with 20 μL loop. Thin layer flow cell are the three electrode type, WE: working electrode, AE: stainless steel tube and RE: Ag/AgCl electrode.

3.6 Sample preparation

Eleven commercial products of beverages were employed in validation of the method. Picture of samples used in this work, shown in Figure 3.4. Those products were bought from Tesco Lotus and One Tambon One Product (OTOP) in Ubon Ratchathani province. In the analysis, sample was filtered with syringe filter (nylon, 13 mm, 0.22 μm). Then 5 mL of sample was added into 10 mL volumetric flask and diluted with 0.1 M phosphate buffer pH 7.0.



Figure 3.4 Sample of beers (Chang, Hienegen and Singha) and wines (French white wine, Mamaow wine, Mulberry, Berri estates bin 777, Sicilian, Berri estates bin 222, Marsol and South Africa).

3.7 Procedure

3.7.1 Part I: Electrochemical detection of sulfite oxidation on sulfite based-biosensor

3.7.1.1 Cyclic voltammetric study of sulfite oxidation

The unique electrochemical behavior of sulfite oxidation was studied at the modified electrode compared with bare GC electrode. The cyclic voltammograms at the bare GC (a) and modified electrode of GC/CNTs-PDDA-AuNPs/SOx (b) in the absence and presence of sulfite were measured using cyclic voltammetry. The results discussed in Section 4.1.1.

3.7.1.2 Studied of parameters that affect the sensitivity of biosensor

1) Effect of CNTs-PDDA loading

Optimization of the CNTs-PDDA modified amount was investigated using amperometry to find the most sensitivity condition for sulfite detection. CNTs-PDDA was studied in the range 0-8 mg mL⁻¹. Results of CNTs-PDDA amount are discussed in Section 4.1.2.1.

2) Effect of gold nanoparticles (AuNPs) loading

The effect of AuNPs concentration in modified solution was studied in the range 0-0.1 %. Results are discussed in Section 4.1.2.2.

3) Effect of cytochrome C (Cyt C) loading

The effect of Cyt C concentration used for the modification was investigated in the range 0-16 mg mL⁻¹. The result was illustrated in Section 4.1.2.3.

4) Effect of sulfite oxidase enzyme (SOx) loading

The influence of SOx loading was studied in the concentration range of 0-0.3 mg mL⁻¹. Results are presented in Section 4.1.2.4.

5) Effect of buffer pH (phosphate buffer solution), 0.1 M

The effect of buffer pH on oxidation peak current of sulfite at the GC/CNTs-PDDA-AuNPs/SOx electrode was investigated over the range -5-9 using 0.1 M phosphate buffer solution as supporting electrolyte. Cyclic voltammograms of sulfite were recorded using electrolyte solution of varying pH. The results are presented in Section 4.1.2.5.

3.7.1.3 Cyclic voltammetry (CV) of potential interferences

In order to test possibility of using the developed biosensor with beverage samples, the signals of foreign ions on the biosensor were investigated. The cyclic voltamograms of potential interferences (glucose, fructose, sucrose, NaNO_3 , $\text{CH}_3\text{CH}_2\text{OH}$, NaH_2PO_4 , KI , ascorbic acid, NaCl and Na_2SO_4) on the sulfite biosensor were examined in 0.1 M phosphate buffer pH 8.0. The results are presented in Section 4.1.3.

3.7.1.4 The apparent Michaelis-Menten constant (K_m^{app})

The apparent Michaelis-Menten constant (K_m^{app}), can be calculated by the Lineweaver-Burk equation follow by equation 4.1. The Michaelis-Menten equation is used to determine the kinetic properties of isolated enzymes. It is also used in modeling the dynamics of enzyme systems and displayed oscillatory behavior. If low oscillatory reactions is shown the many biochemical processes catalyzed by enzymes. K_m^{app} was studied in the range 0.025–0.25 mM using amperometry in phosphate buffer pH 8.0. The results are presented in Section 4.1.4

3.7.1.5 Scan rate dependence study

The cyclic voltammograms of sulfite on the sulfite biosensor were examined in 0.1 M phosphate buffer pH 8.0 using various scan rate. The peak currents of sulfites oxidation at various potential scan rates (0.01, 0.02, 0.03, 0.05, 0.06 and 0.10 V s^{-1}) were investigated. The results are discussed in Section 4.1.5.

3.7.1.6 Stability study

The stability of the GC/CNTs-PDDA-AuNPs/SOx biosensor for detection of sulfite oxidation was studies. The GC/CNTs-PDDA-AuNPs/SOx electrode was stored in vial over a 0.1 M phosphate buffer pH 7.0 and kept at 4 °C when not use. The sulfite oxidation current were measured at a GC/CNTs-PDDA-AuNPs/SOx electrode when stored for 0, 1, 2, 3, 4, 5, 7, 14 and 30 days. Results are presented in Section 4.1.6.

3.7.1.7 Amperometric detection of sulfite in the developed FIA system

1) Optimum potential for amperometric detection

The influence of potential for amperometric detection was studied in the range 0-1 V. Results are discussed in Section 4.1.7.1

2) Optimum flow rate

Optimization of flow rate for sulfite detection was studied between 0.5 to 2.0 mL min⁻¹. Results are presented in Section 4.1.7.2.

3) Analytical features

- Linear concentration range

Standard calibration of sulfite were prepared by diluting the appropriate amount in 0.1 M phosphate buffer pH 8.0 to give working solution in the range 2–200 mg L⁻¹. 20 µL of each standard was injected into the FIA system using flow rate of 1.0 mL min⁻¹ and 0.1 M phosphate buffer pH 8.0 as a carrier solution. Amperometric responses were recorded using the applied potential of 0.3 V. Results were shown in Section 4.1.7.3, 1).

- Limit of detection

In this study, the limit of detection was calculated by injecting 5 mg L⁻¹ of standard sulfite solution 20 times. The signal value of 3 times standard deviation (3SD) was calculated. Results were presented in Section 4.1.7.3, 2).

- Interference study

In this study, the effect of foreign ions, including compounds that are likely to exist in the sample was investigated. The concentration of the foreign species that provide signal change greater than 5% was considered as the tolerance limit. The foreign ions used in this study were glucose, fructose, sucrose, NaNO₃, CH₃CH₂OH, NaCH₃COO, KI, ascorbic acid, NaCl and Na₂SO₄. The results are discussed in Section 4.1.7.3, 3).

- Method validation

Standard method (Iodometric method)

The iodometric titration of sulfite was performed according to the official method. A back titration mode was used to avoid sulfite loss in the form of SO₂ in acidic environment. 5 mL of standard 0.0002 M potassium iodate (KIO₃) was added in the 250.0 mL conical flask followed by 2.5 mL of 3 M sulfuric acid (H₂SO₄). Then 2.5 mL of 0.1500 M potassium iodide (KI) was pipetted into the conical flask and 5.0 mL of sample was added. After that, this mixture solution was immediately titrated with 0.0025 M sodium thiosulfate (Na₂S₂O₃) to a light yellow color. Then 0.5 mL of starch indicator was added and continued the titration until the iodine-starch complex become colorless.

FI-sulfite biosensor

The samples were diluted 2 times using 0.1 M phosphate buffer pH 8.0 prior to the FIA system. The sulfite concentration was calculated using external calibration curve. Results are presented in Section 4.1.7.3, 4).

3.7.2 Part II: Indirect method for sulfite based-biosensor

3.7.2.1 Cyclic voltammetric study of H_2O_2 reduction

The unique electrochemical behavior of sulfite reduction was studied at different modified electrode materials. The cyclic voltammograms at the bare GC (a) and sulfite biosensor (GC/CNTs-PDDA-AuNPs/SOx) (b) in the absence and presence of H_2O_2 were measured using cyclic voltammetry. The results discussed in Section 4.2.1.

3.7.2.2 Optimum potential for amperometric detection of H_2O_2

Optimization of the potential for amperometric detection was investigated between 0 to -0.1 V using amperometry. Results are discussed in Section 4.2.2.

3.7.2.3 Analytical feature

1) Linear range

Calibration standards of sulfite were prepared by diluting the appropriate amount in 0.1 M phosphate buffer pH 8.0 to give working solution in the range 500-2000 $mg\ L^{-1}$. 20 μL of each standard was injected into the FIA system using flow rate of 1.0 $mL\ min^{-1}$ and 0.1 M phosphate buffer pH 8.0 as a carrier solution. Amperometric responses were recorded using the applied potential of -0.4 V. Results were shown in Section 4.2.3.1.

2) Limit of detection

In this study, the limit of detection was investigated by repetitive injections of 500 $mg\ L^{-1}$ sulfite standard solution ($n=20$). The signal value of 3 times standard deviation was calculated. Results were presented in Section 4.2.3.2.

3.7.3 Characterization of the nanocomposites

3.7.3.1 UV-Visible spectroscopy

UV-Visible spectra were measured in a 1 cm path length quartz cell using a Lamda 25 spectrophotometer from Perkin Elmer company. The samples were dissolved in deionization water. Results were presented in Section 4.3.1.

3.7.3.2 Infrared spectroscopy (IR)

Infrared spectroscopy is an important technique in the functional groups identification in molecules. The study was carried out with FT-IR spectrometry from Perkin-Elmer, model: Spectrum RX 1 as shown in Figure 3.6. The range of measurement was set between 500 cm^{-1} and 4000 cm^{-1} . Results are discussed in Section 4.3.2.

3.7.3.3 Scanning electron microscopy (SEM)

The morphology of the composite material modified electrode (CNT-COOH, CNTs-PDDA, CNTs-PDDA-AuNPs and CNTs-PDDA-AuNPs/SOx) surface was studied with scanning electron microscopy (JSM 5410-I.V, JEOL). Sample was attached on SEM stubs and then sputter coated with gold before investigated by SEM. Results are presented in Section 4.3.3.

3.7.3.4 Atomic force microscopy (AFM)

The surface morphology of the composite material modified electrode (CNT-COOH, CNTs-PDDA, CNTs-PDDA-AuNPs and CNTs-PDDA-AuNPs/SOx) surface was studied by using AFM model XE-100. Results are discussed in Section 4.3.4.

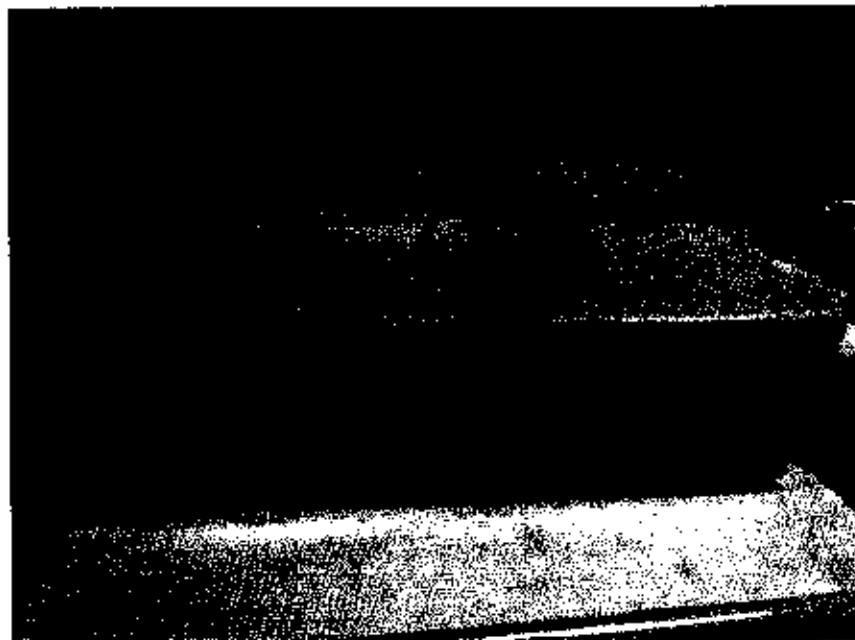


Figure 3.5 UV-Vis spectrometer (Lambda 25, Perkin Elmer)

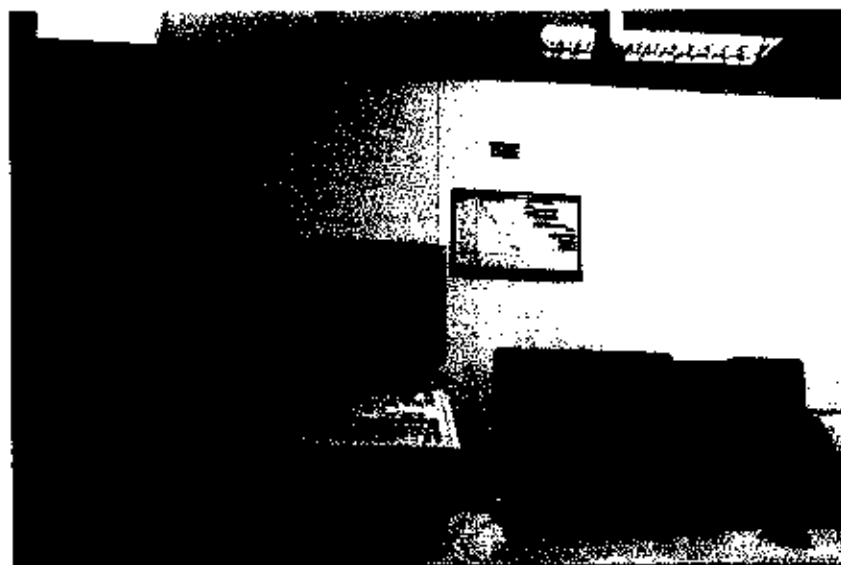


Figure 3.6 FT-IR spectrometer (Spectrum RX 1, Perkin-Elmer)



Figure 3.7 Scanning electron microscope (JSM 5410-LV, JEOL).

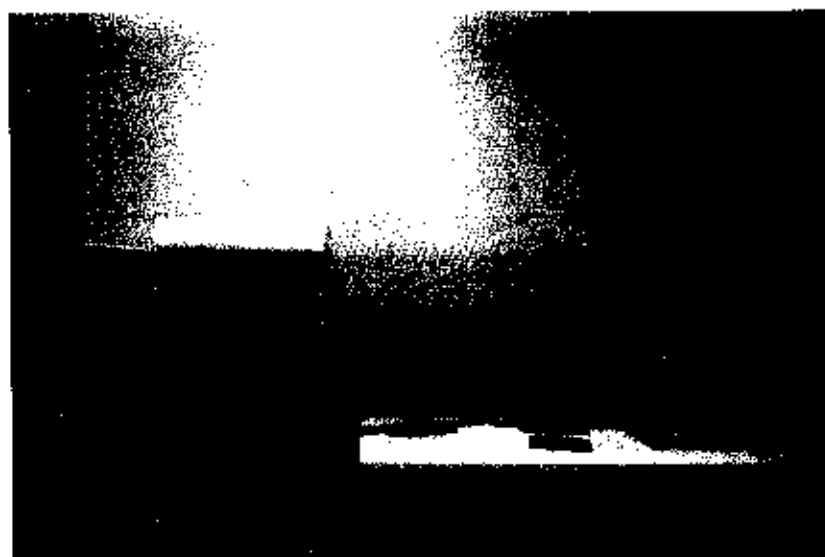


Figure 3.8 Atomic force microscope (XE-100, Park System)

CHAPTER 4

RESULTS AND DISCUSSION

4.1 Part I: Electrochemical detection of sulfite oxidation on the developed sulfite biosensor

4.1.1 Cyclic voltammetric study of sulfite oxidation

The electrochemical behavior of sulfite at modified sulfite biosensor (GC/CNTs-PDDA-AuNPs/SOx) was studied using cyclic voltammetry (CV). The GC or sulfite biosensor was used as a working electrode, Ag/AgCl as a reference electrode and Pt wire as an auxiliary electrode. Figure 4.1 compared the response obtained from bare GC and the developed sulfite biosensor toward the electro-oxidation of sulfite in 0.1 M phosphate buffer (pH 7.0). Sulfite oxidation is an electrochemically irreversible process. Bare GC electrode results in a peak shape signal at about 0.85 V versus Ag/AgCl, whereas the developed sulfite biosensor provides the oxidation peak at 0.30 V. These results show that sulfite oxidase (SOx) immobilized on the CNTs-PDDA-AuNPs composite reduces the overpotential of sulfite oxidation and imparts electrocatalytic activity for sulfite oxidation. Enzyme SOx was effectively immobilized on the biocompatible matrix of CNTs-PDDA-AuNPs and cytochrome C (Cyt C) to produce a selective and sensitive electrode for sulfite detection.

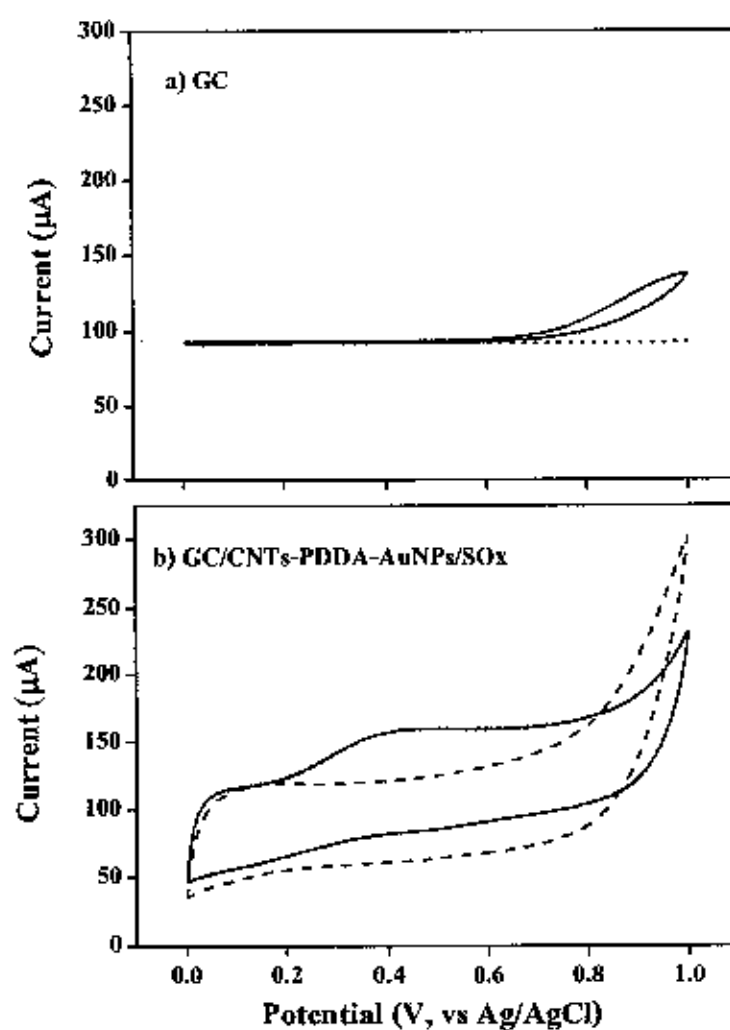


Figure 4.1 Solid lines are the cyclic voltammograms obtained for 4 mM sulfite on a) bare glassy carbon electrode (GC) and b) modified sulfite biosensor (GC/CNTs-PDDA-AuNPs/SOx). Background voltammograms (0.1 M phosphate buffer, pH 7.0) are also shown as dotted for both electrodes. The scan rate was fixed at 50 mV s^{-1} .

4.1.2 Studied of parameters that effect the sensitivity of the developed biosensor

4.1.2.1 Effect of CNTs-PDDA loading

Parameters affecting amperometric detection of sulfite at modified sulfite biosensor were examined using the potential of 0.3 V. The effect of CNTs-PDDA concentration used for electrode modification on the current signal was studied from 0 to 8 mg mL⁻¹. As shown in Figure 4.2 the current response increased with increasing CNTs-PDDA loading from 0 to 4 mg mL⁻¹. A slightly decreased of current response from 4 to 8 mg mL⁻¹. As demonstrated, a cationic polyelectrolyte of PDDA was absorbed on the surface of the CNTs by electrostatic interaction between negatively charged of carboxyl groups on the CNT's surface and positively charged of polyelectrolyte chain [58]. As the results, the CNTs-PDDA properties of promoted electron transfer between the electroactive species and electrode was described by Y.C. Tasi. et al. [59]. Therefore, 4 mg mL⁻¹ CNTs-PDDA was chosen for modified electrode and for further experiments.

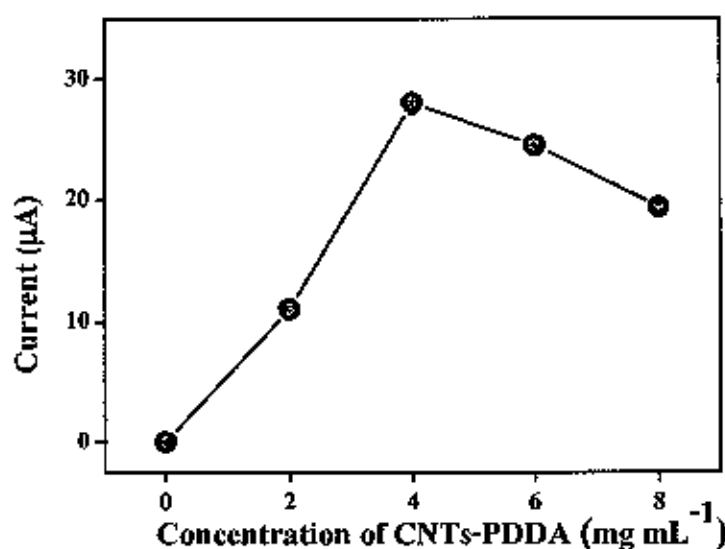


Figure 4.2 The effect of the concentration of CNTs-PDDA (mg mL⁻¹) on the amperometric response of oxidation current to 0.5 mM sulfite solution in 0.1 M phosphate buffer solution pH 8.0 at potential of 0.3 V.

4.1.2.2 Effect of gold nanoparticles (AuNPs) loading

The concentration of AuNPs is a key factor in this enzyme-based biosensor. In this study, optimization was investigated. Figure 4.3 is shown the effect of AuNPs loading between 0–0.1% on the oxidation current of sulfite. The current increased with increasing amount of AuNPs from 0 to 0.02%. This was probably because the amount of absorbed enzyme increased due to increasing surface area. For the amount of AuNPs above 0.02% the oxidation current declined probably because the discontinuous assembly of enzymes on too many AuNPs or mass-transfer processes of substrate and product. Therefore, AuNPs concentration of 0.02% which provided the maximum current was selected as the optimum for the biosensor fabrication.

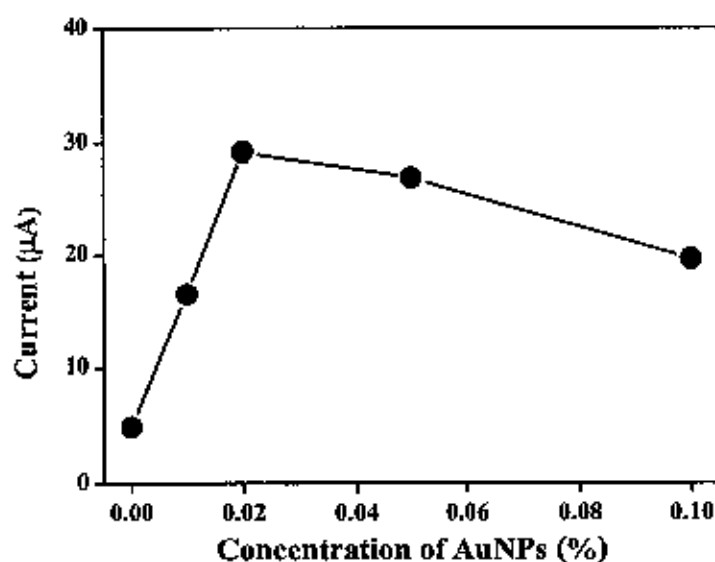


Figure 4.3 Dependence of AuNPs concentration (%) on the oxidation current. The concentration of sulfite is 0.5 mM in 0.1 M phosphate buffer solution of pH 8.0 at potential of 0.3 V.

4.1.2.3 Effect of cytochrome C (Cyt C) loading

The effect of Cyt C loading on current response was studied to optimize the electrode performance. As seen in Figure 4.4, the current responses increased with the increase of Cyt C concentration from 0 to 4 mg mL⁻¹. The results indicated that the Cyt C promoted the electron transfer of SOx. The electrons transfer might be attributed to the following factor. First, the co-immobilization between Cyt C and SOx might results in an optimal conformation to facilitate electron transfer. Second, the electron produced from one protein could transfer to electron surface by the other protein. Finally, the interaction between SOx and Cyt C might result in porous structure which was helpful for the electron transfer by the diffusion of electrolyte between proteins and electrode surface [60]. The oxidation current declined when amount of Cyt C above 4 mg mL⁻¹. The decreasing of the current responses might be ascribed to the thick and dense Cyt C and SOx layer, especially the protein part of Cyt C and SOx, which hindered the electron transfer. Thus, to make a sensitive biosensor, 4 mg mL⁻¹ of Cyt C concentration was selected for further investigations.

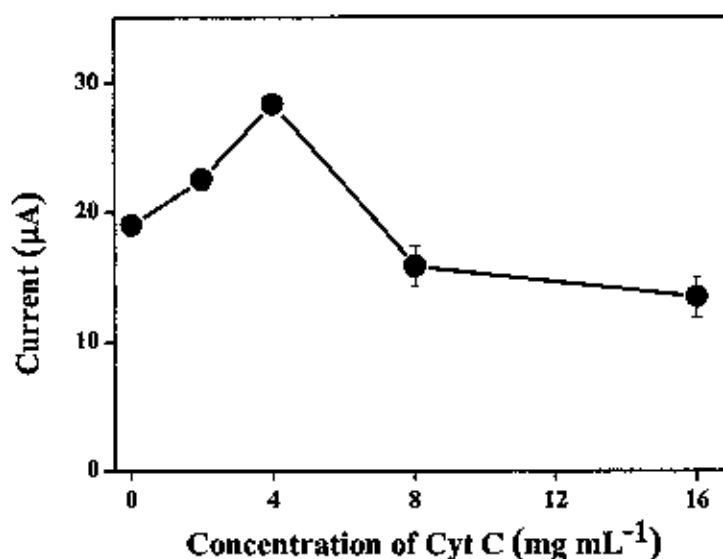


Figure 4.4 Dependence of cytochrome C concentration (mg mL⁻¹) on the oxidation current. The concentration of sulfite is 0.5 mM in 0.1 M phosphate buffer solution of pH 8.0 at potential of 0.3 V.

4.1.2.4 Effect of sulfite oxidase enzyme (SOx) loading

The effect of SOx concentration on the biosensor response was studied. The results are illustrated in Figure 4.5. It was found that the current responses increased with increasing the SOx concentration and reached the maximum value at 0.1 U mL^{-1} . Further increasing of the SOx concentration, the oxidation current tended to decrease. This behavior is typical for the enzyme-based biosensors [61, 62]. Using of higher enzyme activity resulted in a gradual decrease in biosensor response (concentration above 0.1 U mL^{-1}) probably due to the more intensive crosslinking which constituted a diffusion barrier for the substrate. This result was consistence with the study investigated by Dinckaya, et al. [48]. Thus, 0.1 U mL^{-1} SOx was chosen for subsequent experiments.

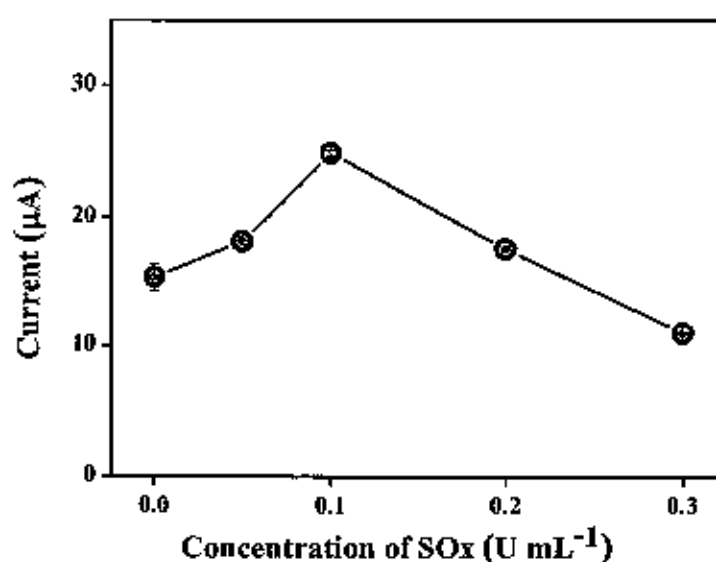


Figure 4.5 Dependence of sulfite oxidase enzyme concentration (U mL^{-1}) on the oxidation current.

The concentration of sulfite is 0.5 mM in 0.1 M phosphate buffer solution of $\text{pH } 8.0$ at potential of 0.3 V .

4.1.2.5 Effect of buffer pH (phosphate buffer solution), 0.1 M

The influence of pHs were studied because it is a critical parameter in the determination of enzyme activity. The effects of pHs on the analytical response of modified sulfite biosensor were studied in the range 5.0 to 9.0 in 0.1 M phosphate buffer solution using cyclic voltammetry. Figure 4.6a is shown the signal of 4 mM sulfite at various buffers. It was observed that the peak potential values of peak shifted slightly towards less values (Figure 4.6b), when the pH is increased. Figure 4.6c is shown that increasing of current responses when the pH is increased until the pH 8.0 and above pH 8.0 the current responses is decreased. This indicated that pH 8.0 was the optimum pH. This pH, biomolecules retain their natural structures and its do not get denatured. These results were similar to previous work reported by P. Kalimuthu, et al. [63]. Therefore, 0.1 M phosphate buffer pH 8.0 was selected for further study.

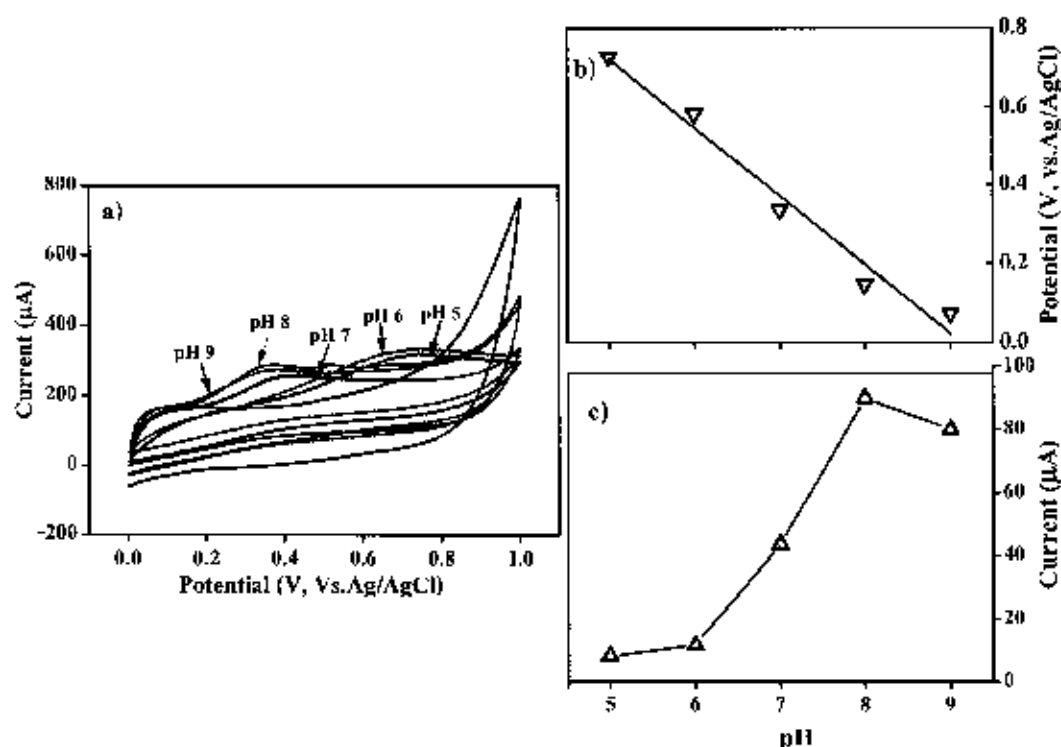


Figure 4.6 a) Cyclic voltammetric responses of 4 mM sulfite at various buffer pHs and the dependence of buffer pH on the b) peak potential c) peak current obtained from the biosensor, scan rate 50 mV s^{-1} .

4.1.3 Cyclic voltammetry (CV) of the potential interferences

The selectivity of modified sulfite biosensor was studied by cyclic voltammetry. The cyclic voltammograms of potential interferences such as sugar, ions and vitamins were measured in a 0.1 M phosphate pH 8.0 with the modified sulfite biosensor as a working electrode, Ag/AgCl as a reference electrode and Pt wire as an auxiliary electrode. These interferences (sugar, ions and vitamins) contain the wines and beers sample. Figure 4.7 is shown the cyclic voltammograms of substances including glucose, fructose, NaNO_3 , Na_2SO_4 , sucrose, NaCl, NaCH_3COO , $\text{CH}_3\text{CH}_2\text{OH}$ and ascorbic acid. The cyclic voltammograms of these substances were not well appeared peaks at the potential from 0 to 1 V. But the oxidation wave of KI was observed at about 0.5 V. The results indicated that most of the sample constituents such as glucose, fructose, NaNO_3 , Na_2SO_4 , sucrose, NaCl, NaCH_3COO , $\text{CH}_3\text{CH}_2\text{OH}$, ascorbic acid and KI did not interfere with the detection of sulfite at the developed biosensor. This indicated that the developed modified sulfite biosensor was selective for sulfite determination.

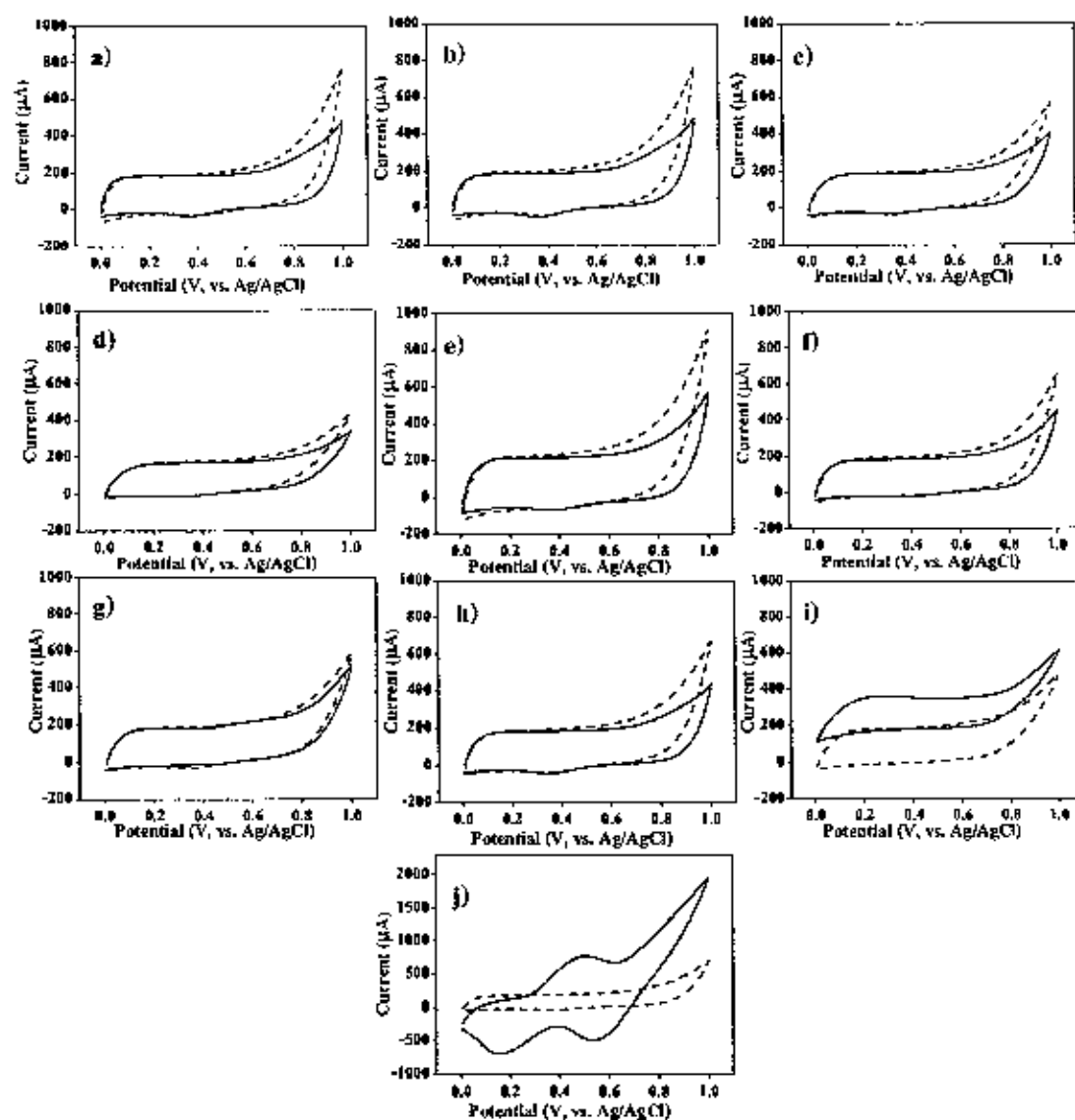


Figure 4.7 Cyclic voltammogram of substances, a) fructose, b) glucose, c) NaNO_3 , d) Na_2SO_4 , e) sucrose, f) NaCl , g) NaCH_3COO , h) $\text{CH}_3\text{CH}_2\text{OH}$, i) ascorbic acid and j) KI concentration of 12 mM in 0.1 M phosphate buffer pH 8.0. The scan rate was fixed at 50 mV s^{-1} .

4.1.4 The apparent Michaelis-Menten constant (K_m^{app})

The amperometric measurements using the modified sulfite biosensor was investigated by successively adding sulfite to a continuous stirring 20 mL of 0.1 M phosphate buffer pH 8.0 under the optimized condition (The amperogram is shown in Figure A.5). Figure 4.8a is shown the dependency of current response on sulfite concentration. The current increases when the concentration of sulfite increases. The K_m^{app} gave an indication of enzyme-substrate kinetics, could be estimated from the electrochemical version of the Lineweaver-Burk equation (4.1) [64].

$$\frac{1}{I_{ss}} = \frac{1}{I_{max}} + \frac{K_m^{app}}{I_{max}c} \quad (4.1)$$

Where c is a substrate concentration in a bulk solution, I_{ss} the steady-state current after the addition of substrate and I_{max} is the maximum current measured under saturated substrate conditions. A low K_m^{app} value indicates a strong substrate binding and demonstrates a higher affinity of sulfite for the modified electrode. On the other hand, a high K_m^{app} value means a lot of substrate must be present to saturate the enzyme, meaning the enzyme has low affinity for the substrate. Figure 4.8b is shown the Lineweaver-Burk plot of SOx immobilized on the modified electrode in the presence of different concentration of sulfite. The calculated K_m^{app} is 0.49 mM, indicating that the modified sulfite electrode obtained represents a strong substrate binding and demonstrates a high affinity of sulfite for the modified electrode.

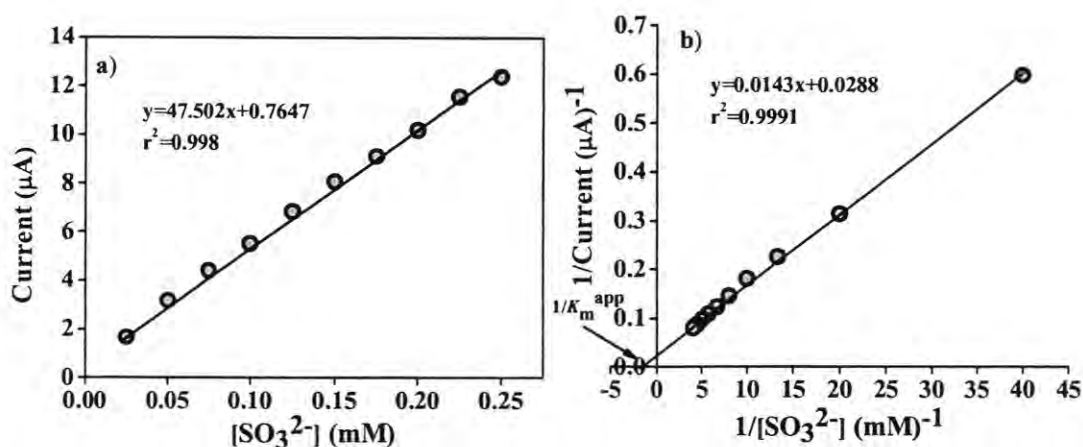


Figure 4.8 a) Amperometric response of modified sulfite biosensor toward sulfite in the concentration range 0.025-0.25 mM and b) Linerweaver-Bulk plot of sulfite immobilized on the sulfite biosensor.

4.1.5 Scan rate dependence study

Cyclic voltammograms of sulfite on the sulfite biosensor (GC/CNTs-PDDA-AuNPs/SOx) were investigated at different scan rates, the results are shown in Figure 4.9. It can be observed in Figure 4.9a that the oxidation peak potential shift to more positive potentials with increasing scan rate. Because increasing the scan rate can decrease the effect of a coupled chemical reaction, since the reaction has less time to occur. Also, a plot of peak current versus the square root of scan rate was found to be linear in the range from 0.01 to 0.1 V s⁻¹. Linear regression equation gave $y = 769.51x - 48.68$ ($r^2 = 0.9942$). This indicated that the sulfite oxidation is a diffusion controlled process [65].

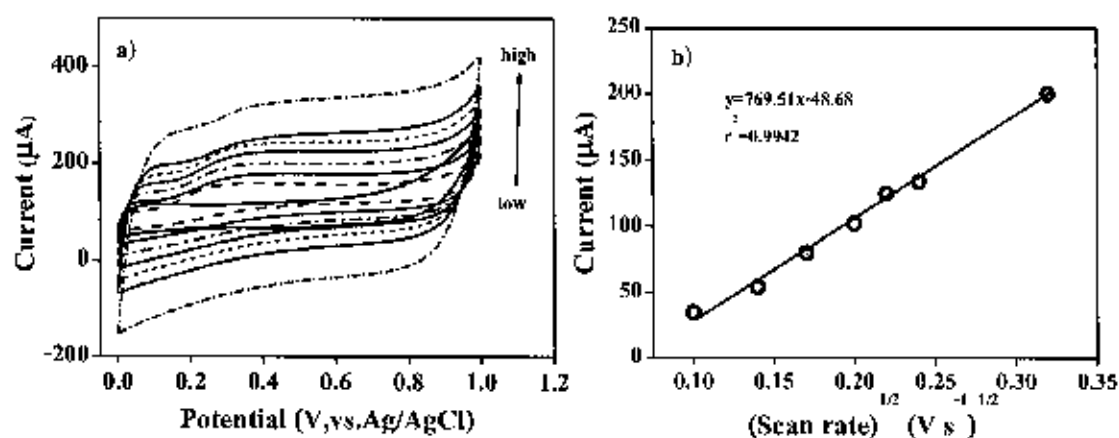


Figure 4.9 a) Cyclic voltammograms, obtained at various scan rates for 4 mM sulfite in 0.1 M phosphate buffer (pH 8.0) at modified sulfite biosensor and b) linear relationship between oxidation peak currents and square root of the scan rate.

4.1.6 Stability study

The storage stability of the developed sulfite sensor was investigated in 0.1 M phosphate buffer pH 7.0. The sulfite oxidation current was measured when stored for 0, 1, 2, 3, 4, 5, 6, 7, 15 and 30 days. The relative oxidation current was calculated and plotted versus storage time. Relationship between percentages of relative oxidation currents and storage time (day) was shown in Figure 4.10. The results indicated that relative oxidation current of 80 % can be obtained after stored for 30 days. This indicated high stability of the developed biosensor.

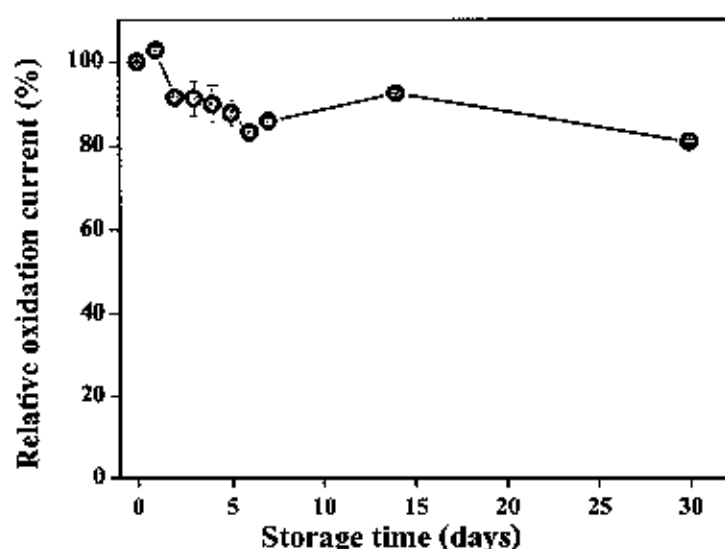


Figure 4.10 The storage stability of the GC/CNTs-PDDA-AuNPs/SOx using 0.05 mM sulfite.

4.1.7 Amperometric detection of sulfite in the developed FIA system

4.1.7.1 Optimum potential for amperometric detection

The detection potential affects the sensitivity of current signal of an analyte. In order to obtain the optimal potential for amperometric detection in FIA, hydrodynamic voltammetric behavior of sulfite was investigated. 10 mg L^{-1} of sulfite solution was injected into the flow system with varying detection potential from 0.0 to 1.0 V. As shown in Figure 4.11, the oxidation current rises from the potential range 0.0 to 0.3 V, then decrease rapidly above 0.3 V and saturated at potential above 0.6 V. The potential at 0.3 V provided the maximum peak area and therefore it was selected as the optimum potential. The results indicated that electrocatalytic activity of enzyme SOx incorporated with the matrix GC/CNTs-PDDA-AuNPs/SOx toward the oxidation of sulfite enables the biosensor can be effectively detect at low potential. The advantage of detection at low potential is low noise and background current [66]. This potential was similar to previous work reported by R. Rewal. et al. [67], who studied amperometric sulfite biosensor based on SOx/PBNPs (Prussian blue nanoparticle)/PPY (polypyrrole composite) electrodeposition onto the surface of indium tin oxide (ITO) electrode.

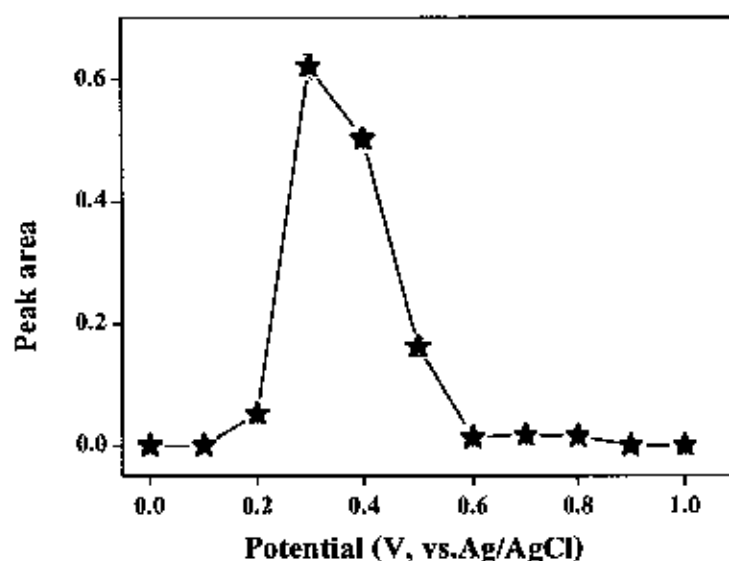


Figure 4.11 Influence of the applied potential on the biosensor response for 10 mg L^{-1} sulfite.

4.1.7.2 Optimum flow rate

In order to achieve the satisfactory sensitivity and sample throughput, the effect of flow rate on the modified sulfite biosensor response was optimized by injection of 10 mg L^{-1} sulfite into the carrier stream (0.1 M phosphate buffer pH 8.0). The flow rate was between 0.5 to 2 mL min^{-1} . Figure 4.12 is shown that the responses decrease with the increasing flow rate from 0.5 to 2 mL min^{-1} . This behavior is in agreement with theoretical expectations based on laminar flow assumptions under conditions of mass transport control [68]. However, increasing flow rate increases sample throughput. To balance between response and sample throughput, the flow rate of 1.0 mL min^{-1} was selected as the optimum for future experimental.

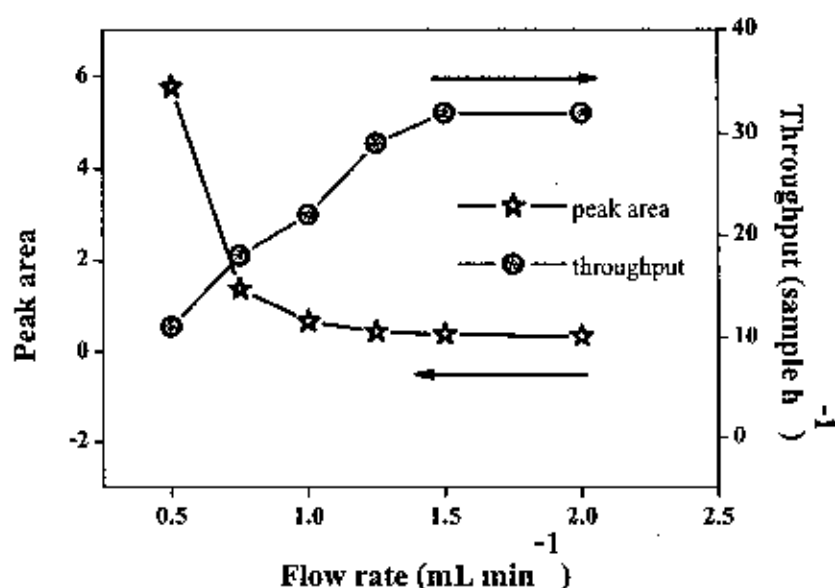


Figure 4.12 Effect of the flow rate on sulfite biosensor response and sample throughput.

4.1.7.3 Analytical feature

1) Linear concentration range

The analytical performance of the FI method with amperometric detection at the developed sulfite biosensor was examined. Figure 4.13 shows the effect of sulfite concentration on current signal with different concentration between 2-200 mg L⁻¹, with the three replicate injections. The results demonstrated the regression equation $y=204.66x-715.65$ ($r^2=0.9991$), when y and x are the peak area ($\mu\text{A} \cdot \text{min}$) and sulfite concentration (mg L⁻¹), respectively.

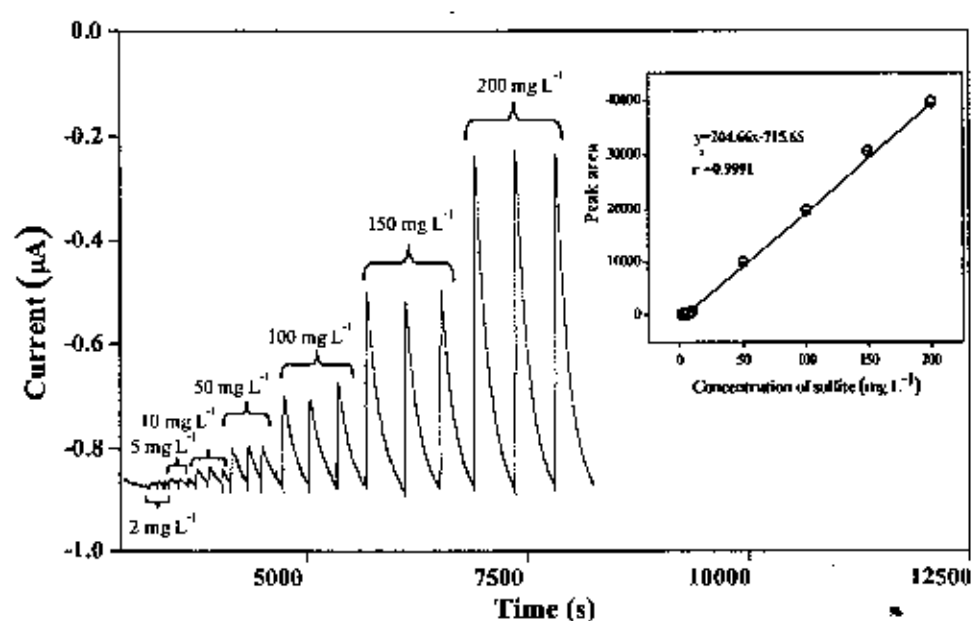


Figure 4.13 FIA grams obtained from injections of sulfite standards. The inset shows the linear relationship between the signal of sulfite and the concentration.

2) Limit of detection

The detection limit was performed by 5 mg L^{-1} sulfite with the twenty replicate injections into a carrier solution of 0.1 M phosphate buffer pH 8.0. The result is shown in Figure 4.14. The detection limit (3σ) was 1.3 mg L^{-1} . The system provides an impressively good precision (%R.S.D.=3.8, $n=20$). High precision of the developed system demonstrates good stability of the immobilized enzyme in spite of the hydrodynamic condition. Throughput of sample is 57 samples h^{-1} .

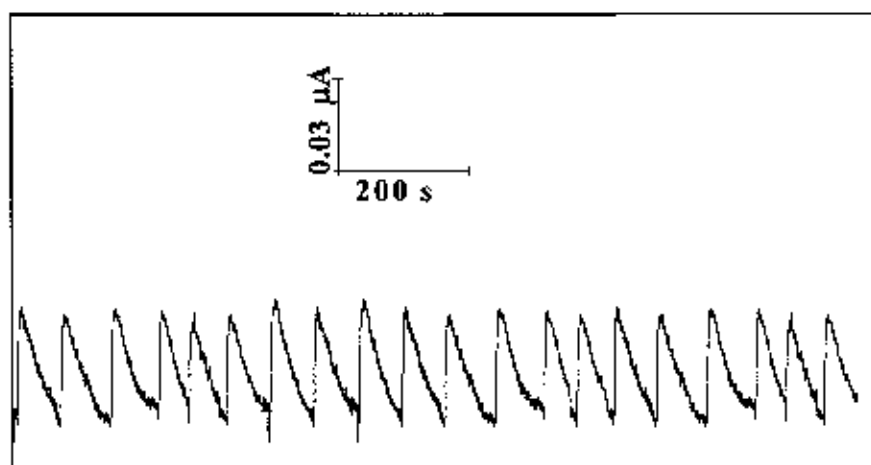


Figure 4.14 FI amperometric response obtained from the developed sulfite biosensor for 20 repetitive injection of 5 mg L^{-1} sulfite. Carrier solution is 0.1 M phosphate buffer pH 8.0, applied potential at 0.3 V using 1.0 mL min^{-1} of flow rate.

3) Interference study

Effect of possible interferences from beers and wines matrixes to the FI-sulfite biosensor method was studied. The effect of foreign ions including fructose, glucose, NaNO_3 , NaSO_4 , sucrose, NaCl , NaCH_3COO , $\text{CH}_3\text{CH}_2\text{OH}$, KI and ascorbic acid on the alteration of amperometric signal obtained from 10 mg L^{-1} sulfite was investigated. The tolerance limits of possible coexisting ions are summarized in Table 4.1. The results from this study could be roughly divided into three groups.

Group I: do not interfere. The foreign ions in this group were fructose, glucose, NaNO_3 , Na_2SO_4 .

Group II: very low interfering potentials. In this group, tolerance limit were in between 500 to 1000 mg L^{-1} these foreign were including sucrose, NaCl , NaCH_3COO , $\text{CH}_3\text{CH}_2\text{HO}$, and KI .

Group III: low interfering potential. In this group, tolerance limit was less than 15 mg L^{-1} which was ascorbic acid.

The results indicated that the selectivity of the developed method is satisfied.

Table 4.1 Effect of foreign ions on the alteration of FI amperometric signal obtained from replicate injections (n=3) of 10 mg L^{-1} standard sulfite.

Foreign species/ added as	Investigated concentration (mg L^{-1})	Tolerance limit ^a (mg L^{-1})
1. fructose/ $\text{C}_6\text{H}_{12}\text{O}_6$	10-1000	does not interfere
2. glucose/ $\text{C}_6\text{H}_{12}\text{O}_6$		
3. sodium nitrate/ NaNO_3		
4. sodium sulfate/ Na_2SO_4		
5. sucrose/ $\text{C}_{12}\text{H}_{22}\text{O}_{11}$		1000
6. sodium chloride/ NaCl		
7. sodium acetate/ NaCH_3COO		
8. ethanol/ $\text{CH}_3\text{CH}_2\text{OH}$		500
9. potassium iodide/ KI		
10. ascorbic acid/ $\text{C}_6\text{H}_8\text{O}_6$	10-15	15

^a Greater than $\pm 5\%$ signal alteration is classified as interfering condition

4) Method validation

The possibility of applying the develop method for beverage samples analysis were studied. Eleven samples including beers (Chang, Hienegen and Singha) and wines (French white wine, Mamaow wine, Mulberry, Berry estates bin 777, Sicilian, Berry estates bin 222, Marsol and South Africa) were investigated using our developed method. The results were compared with those obtained from iodometric method as summarized in Table 4.2.

Table 4.2 Sulfite contents analyzed from the developed method (FI-sulfite sensor) and standard method (iodometric method). Each analysis sample was carried out in triplicate injections.

Samples	FI-sulfite biosensor (mg L ⁻¹)	Iodometric method (mg L ⁻¹)
<i>Beers</i>		
Chang	7.45±0.19	7.56±0.69
Hienegen	7.49±0.56	7.00±0.40
Singha	8.19±0.07	8.68±1.05
<i>Wines</i>		
French white wine	5.71 ± 0.003	4.76±1.43
Mamaow wine	6.49±0.05	6.72±0.69
Mulbery	5.65±0.005	3.92±0.79
Berri eatates bin 777	9.01±1.09	8.96±0.79
Sicilian	6.73±0.06	6.16±1.05
Berri eatates bin 222	8.52±0.22	8.12±1.43
Marsol	6.28±0.05	6.44±1.05
South Africa	6.40±0.02	6.16±1.43

Figure 4.15 displays the values analyzed by the developed method compared with the values from standard method (iodometric method). According to the t-test, sulfite contents determined from the two methods agree significantly well with each other ($t_{\text{observed}}=1.64$, $t_{\text{critical}}=2.23$ at $P=0.05$)

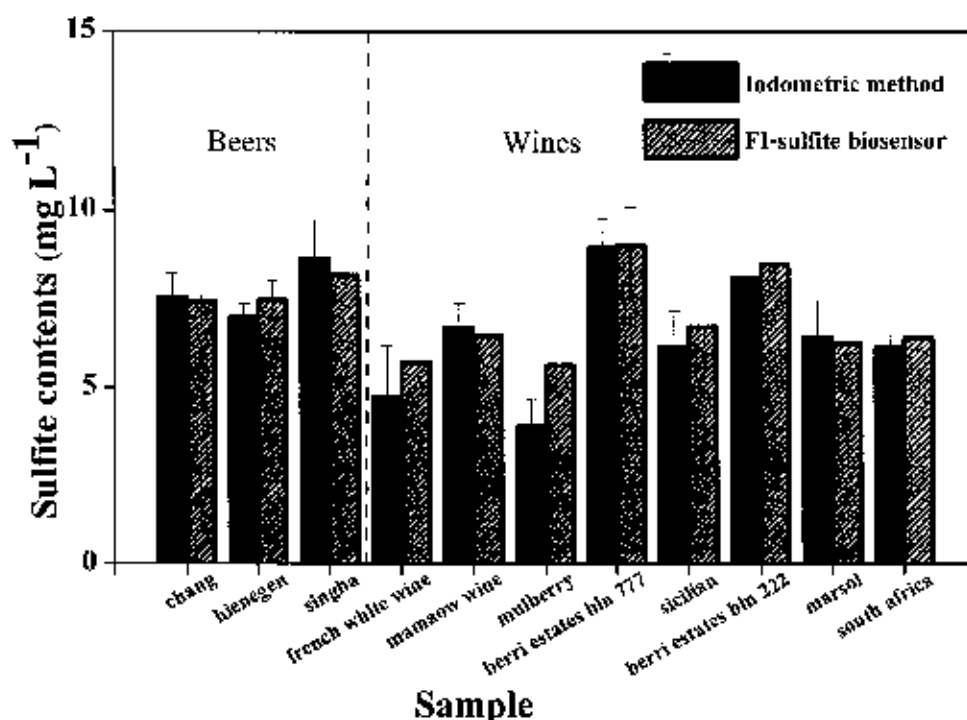


Figure 4.15 Comparison of sulfite content found in wine and beer samples, which were analyzed by the developed method (FI-sulfite biosensor) and iodometric method. Determination by each method was carried out in triplicate runs per sample.

4.2 Part II: Indirect method for detection of sulfite

In this part, indirect method or detection the reduction of hydrogen peroxide were investigated. Flow through electrochemical cell using GC/CNTs-PDDA-AuNPs/SOx as a working electrode, Ag/AgCl as a reference electrode and Pt wire as a counter electrode was applied for the detection.

4.2.1 Cyclic voltammetric study of H₂O₂ reduction

The unique electrochemical behavior of H₂O₂ reduction was studied at GC and sulfite biosensor electrode using cyclic voltammetry (CV). The GC or sulfite biosensor electrode was used as a working electrode, Ag/AgCl as a reference electrode and Pt wire as a auxiliary electrode. Cyclic voltammograms of H₂O₂ was conducted in a 0.1 M phosphate buffer pH 8.0. Figure 4.16 is shown reduction waves of H₂O₂ from bare and modified sulfite biosensor. The

results are shown that the reduction wave was observed at 0 to -1.0 V. These results are correspond with the effective SOx.

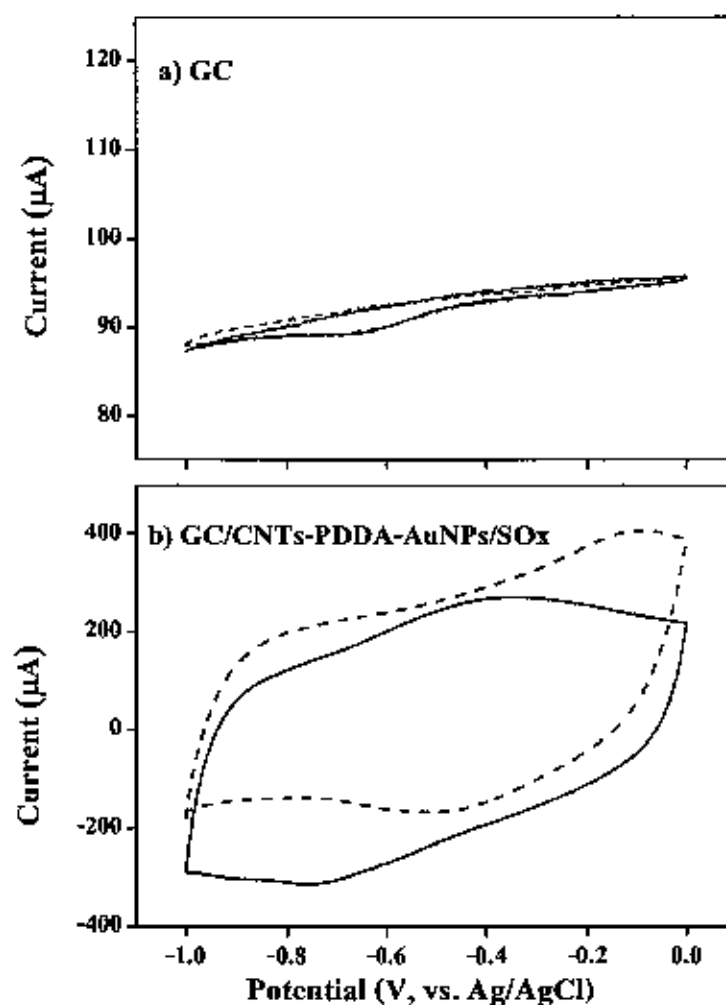


Figure 4.16 Solid lines are the cyclic voltammograms obtained from 4 mM H₂O₂ analysis on a) bare glassy carbon (GC) electrode and b) GC/CNTs-PDDA-AuNPs/SOx. Background voltammograms (0.1 M phosphate buffer pH 8.0) are also shown as dotted for both electrodes. The scan rate was fixed at 50 mV s⁻¹.

4.2.2 Optimum potential for amperometric detection of H_2O_2

Hydrodynamic voltammetric in flow injection system was used to study the influence of applied potential on the amperometric detection of 0.5 mM H_2O_2 at the developed biosensor. The results show in Figure 4.17. The reduction current rises in potential between of 0 up to -0.6 V and decreases rapidly above -0.6 V. This result is shown the potential above -0.6 V indicated that the lost the activity of enzyme SOx. This work, the potential at -0.4 V was selected as the optimum potential for the future experimental. Because this potential have the advantages including i) low noise and background current and thereby enabling detection of low analyte concentration and ii) reduction of the risk of interfering from the sample constituents.

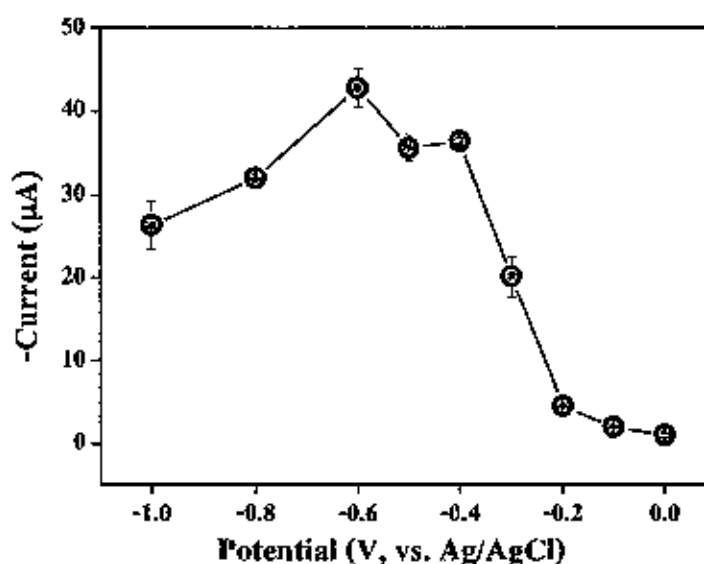


Figure 4.17 Influence of the applied potential on the biosensor response for 0.5 mM H_2O_2 .

4.2.3 Analytical feature

4.3.2.1 Linearity range

Analytical performance of the developed FI-sulfite biosensor (manifold in Figure 3.3a) was examined. Examples of the FI profiles are shown in Figure 4.18. Figure 4.18a displays the signals of sulfite at different concentrations from 500 to 5000 mg L^{-1} with three replicate injections and the corresponded calibration curve is shown in Figure 4.18b. The linear calibration was observed in the range of 500 to 1500 mg L^{-1} . The regression equation is

$y=7.61x-1792.30$ ($r^2 = 0.9697$) where x and y are the peak area ($\mu A \cdot min$) and sulfite concentration ($mg L^{-1}$), respectively.

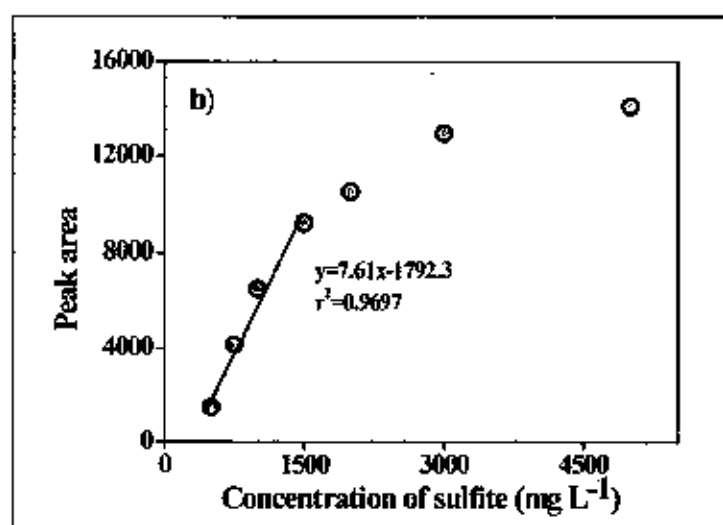
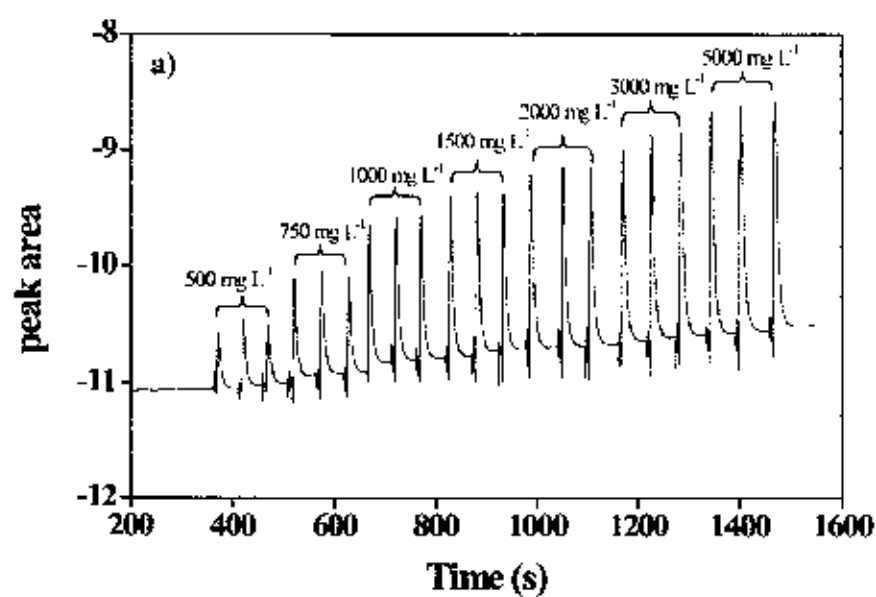


Figure 4.18 FI amperometric responses obtained from the developed sulfite biosensor of a) FIA grams obtained from injection of the various sulfite concentrations ($n=3$) using the amperometric detection on the developed biosensor and b) calibration curve.

4.2.3.2 Limit of detection

In this study, limit of detection of sulfite was investigated by injecting twenty replicate 500 mg L^{-1} sulfite. The result is shown in Figure 4.19. Limit of detection was 44.25 mg L^{-1} , calculated as three times standard deviation of the lowest concentration in calibration curve (500 mg L^{-1}). The FI-amperometric with indirect technique provide good precision (%RSD = 2.93). Sample throughput was $65 \text{ samples h}^{-1}$.

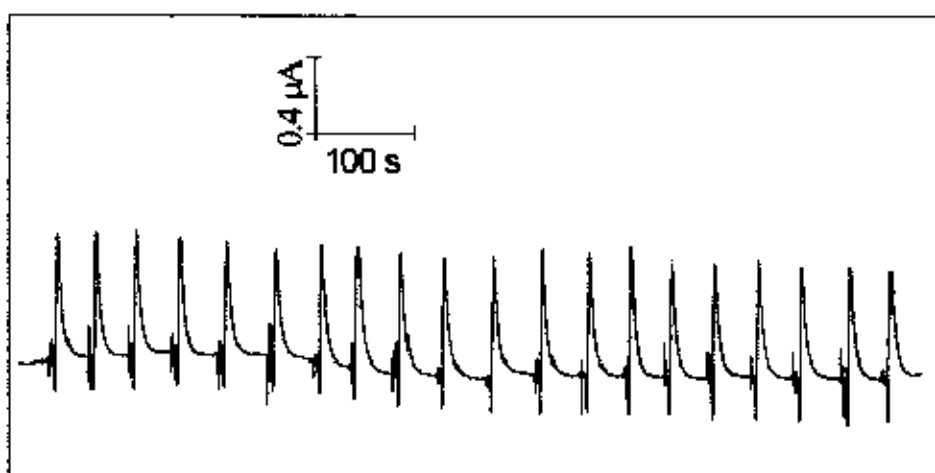


Figure 4.19 FIA grams obtained from the developed sulfite biosensor for 20 times injections of 500 mg L^{-1} sulfite using 0.1 M phosphate buffer pH 8.0, applied potential -0.4 V at flow rate 1.0 mL min^{-1} .

4.3 Characterization of the nanocomposites

4.3.1 UV-Visible spectroscopy

The UV-Visible spectroscopy was used to investigate the absorption spectra of nanocomposites including AuNPs, PDDA and SOx. It can be seen that the PDDA solution (Figure 4.20a) and SOx enzyme solution (Figure 4.20b) did not show an absorption peak, as these molecules do not have chromophores. This result was the similar to the previous work reported by M. Zhang, et al. [69]. According to the previous studies [70], AuNPs show strong absorbance in the visible region which are widely known as a results of surface plasmon absorption (SPR). The absorbance of AuNPs solution (Figure 4.20c) in this work appears at 532 nm . As can be seen, an absorption band of 552 nm was observed when AuNPs were assembled on PDDA (Figure

4.20d). The wavelength shift to the higher than of 20 nm was obtained when compared to that obtained from pure AuNPs. Another absorption band was appended at 660 nm when SOx was adsorbed on PDDA-AuNPs (Figure 4.20e). The reason for this wavelength shifting is related to the color change of AuNPs solution from red to purple when the AuNPs become large or called aggregation [71].

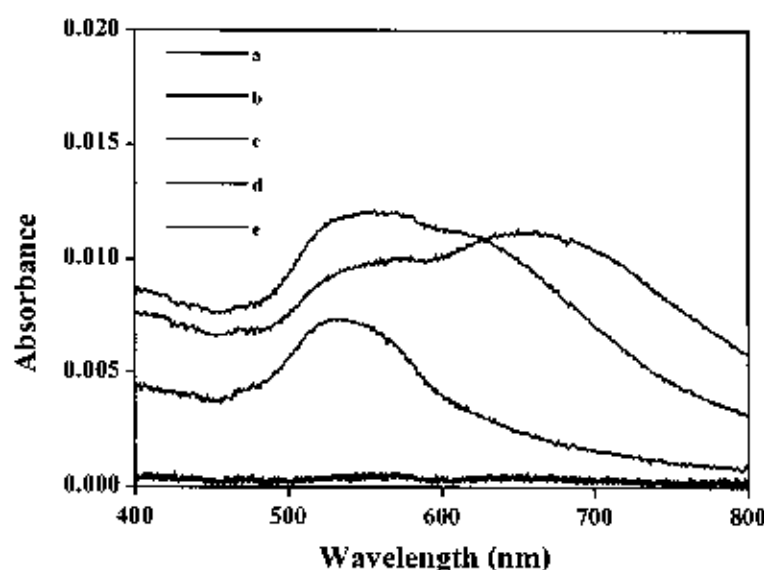


Figure 4.20 UV-Vis spectra of a) PDDA solution, b) SOx enzyme solution, c) AuNPs solution, d) PDDA-AuNPs solution and e) PDDA-AuNPs-SOx solution.

4.3.2 IR spectroscopy

FTIR results display in Figure 4.21. CNTs (Figure 4.21c) is shown a weak two band at 1032 and 1543 cm^{-1} which were originated from the absorption peak of the vibration of C-O stretching and C-C stretching. Absorption peak corresponding to the vibration of C-O stretching (1006 cm^{-1}), C=O stretching (1603 cm^{-1}) and OH stretching (3400 cm^{-1}) over CNT-COOH (Figure 4.21b) indicated that oxygenated groups are produced on the surface of the CNT after treatment with $\text{H}_2\text{SO}_4/\text{HNO}_3$ (3:1). The spectra corresponding to CNTs-PDDA (Figure 4.21a) and CNTs-PDDA-AuNPs (Figure 4.21d) clearly observed OH stretching (3400 cm^{-1}) due to the successful attachment of PDDA and AuNPs to the CNT-COOH, these results was consistent with previous report [72, 73].

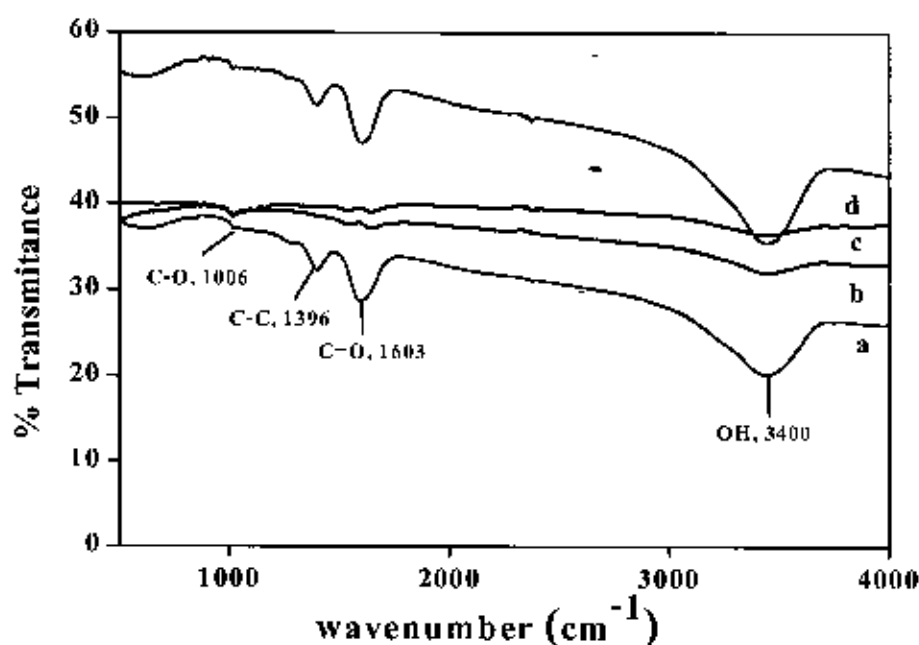


Figure 4.21 FTIR spectra of a) CNTs-PDDA-AuNPs, b) CNT-COOH, c) CNT and d) CNTs-PDDA

4.3.3 Scanning electron microscopy (SEM)

The morphology of nanostructures was initially characterized with SEM. Figure 4.22 is illustrated the SEM image of composite modified electrode. The morphology of CNT-COOH(a) was rough while the CNTs-PDDA(b) was more relatively smooth because PDDA plays a key role in the attachment; it acts as a bridge to connect CNTs. Figure 4.22c is indicated that AuNPs were uniformly spread on the surface of (CNTs-PDDA-AuNPs) composite. CNTs-PDDA-AuNPs-SOx image (Figure 4.22d) shows regular globular structure morphology, indicating the successful immobilization of SOx enzyme to the surface of the CNTs-PDDA-AuNPs [74, 75].

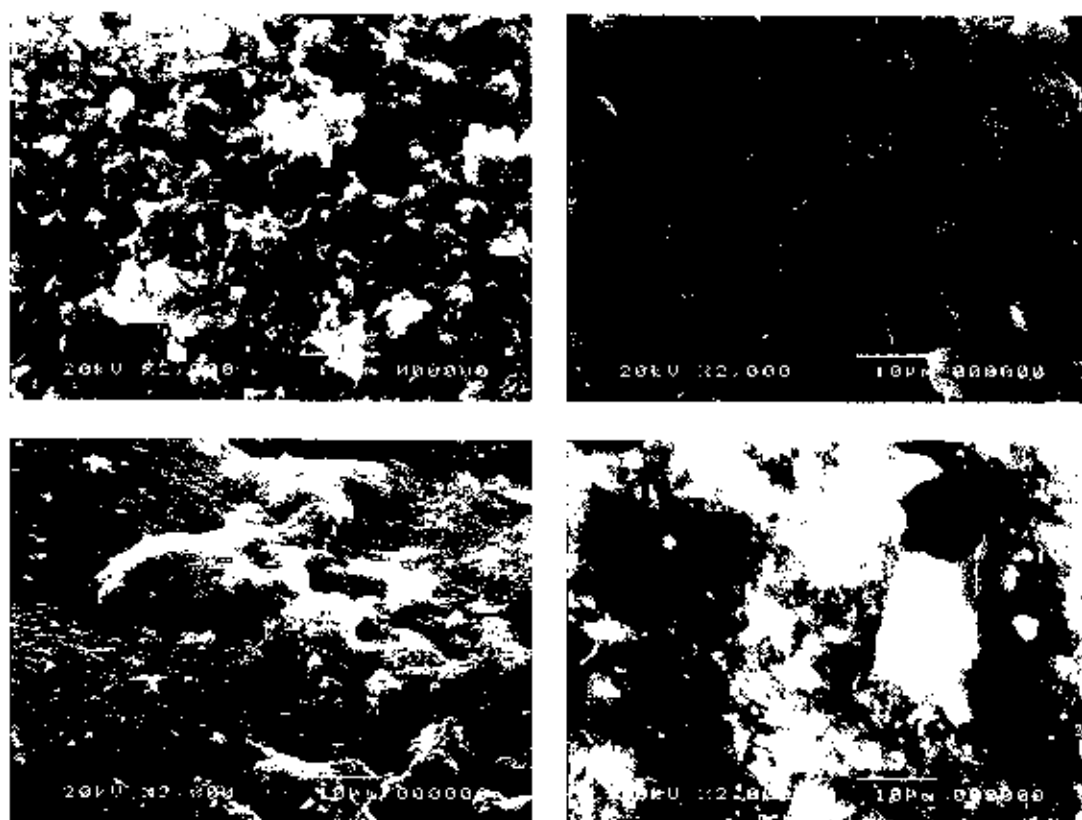


Figure 4.22 SEM images of a) CNT-COOH, b) CNTs-PDDA, c) CNTs-PDDA-AuNPs, d) CNTs-PDDA-AuNPs-SOx

4.3.4 Atomic force microscopy (AFM)

The atomic force microscopy (AFM) is one of the most widely used instruments for morphological study. Figure 4.23 shows the representative AFM images ($5\ \mu\text{m} \times 5\ \mu\text{m}$ scan size) of the composites used in the modified electrode. As shown in Figure 4.23a, the CNT-COOH shows the rough particles. The CNTs-PDDA (Figure 4.23b) shows the presence of spiral shape particle on surface, which is attributed to the presence of PDDA. The CNTs-PDDA-AuNPs (Figure 4.23c) and CNTs-PDDA-AuNPs-SOx (Figure 4.23d) shows the presence of many tiny particle on the surface; some which were rough-like. The results show the electrostatic interaction between positively charged coated on the negatively charged surface of CNTs. These results were ascribed by previous reports [76, 77].

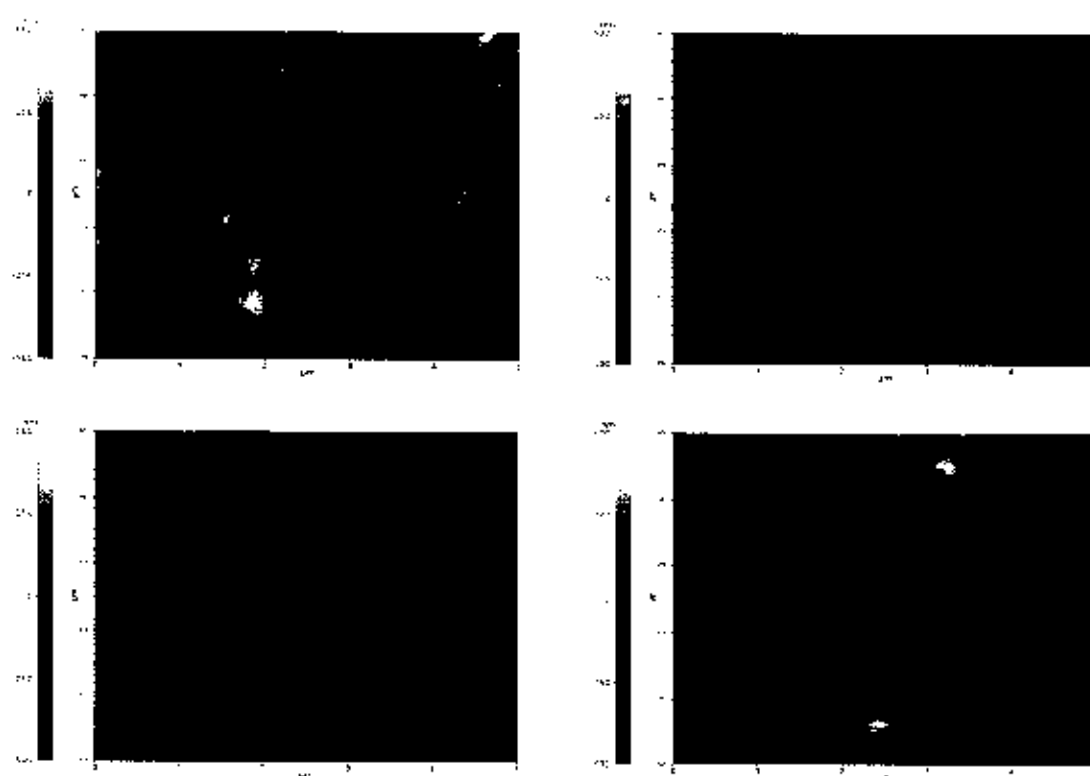


Figure 4.23 AFM images of a) CNT-COOH, b) CNTs-PDDA, c) CNTs-PDDA-AuNPs, d) CNTs-PDDA-AuNPs-SOx

CHAPTER 5

CONCLUSIONS

This work presented the development of a sulfite biosensor for amperometric determination of sulfite using a simple flow injection system. The biosensor was developed based on the hybrid materials, composed of carboxylic functionalized carbon nanotubes, poly(diallyldimethylammoniumchloride) and gold nanoparticle (CNTs-PDDA-AuNPs) coated on a glassy carbon (GC) electrode, which constructed an effective immobilization matrix and made the immobilized components hold high stability and bioactivity. CNTs were initially oxidized by acid treatment (H_2SO_4 : HNO_3 , 3:1) to introduce carboxyl groups on their tips and any defect in the side walls. Then, a cationic electrolyte (PDDA) was absorbed on the surface of the CNTs by electrostatic interaction between carboxyl groups on the CNTs surface and polyelectrolyte chains. In this work, CNTs modified by PDDA were assembled on the activated GC surface, and then AuNPs can be electrostatic absorbed to the CNTs surface. Sulfite oxidase (SOx) was immobilized to CNTs-PDDA-AuNPs and cytochrome C (Cyt C) composites film by using glutaraldehyde (Glu). This developed biosensor (GC/CNTs-PDDA-AuNPs/SOx) was applied in flow injection analysis (FIA). Performances for determination of sulfite using two approaches including direct method or detection the oxidation of sulfite and indirect method or detection the reduction of hydrogen peroxide were investigated. Flow through electrochemical cell using GC/CNTs-PDDA-AuNPs/SOx as a working electrode, Ag/AgCl as a reference electrode and Pt wire as a counter electrode was applied for the detection. Moreover, the nanocomposites for the modified electrode were morphology characterised using UV-Visible spectroscopy, FT-IR spectroscopy, scanning electron microscopy (SEM) and atomic force microscopy (AFM).

Direct method for the oxidation of sulfite biosensor was studied at the developed biosensor (GC/CNTs-PDDA-AuNPs/SOx) using cyclic voltammetry (CV) and amperometry. The oxidation wave of 4 mM sulfite was observed at 0.3 V using the scan rate at 50 mV s^{-1} . Results indicated that the optimum condition for modifying electrode were casting with 40 μL of 4 mg mL^{-1} of, CNTs-PDDA followed by 40 μL of 0.02% of AuNPs. Finally, 15 μL of the mixture

4 mg mL⁻¹ Cyt C:SOx 0.1 U mL⁻¹ with ratio of 2:1. Optimum pH using cyclic voltammetry was 8.0. The estimated apparent Michaelis–Menten constant (K_m^{app}) was 0.49 mM. The developed biosensor was applied in the flow injection system for amperometric detection of sulfite using solution of 0.1 M phosphate buffer (pH 8.0) as a carrier and applying a potential of 0.3 V. The proposed sulfite biosensor exhibits linear calibration over the range of 2–200 mg L⁻¹ of sulfite with slope of 204.66 nA mg⁻¹ L and correlation coefficient of 0.9991. The detection limit (3σ) was 1.3 mg L⁻¹. The developed biosensor also provide good precision (RSD=3.8%) for sulfite signal (5 mg L⁻¹, n=20) with a rapid sample throughput (57 samples h⁻¹). Results from the storage stability of GC/CNTs-PDDA-AuNPs/SOx indicated the relative current response of 80% after stored for 30 days. This implied that the developed biosensor has high storage ability. The method was successfully applied to evaluate sulfite content in beer and wine samples.

In the indirect method, reduction of sulfite biosensor was studied at the developed biosensor (GC/CNTs-PDDA-AuNPs/SOx). The optimum potential for amperometric detection was -0.4 V. Flow injection system was applied for amperometric detection of sulfite using solution of 0.1 M phosphate buffer (pH 8.0) as a carrier and applying a potential of -0.4 V. The linear calibration over the range of 500–1500 mg L⁻¹ was obtained. The regression equation is given by $y = -7.61x - 1792.30$ ($r^2 = 0.9697$), when y and x are the area of peak current (nA) and sulfite concentration (mg L⁻¹). The detection limit (3σ) was 44.25 mg L⁻¹, %RSD=2.93. Sample throughput was 65 samples h⁻¹. Our results indicated that direct method offers higher sensitivity and wider dynamic range than indirect method.

Characterization of the nanocomposites for the modified electrode was studied using UV-Visible spectroscopy, FT-IR spectroscopy, SEM and AFM. The results from UV-Visible spectroscopy, indicated that the absorbance of AuNPs solution was appeared at 532 nm. The PDDA-AuNPs and PDDA-AuNPs-SOx solution was appeared the shift of wavelength because it was related to aggregation. The synthesized CNTs-PDDA is characterized by IR spectroscopy. The results display the vibration of C-O stretching (1006 cm⁻¹), C=O stretching (1603 cm⁻¹) and OH stretching (3400 cm⁻¹). This IR spectrums is demonstrated that PDDA was successfully absorbed on the surface of the CNT-COOH. In addition, stepwise fabrication process of the prepared biosensor (CNTs-PDDA-AuNPs-SOx) was characterized by SEM and AFM. The SEM

image of CNT-COOH is appeared rough, the CNTs-PDDA displays smooth. This results are shown as a the bridge to connect CNTs. The CNTs-PDDA-AuNPs image was shown uniformly and the CNTs-PDDA-AuNPs-SOx image shows a regular globular structure. The AFM image of CNT-COOH shows the rough particles. The CNTs-PDDA displays the Spiral-like shape particle on surface. The CNTs-PDDA-AuNPs and CNTs-PDDA-AuNPs-SOx were show the rough-like. This result indicates the electrostatic interaction between positively charged on the negatively charged surface of CNTs.

REFERENCES

REFERENCES

- [1] Hassan, S. S. M., Hamza, M. S. A. and Mohamed, A. H. K. "A novel spectrophotometric method for batch and flow injection determination of sulfite in beverages", Analytica Chimica Acta. 570: 232-239, 2006.
- [2] Oliveira, S. M. and et al. "Development of a Gas Diffusion Multicommuted Flow Injection System for the Determination of Sulfur Dioxide in Wines, Comparing Malachite Green and Pararosaniline Chemistries", Journal of Agricultural and Food Chemistry. 57: 3415-3422, 2009.
- [3] Satienperakul, S., Phongdong, P. and Liawruangrath, S. "Pervaporation flow injection analysis for the determination of sulphite in food samples utilising potassium permanganate–rhodamine B chemiluminescence detection", Food Chemistry. 121: 893-898, 2010.
- [4] Theisen, S. and et al. "A fast and sensitive HPLC method for sulfite analysis in food based on a plant sulfite oxidase biosensor", Biosensors and Bioelectronics. 26: 175-181, 2010.
- [5] Yilmaz, Ü. T. and Somer, G. "Determination of trace sulfite by direct and indirect methods using differential pulse polarography", Analytica Chimica Acta. 603: 30-35, 2007.
- [6] Rawal, R. and Pundir, C. S. "Development of electrochemical sulfite biosensor based on SOX/PBNPs/PPY modified Au electrode", Biochemical Engineering Journal. 71: 30-37, 2013.
- [7] Feng, C., Tollin, G. And Enemark, J. H. "Sulfite oxidizing enzymes", Biochimica et Biophysica Acta (BBA)-Proteins and Proteomics. 1774: 527-539, 2007.
- [8] Spricigo, R. and et al. "Electrocatalytic sulfite biosensor with human sulfite oxidase co-immobilized with cytochrome c in a polyelectrolyte-containing multilayer", Anal Bioanal Chem. 393: 225-233, 2009.
- [9] Ferapontova, E. E., Ruzgas, T. and Gorton, L. "Direct Electron Transfer of Heme- and Molybdopterin Cofactor-Containing Chicken Liver Sulfite Oxidase on Alkanethiol-Modified Gold Electrodes", Analytical Chemistry. 75: 4841-4850, 2003.
- [10] Gooding, J. J. "Nanostructuring electrodes with carbon nanotubes: A review on electrochemistry and applications for sensing", Electrochimica Acta. 50: 3049-3060, 2005.

REFERENCES (CONTINUED)

- [11] Marcelo, G., Tarazona, M. P. and Saiz, E. "Solution properties of poly(diallyldimethylammonium chloride) (PDDA)", Polymer. 46: 2584-2594, 2005.
- [12] Jiang, S. P. and et al. "Synthesis and characterization of PDDA-stabilized Pt nanoparticles for direct methanol fuel cells", Electrochimica Acta. 51: 5721-5730, 2006.
- [13] Ensafi, A. A., Heydari-Bafrooei, E. and Rezaei, B. "DNA-Based Biosensor for Comparative Study of Catalytic Effect of Transition Metals on Autoxidation of Sulfite", Analytical Chemistry. 85: 991-997, 2012.
- [14] Nashar, R. M. E. "Flow injection catalase activity measurement based on gold nanoparticles/carbon nanotubes modified glassy carbon electrode", Talanta. 96: 161-167, 2012.
- [15] Song, Y. and et al. "A novel bi-protein bio-interphase of cytochrome c and glucose oxidase: Electron transfer and electrocatalysis", Electrochimica Acta. 93: 17-24, 2013.
- [16] Hu, J. and et al. "One-step synthesis of graphene-AuNPs by HMTA and the electrocatalytic application for O₂ and H₂O₂", Talanta. 93: 345-349, 2012.
- [17] Adhikari, B. and Majumdar, S. "Polymers in sensor applications", Progress in Polymer Science. 29: 699-766, 2004.
- [18] Koyun, A., Ahlatcioglu, E., and Ipek, Y. K., "biosensors and their principles", A Roadmap of Biomedical Engineers and Milesstones. 115-130.
- [19] Ng, K.-W. and Lam, W.-H.; Pichiah, S. "A review on potential applications of carbon nanotubes in marine current turbines", Renewable and Sustainable Energy Reviews. 28: 331-339, 2013.
- [20] Ren, X. and et al. "Carbon nanotubes as adsorbents in environmental pollution management: A review", Chemical Engineering Journal. 170: 395-410, 2011.
- [21] Ma, P.-C. and et al. "Dispersion and functionalization of carbon nanotubes for polymer based nanocomposites: A review", Composites Part A: Applied Science and Manufacturing. 41: 1345-1367, 2010.
- [22] Gil, R., and et al. "Speciation analysis of thallium using electrothermal AAS following on-line pre-concentration in a microcolumn filled with multiwalled carbon nanotubes", Microchim Acta. 167: 187-193, 2009.

REFERENCES (CONTINUED)

- [23] Yu, Y. and et al. "Direct electron transfer of glucose oxidase and biosensing for glucose based on PDDA-capped gold nanoparticle modified graphene/multi-walled carbon nanotubes electrode", Biosensors and Bioelectronics. 52: 147-152, 2014.
- [24] Wang, Y. and et al. "Dispersion of single-walled carbon nanotubes in poly(diallyldimethylammonium chloride) for preparation of a glucose biosensor", Sensors and Actuators B: Chemical. 130: 809-815, 2008.
- [25] Francis, S. and et al. "Sunlight mediated synthesis of PDDA protected concave gold nanoplates", J Nanopart Res. 15: 1-9, 2013.
- [26] Yang, D.-Q.; Rochette, J.-F. And Sacher, E. "Spectroscopic Evidence for π - π Interaction between Poly(diallyldimethylammonium) Chloride and Multiwalled Carbon Nanotubes", The Journal of Physical Chemistry B. 109: 4481-4484, 2005.
- [27] Zayed, M. F. and Eisa, W. H. "Phoenix dactylifera L. leaf extract phytosynthesized gold nanoparticles; controlled synthesis and catalytic activity", Spectrochimica Acta Part A: Molecular and Biomolecular Spectroscopy. 121: 238-244, 2014.
- [28] Sakai, T. and et al. "Hydrogen-assisted fabrication of spherical gold nanoparticles through sonochemical reduction of tetrachloride gold(III) ions in water", Ultrasonics Sonochemistry. 21: 946-950, 2014.
- [29] Pingarrón, J. M.; Yáñez-Sedeño, P. and González-Cortés, A. "Gold nanoparticle-based electrochemical biosensors", Electrochimica Acta, 53: 5848-5866, 2008.
- [30] Ding, S.-F., Wei, W. and Zhao, G.-C. "Direct electrochemical response of cytochrome c on a room temperature ionic liquid, N-butylpyridinium tetrafluoroborate, modified electrode", Electrochemistry Communications. 9: 2202-2206, 2007.
- [31] Song, Y. and et al. "A Novel Tri-Protein Bio-Interphase Composed of Cytochrome c, Horseradish Peroxidase and Concanavalin A: Electron Transfer and Electrocatalytics", 7:11206-11218, 2012.
- [32] Bilen, S. and Dick, W. "Sulfite oxidase enzyme activity in soil", Biol Fertil Soils. 47: 647-654, 2011.

REFERENCES (CONTINUED)

- [33] Klein, E. L. and et al. "Applications of pulsed EPR spectroscopy to structural studies of sulfite oxidizing enzymes", Coordination Chemistry Reviews. 257: 110-118, 2013.
- [34] Hernandez-Marin, E. and Ziegler, T. "Theoretical Study of the Oxidation Reaction and Electron Spin Resonance Parameters Involving Sulfite Oxidase", Inorganic Chemistry. 48: 1323-1333, 2009.
- [35] <http://www.cdph.ca.gov/pubsforms/Guidelines/Documents/fdb%20Sulfites.pdf>. March, 2013.
- [36] Zhao, M., Hibbert, D. B. and Gooding, J. J. "Determination of sulfite in beer samples using an amperometric fill and flow channel biosensor employing sulfite oxidase", Analytica Chimica Acta. 556: 195-200, 2006.
- [37] Gasana, E. and et al. "A wall-jet disc electrode for simultaneous and continuous on-line measurement of sodium dithionite, sulfite and indigo concentrations by means of multistep chronoamperometry", Analytica Chimica Acta. 486: 73-83, 2003.
- [38] Casella, I. G. and Marchese, R. "Sulfite oxidation at a platinum glassy carbon electrode. Determination of sulfite by ion exclusion chromatography with amperometric detection", Analytica Chimica Acta. 311: 199-210, 1995.
- [39] Isaac, A. and et al. "Electroanalytical methods for the determination of sulfite in food and beverages", TrAC Trends in Analytical Chemistry. 25: 589-598, 2006.
- [40] MacLeod, R.M. and et al. "Enzymatic Assay of SULFITE OXIDASE (EC 1.8.3.1)", Journal of Biological Chemistry. 236: 1841-1843, 1961.
- [41] Abass, A. K., Hart, J. P. and Cowell, D. "Development of an amperometric sulfite biosensor based on sulfite oxidase with cytochrome c, as electron acceptor, and a screen-printed transducer", Sensors and Actuators B: Chemical. 62: 148-153, 2000.
- [42] Wang, J. Analytical Electrochemistry. New York: Wiley-VCH. 1994.
- [43] Compton, R. G., Ward, K. R. and Laborda, E. "Understanding Voltammetry Simulation of Electrode Processes", Imperial College Press. 25-27, 2007.
- [44] Grieshaber, D. and et al. "Electrochemical Biosensors-Sensor Principles and Architectures", Sensors, 8: 1400-1458, 2008.

REFERENCES (CONTINUED)

- [45] Henze, F. G. T. a. G. Introduction to voltammetric Analysis Theory and Paractice. Australia, Csiro. 2001.
- [46] Hart, J. P., Abass, A. K. and Cowell, D. "Development of disposable amperometric sulfur dioxide biosensors based on screen printed electrodes", Biosensors and Bioelectronics. 17: 389-394, 2002.
- [47] Adcloju, S. B., Ohanessian, A. and Duc, N. N. "Electrosynthesis and Characterization of Composite Polypyrrole-Dextran-Sulfite Oxidase Films", Synthetic Metals. 153: 17-20, 2005.
- [48] Dinçkaya, E. and et al. "Sulfite determination using sulfite oxidase biosensor based glassy carbon electrode coated with thin mercury film", Food Chemistry. 101: 1540-1544, 2007.
- [49] Qiu, J.-D. and et al. "Synthesis, Characterization, and Immobilization of Prussian Blue-Modified Au Nanoparticles: □ Application to Electrocatalytic Reduction of H_2O_2 ", Langmuir. 23: 2133-2137, 2007.
- [50] Cui, R. and et al. "Horseradish peroxidase-functionalized gold nanoparticle label for amplified immunoanalysis based on gold nanoparticles/carbon nanotubes hybrids modified biosensor", Biosensors and Bioelectronics. 23: 1666-1673, 2008.
- [51] Bahmani, B. and et al. "Development of an electrochemical sulfite biosensor by immobilization of sulfite oxidase on conducting polyaniline film", Synthetic Metals. 160: 2653-2657, 2010.
- [52] Rawal, R. and et al. "Development of an amperometric sulfite biosensor based on a gold nanoparticles/chitosan/ multiwalled carbon nanotubes/polyaniline-modified gold electrode", Anal Bioanal Chem. 401: 2599-2608, 2011.
- [53] Eguílaz, M. and et al. "Gold nanoparticles: Poly(diallyldimethylammonium chloride)- carbon nanotubes composites as platforms for the preparation of electrochemical enzyme biosensors: Application to the determination of cholesterol", Journal of Electroanalytical Chemistry. 661: 171-178, 2011.

REFERENCES (CONTINUED)

- [54] Salimi, A. and et al. "A novel non-enzymatic hydrogen peroxide sensor based on single walled carbon nanotubes-manganese complex modified glassy carbon electrode", Electrochimica Acta. 56: 3387-3394, 2011.
- [55] Ping, J. and et al. "An amperometric sensor based on Prussian blue and poly(o-phenylene-diamine) modified glassy carbon electrode for the determination of hydrogen peroxide in beverages", Food Chemistry. 126: 2005-2009, 2011.
- [56] Moghaddam, H. M. and et al. "Nanostructured Base Electrochemical Sensor for Determination of Sulfite", International Journal of ELECTROCHEMICAL SCIENCE. 9: 327-341, 2014.
- [57] Zhou, Y. and et al. "Enhanced ultrasensitive detection of Cr(III) using 5-thio-2-nitrobenzoic acid (TNBA) and horseradish peroxidase (HRP) dually modified gold nanoparticles (AuNPs)", Sensors and Actuators B: Chemical. 161: 1108-1113, 2012.
- [58] Cui, Z. and et al. "Pd nanoparticles supported on HPMo-PDDA-MWCNT and their activity for formic acid oxidation reaction of fuel cells", International Journal of Hydrogen Energy. 36: 8508-8517, 2011.
- [59] Tsai, Y.-C. and Chiu, C.-C. "Amperometric biosensors based on multiwalled carbon nanotube-Nafion-tyrosinase nanobiocomposites for the determination of phenolic compounds", Sensors and Actuators B: Chemical. 125: 10-16, 2007.
- [60] Wan, L. and et al. "Electron Transfer of Co-immobilized Cytochrome c and Horseradish Peroxide in Chitosan-Graphene Oxide Modified Electrode", International Journal of ELECTROCHEMICAL SCIENCE. 6: 4700-4713, 2011.
- [61] Solanki, P. R. and et al. "Multi-walled carbon nanotubes/sol-gel-derived silica/chitosan nanobiocomposite for total cholesterol sensor", Sensors and Actuators B: Chemical. 137: 727-735, 2009.
- [62] Lan, D., Li, B. and Zhang, Z. "Chemiluminescence flow biosensor for glucose based on gold nanoparticle-enhanced activities of glucose oxidase and horseradish peroxidase", Biosensors and Bioelectronics. 24: 934-938, 2008.

REFERENCES (CONTINUED)

- [63] Kalimuthu, P.; Tkac, J.; Kappler, U.; Davis, J. J.; Bernhardt, P. V., "Highly Sensitive and Stable Electrochemical Sulfite Biosensor Incorporating a Bacterial Sulfite Dehydrogenase", Analytical Chemistry, 82: 7374-7379, 2010.
- [64] Hong, J. and et al. "Direct electron transfer of horseradish peroxidase on Nafion-cysteine modified gold electrode", Electrochimica Acta. 52: 6261-6267, 2007.
- [65] Sartori, E. R., Vicentini, F. C. and Fatibello-Filho, O. "Indirect determination of sulfite using a polyphenol oxidase biosensor based on a glassy carbon electrode modified with multi-walled carbon nanotubes and gold nanoparticles within a poly(allylaminehydrochloride) film", Talanta. 87: 235-242, 2011.
- [66] Alamo, L. S. T., Tangkuaram, T. and Saticnprakul, S. "Determination of sulfite by pervaporation-flow injection with amperometric detection using copper hexacyanoferrate-carbon nanotube modified carbon paste electrode", Talanta. 81: 1793-1799, 2010.
- [67] Rawal, R. and Pundir, C. S. "Development of an amperometric sulfite biosensor based on SO₃/PBNPs/PPY modified ITO electrode", International Journal of Biological Macromolecules. 51: 449-455, 2012.
- [68] Casella, I. G. and Marchese, R. "Sulfite oxidation at a platinum glassy carbon electrode. Determination of sulfite by ion exclusion chromatography with amperometric detection", Analytical Chimica Acta. 311: 199-210, 1995.
- [69] Blakey, I. and et al. "Interactions of Phenylthioesters with Gold Nanoparticles (AuNPs): Implications for AuNP Functionalization and Molecular Barcoding of AuNP Assemblies", Langmuir. 26: 692-701, 2009.
- [70] Zhang, M. and et al. "Glucose biosensor based on titanium dioxide-multiwall carbon nanotubes-chitosan composite and functionalized gold nanoparticles", Bioprocess Biosyst Eng. 34: 1143-1150, 2011.
- [71] He, L. and et al. "Colorimetric Sensing of Tetracyclines in Milk Based on the Assembly of Cationic Conjugated Polymer-Aggregated Gold Nanoparticles", Food Anal. Methods. 6: 1704-1711, 2013.

REFERENCES (CONTINUED)

- [72] Gutierrez, F., Rubianes, M. D. and Rivas, G. A. "Dispersion of multi-wall carbon nanotubes in glucose oxidase: Characterization and analytical applications for glucose biosensing", Sensors and Actuators B: Chemical. 161: 191-197, 2012.
- [73] Mohammadi Meman, N. and et al. "Synthesis, characterization and operation of a functionalized multi-walled CNT supported MnOx nanocatalyst for deep oxidative desulfurization of sour petroleum fractions", Journal of Industrial and Engineering Chemistry:
- [74] Jie, G. and et al. "Enhanced electrochemiluminescence of CdSe quantum dots composited with CNTs and PDDA for sensitive immunoassay", Biosensors and Bioelectronics. 24: 3352-3358, 2009.
- [75] Rawal, R., Chawla, S. and Pundir, C. S. "Polyphenol biosensor based on laccase immobilized onto silver nanoparticles/multiwalled carbon nanotube/ polyaniline gold electrode", Analytical Biochemistry. 419: 196-204, 2011.
- [76] Carson, L. and et al. "Synthesis, characterization and stability of chitosan and poly(methyl methacrylate) grafted carbon nanotubes", Spectrochimica Acta Part A: Molecular and Biomolecular Spectroscopy. 96: 380-386, 2012.
- [77] Ensafi, A. A., Amini, M. and Rezaei, B. "Biosensor based on ds-DNA decorated chitosan modified multiwall carbon nanotubes for voltammetric biodetection of herbicide amitrole", Colloids and Surfaces B: Biointerfaces. 109: 45-51, 2013.

APPENDICES

APPENDIX A

Electrochemical detection of sulfite oxidation on developed sulfite biosensor

Effect of CNTs-PDDA modified amount on the detection of sulfite (raw data for Figure 4.2)

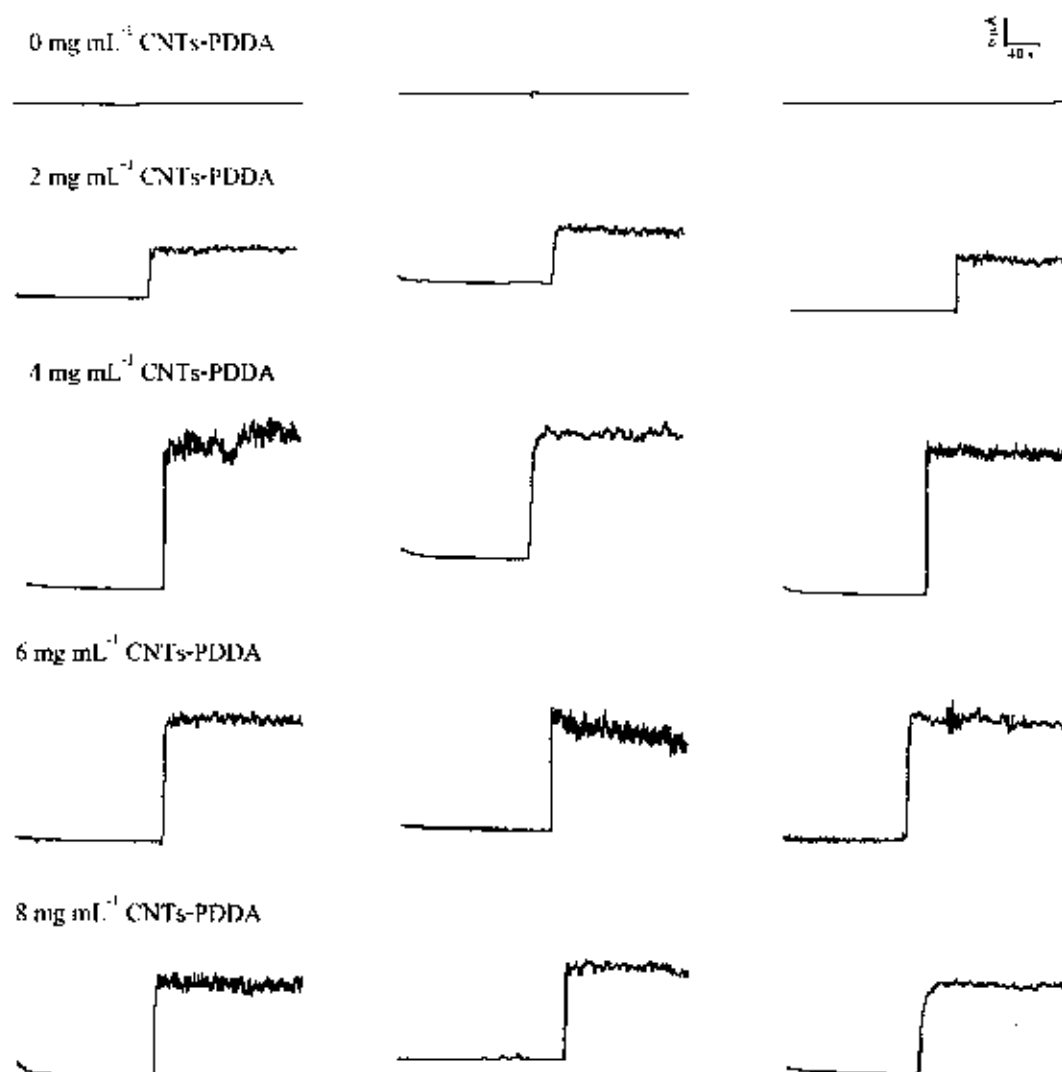
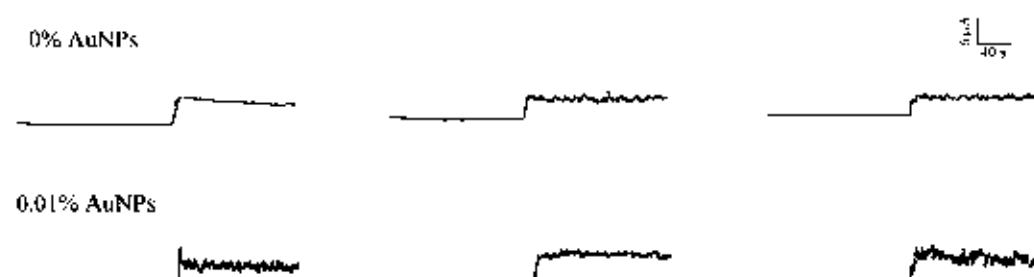


Figure A.1 Amperogram of concentration of CNTs-PDDA (mg mL⁻¹)

Effect of gold nanoparticles (AuNPs) concentration in modified solution (raw data for Figure 4.3)



Effect of gold nanoparticles (AuNPs) concentration in modified solution (raw data for Figure 4.3)

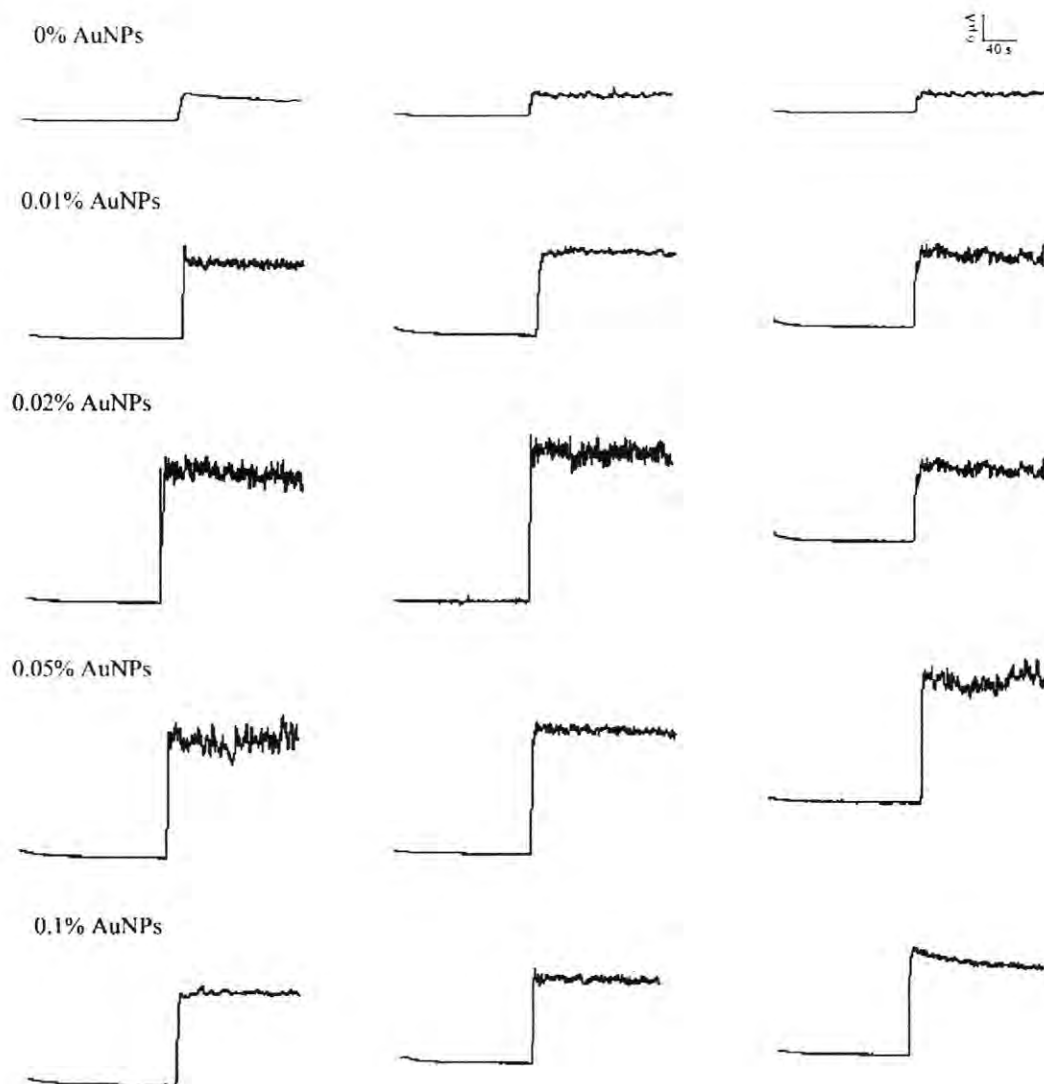


Figure A.2 Amperogram of concentration of AuNPs (%)

Effect of cytochrome c (Cyt C) concentration (raw data for Figure 4.4)

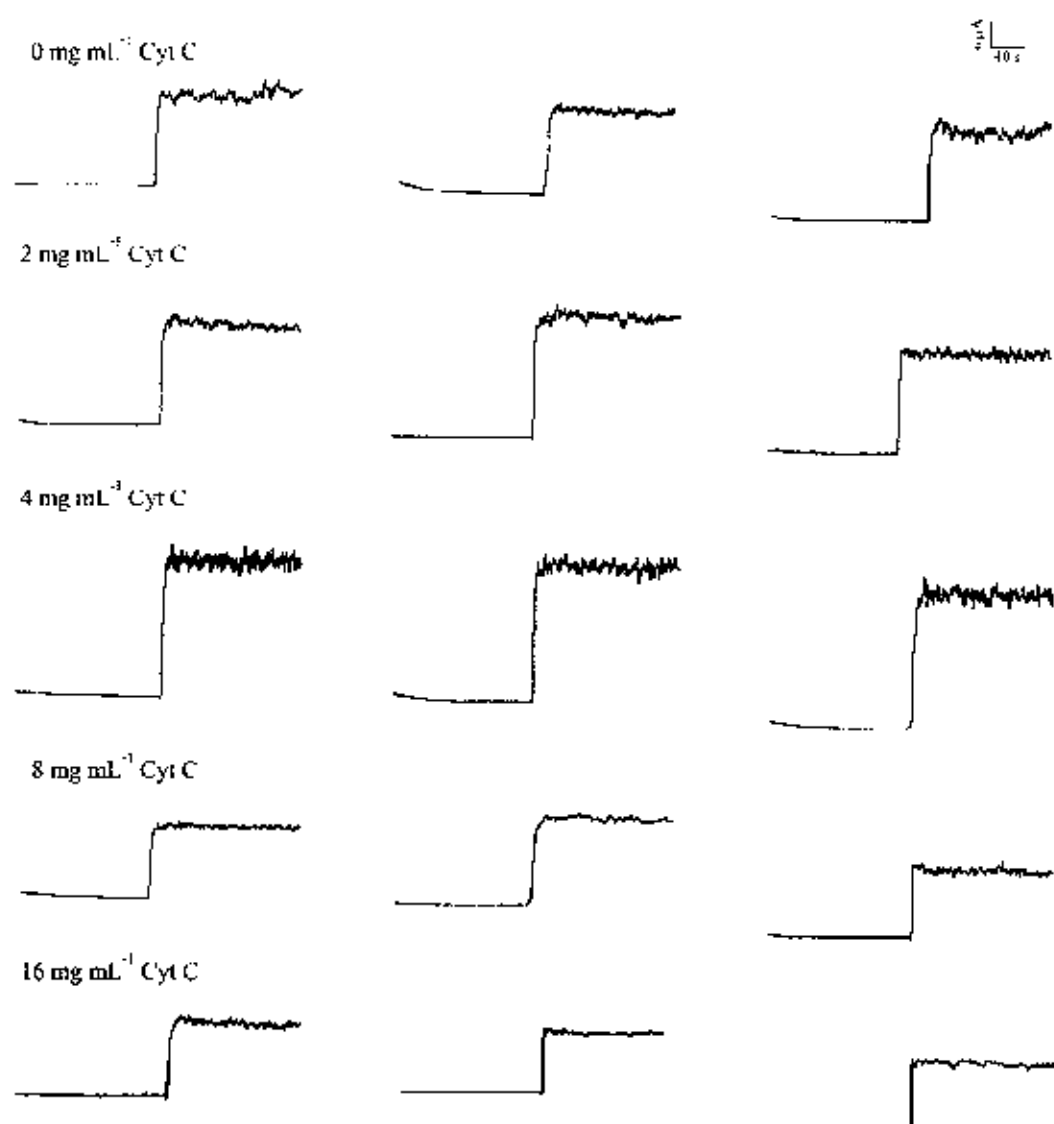


Figure A.3 Amperogram of concentration of Cyt C (mg mL⁻¹)

Effect of sulfite oxidase enzyme (SOx) loading (raw data for Figure 4.5)

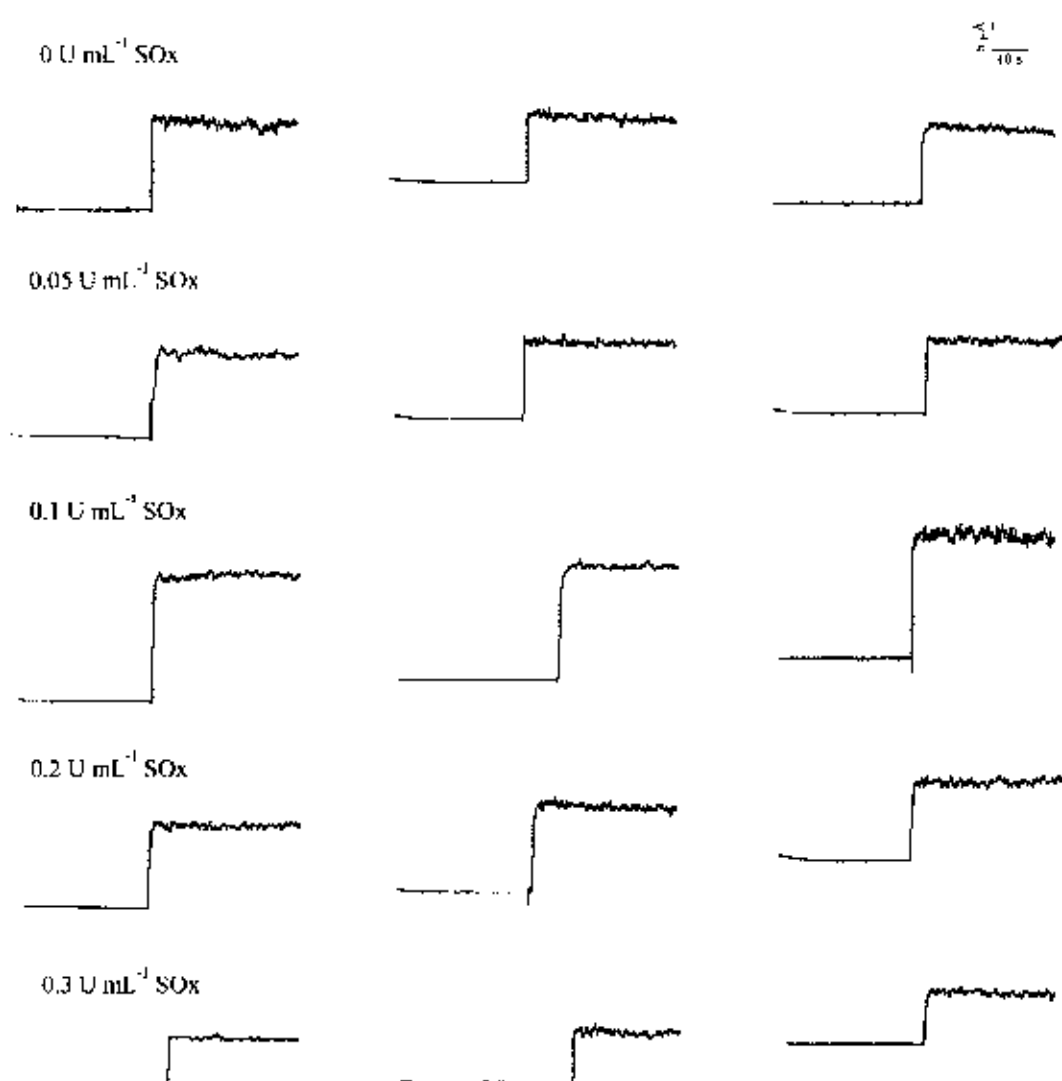


Figure A.4 Amperogram of concentration of SOx (U mL⁻¹)

The apparent Michaelis-Menten constant (K_m^{app}) (raw data for Figure 4.8)

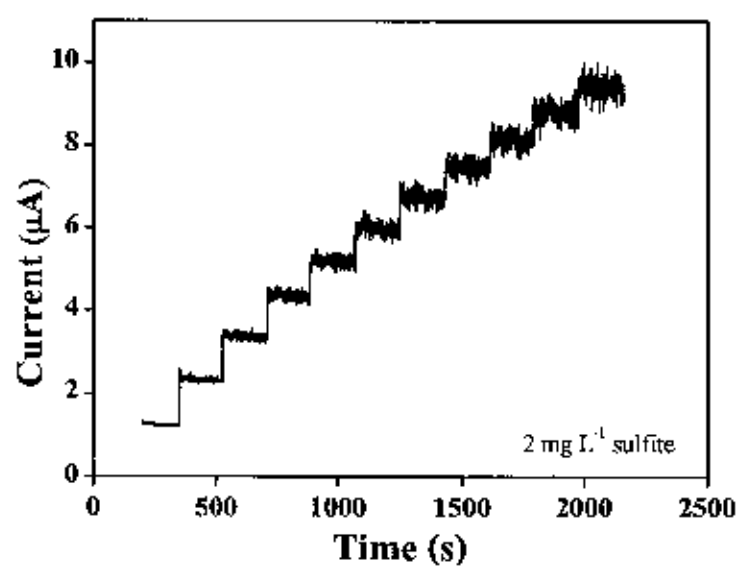
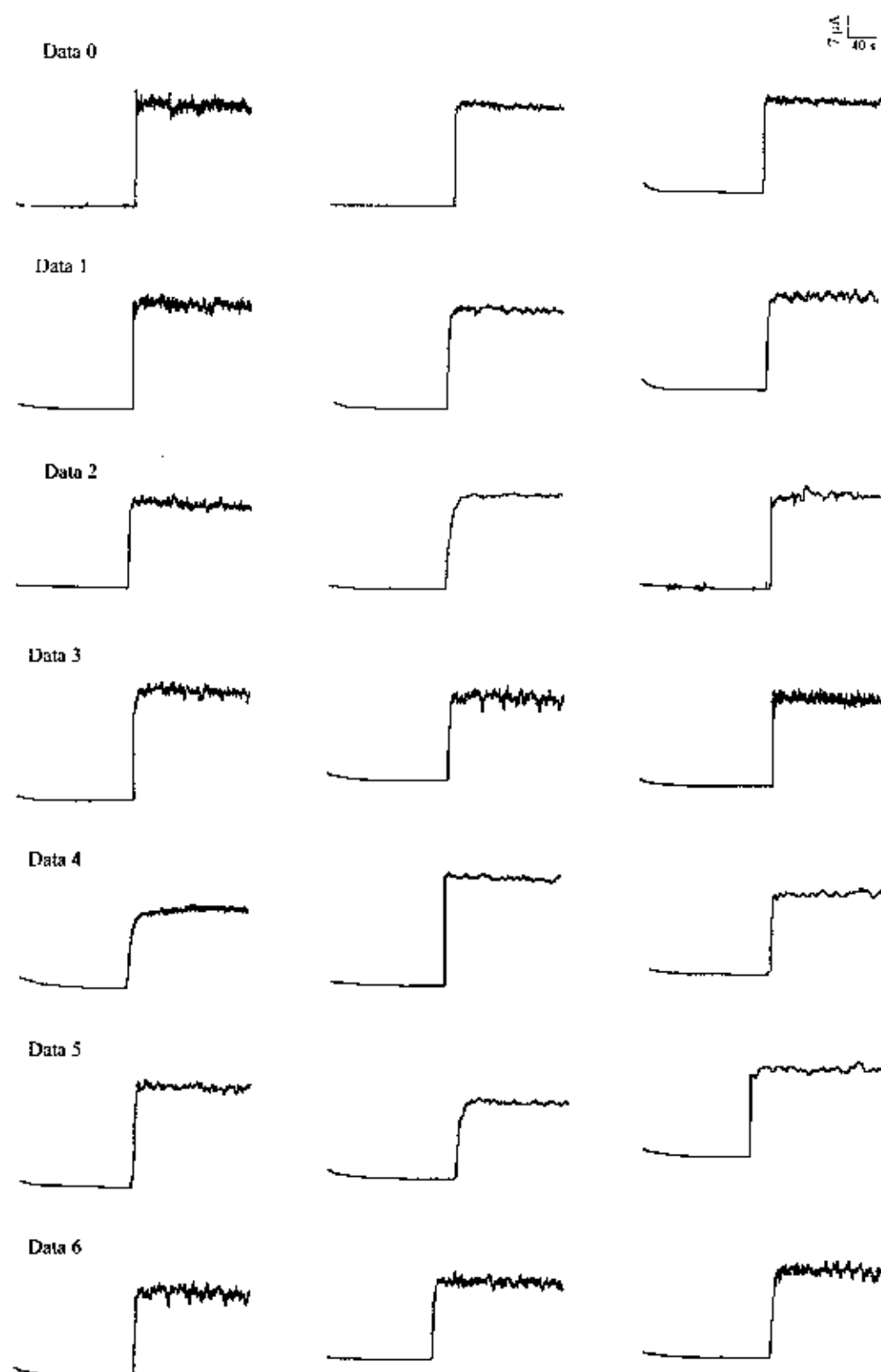
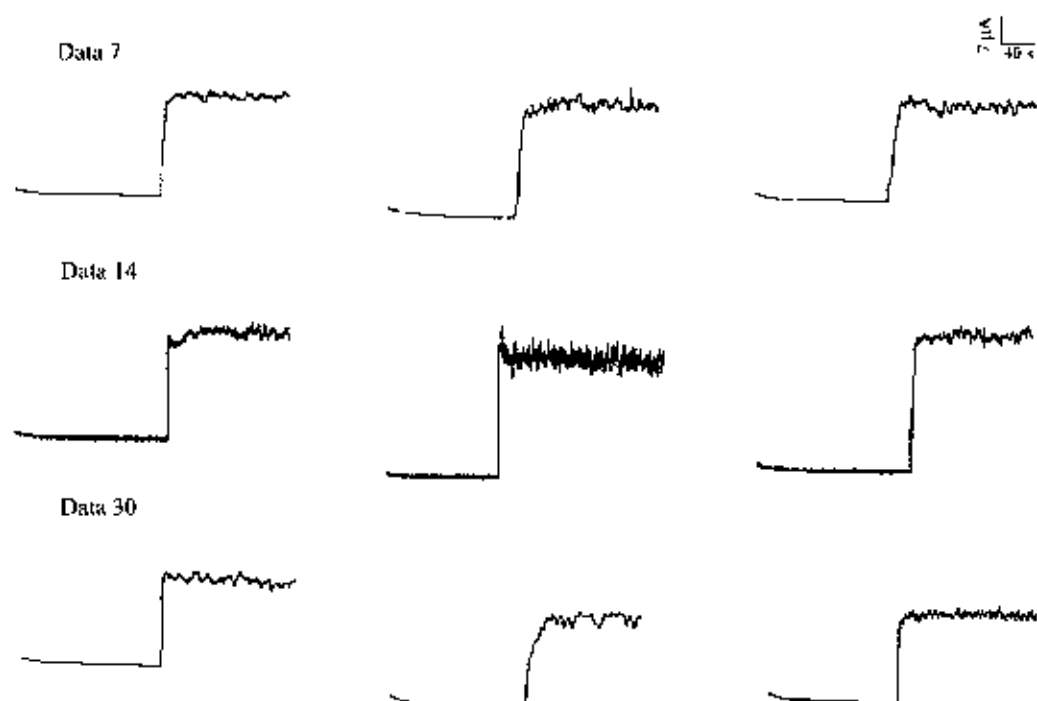


Figure A.5 Amperogram of concentration of sulfite in the rang 2 to 20 mg L⁻¹

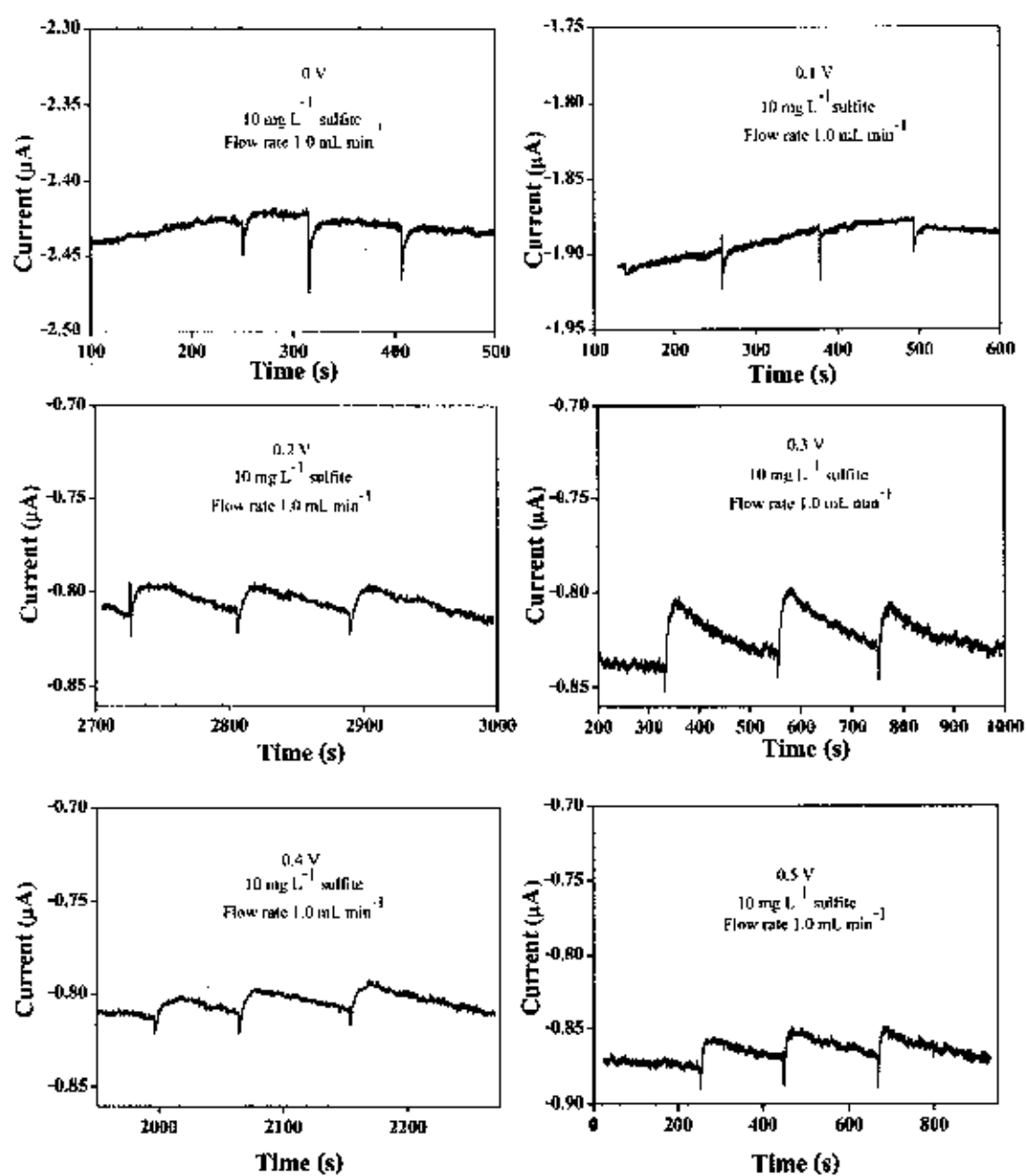
Stability study (raw data for Figure 4.10)



Stability study (raw data for Figure 4.10) (Continued)

**Figure A.6** Amperogram of stability using 0.5 mM sulfite

Optimum potential for amperometric detection (raw data for Figure 4.11)



Optimum potential for amperometric detection (raw data for Figure 4.11) (continued)

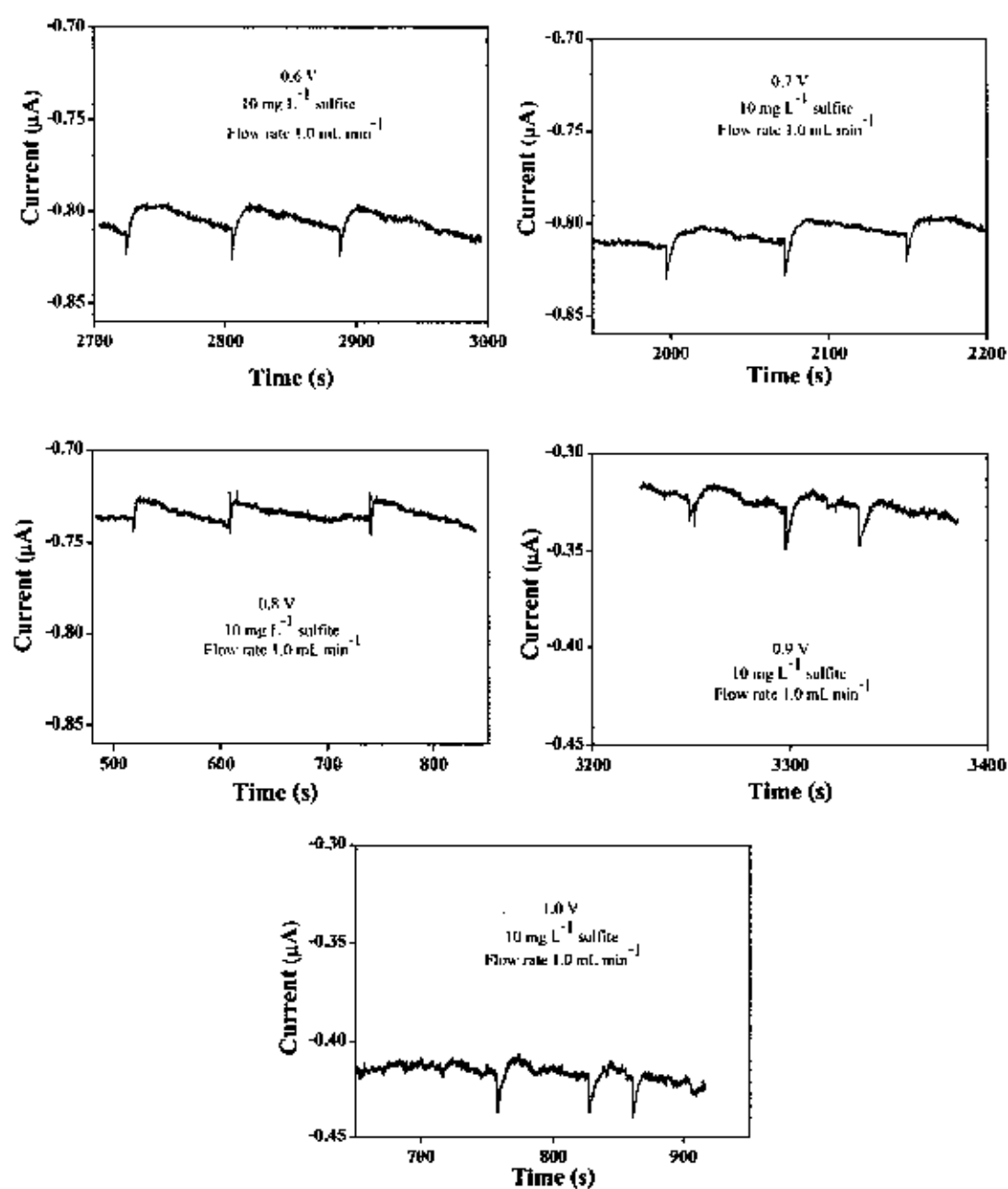


Figure A.7 FIA grams of the applied potential on the sulfite biosensor response 10 mg L^{-1} sulfite

Optimum flow rate (raw data for Figure 4.12)

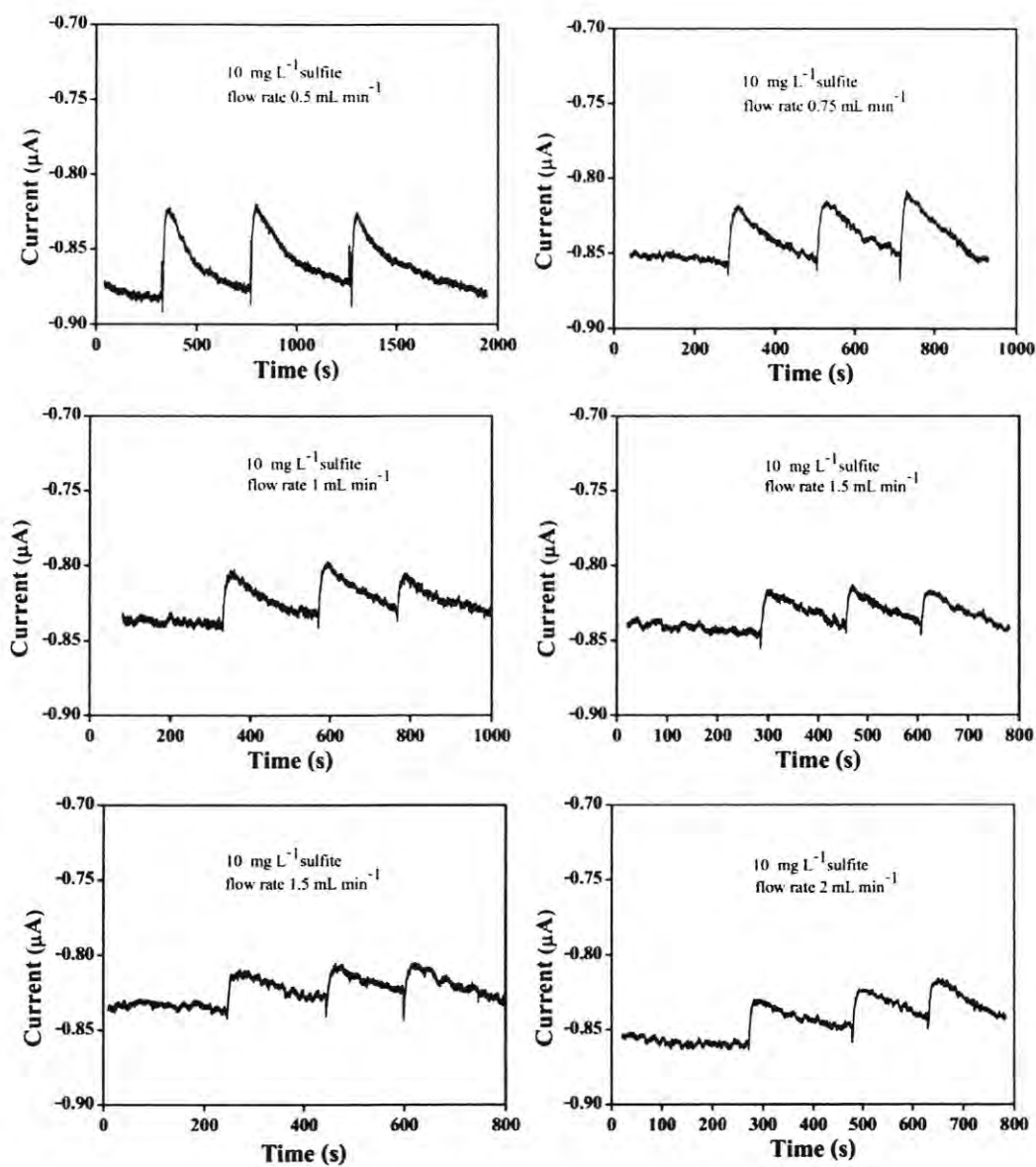
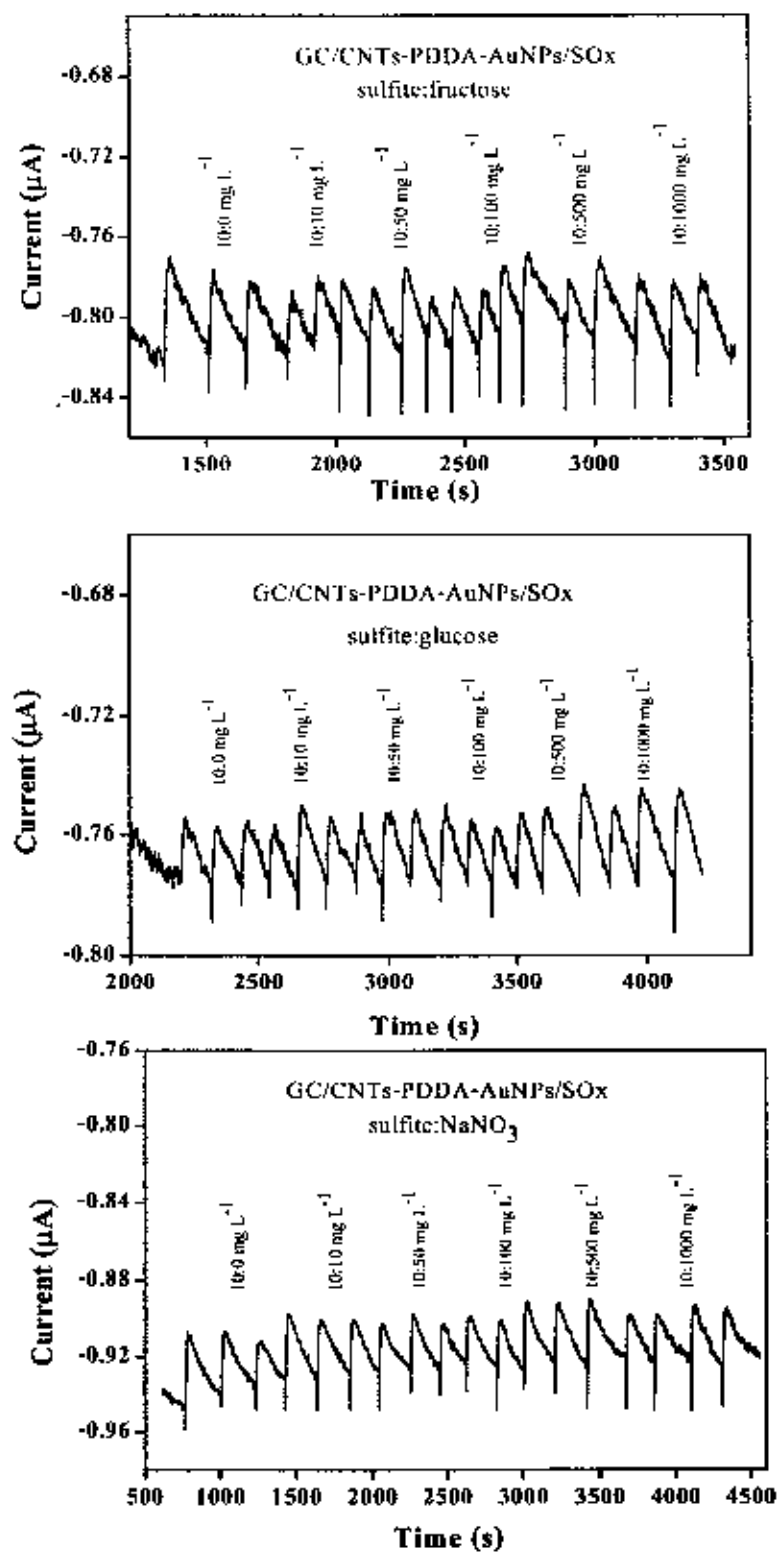
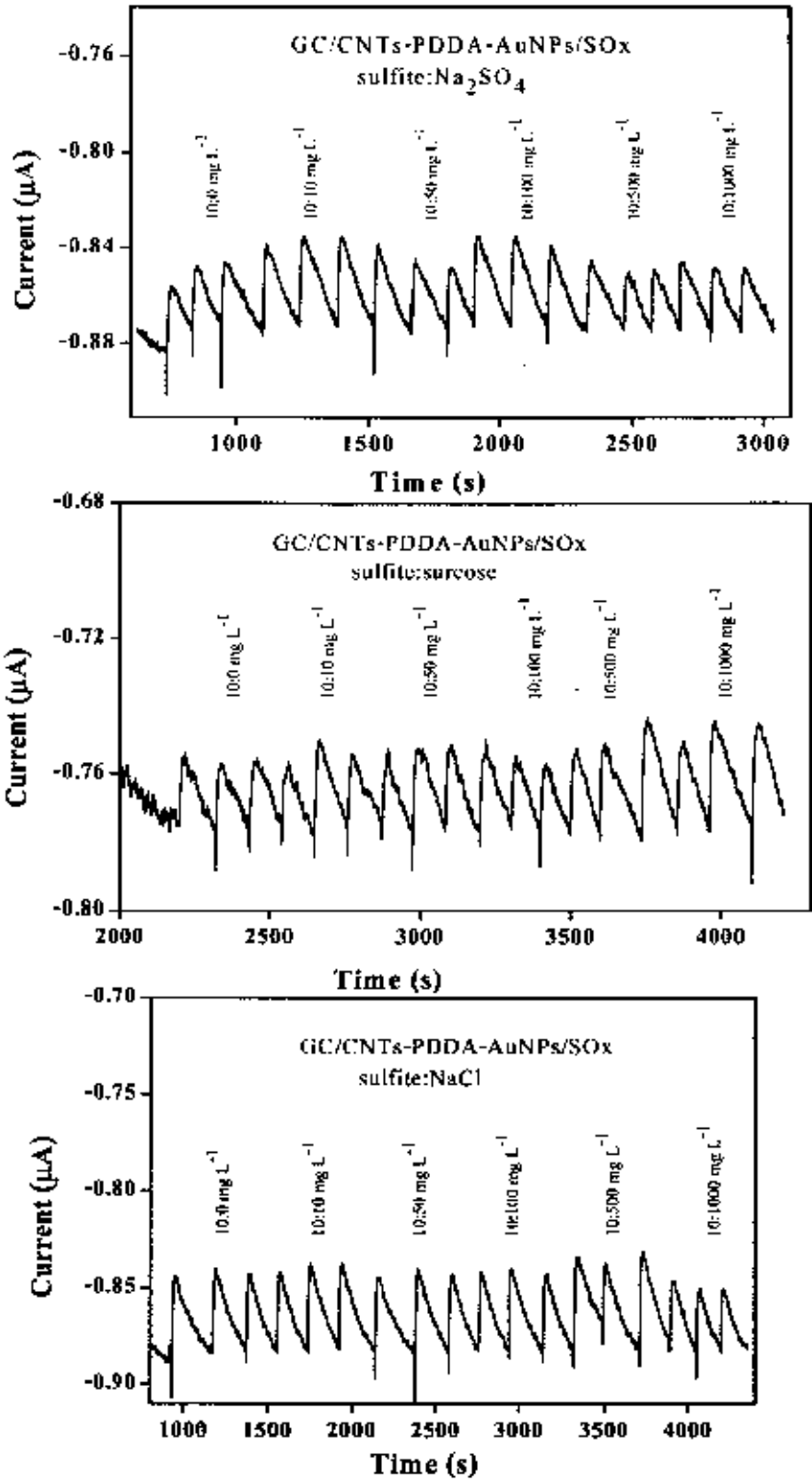


Figure A.8 FIA grams of the flow rate on the sulfite biosensor response 10 mg L^{-1} sulfite

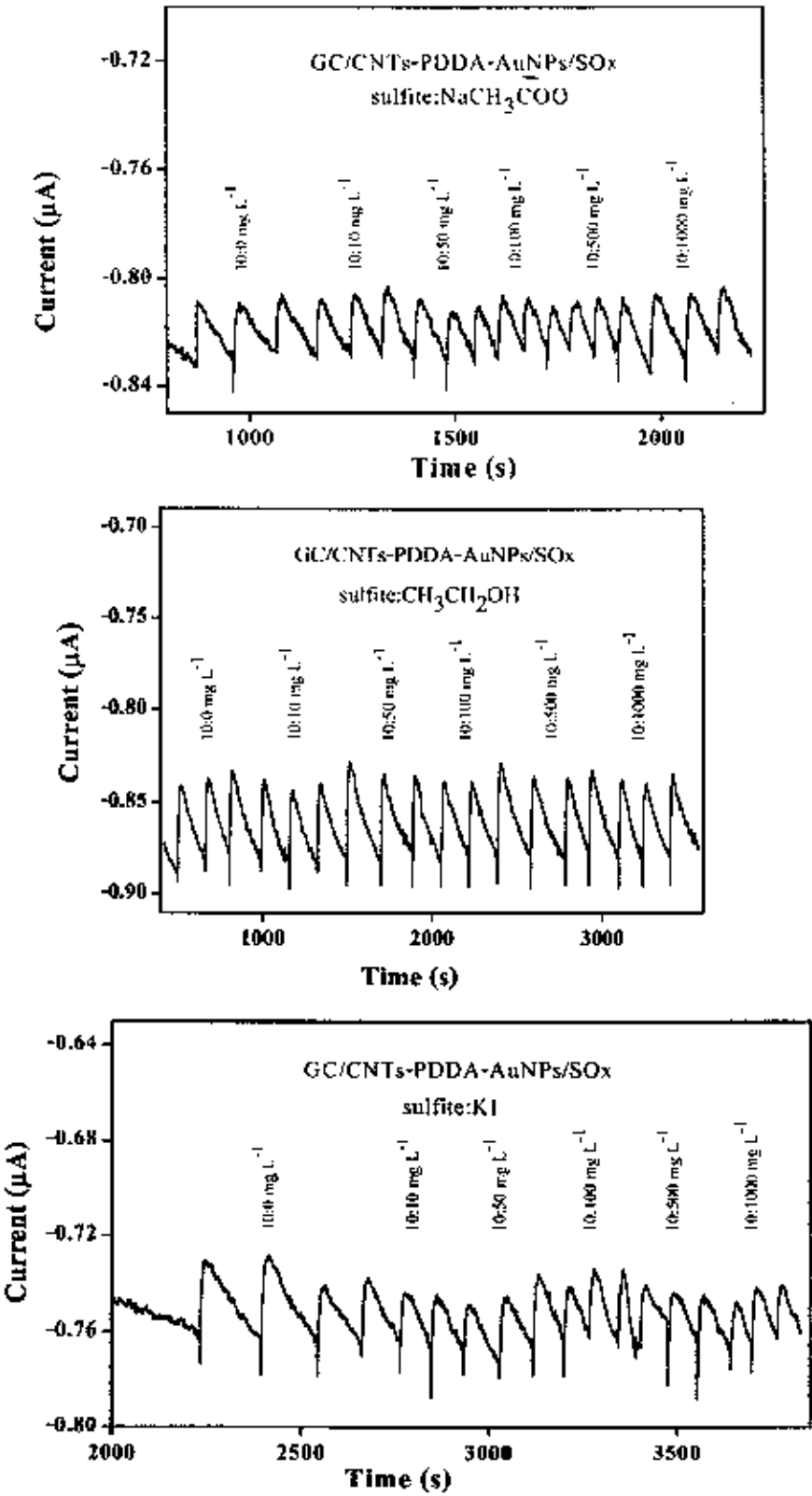
Interference study (raw data for Table 4.1)



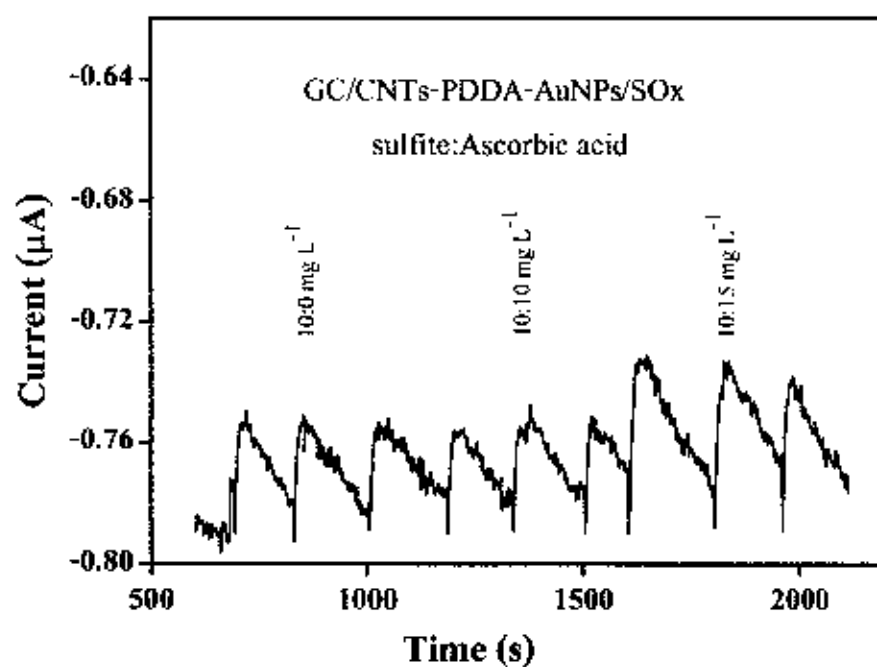
Interference study (raw data for Table 4.1) (Continued)



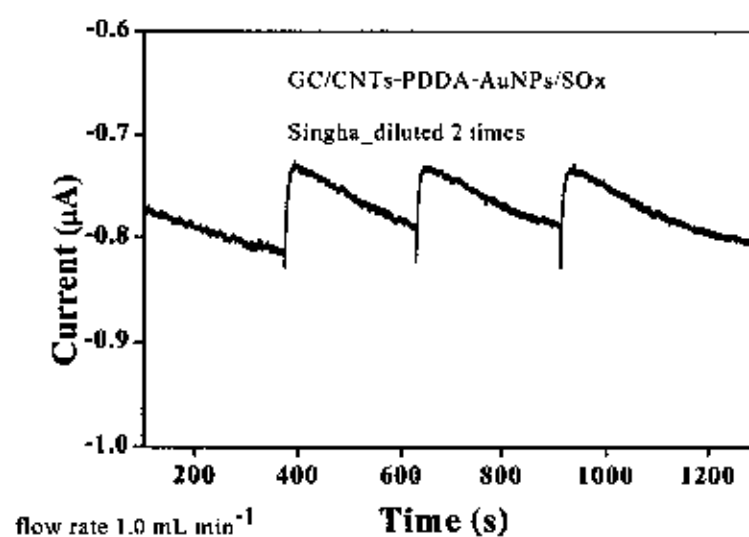
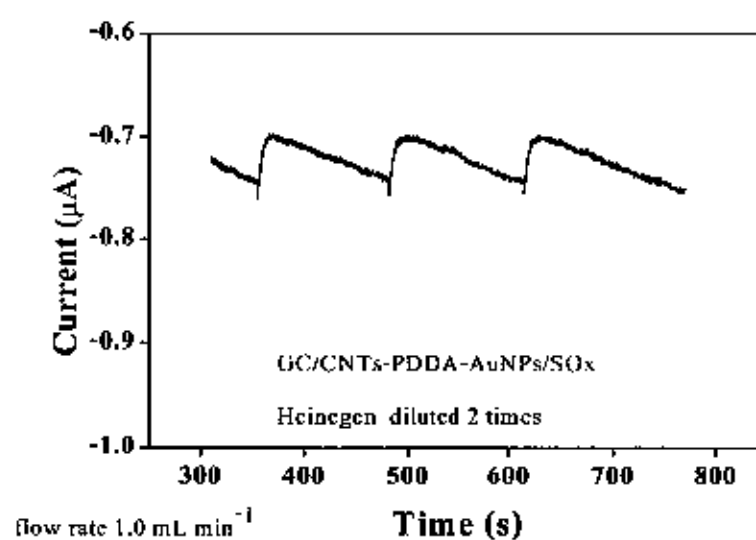
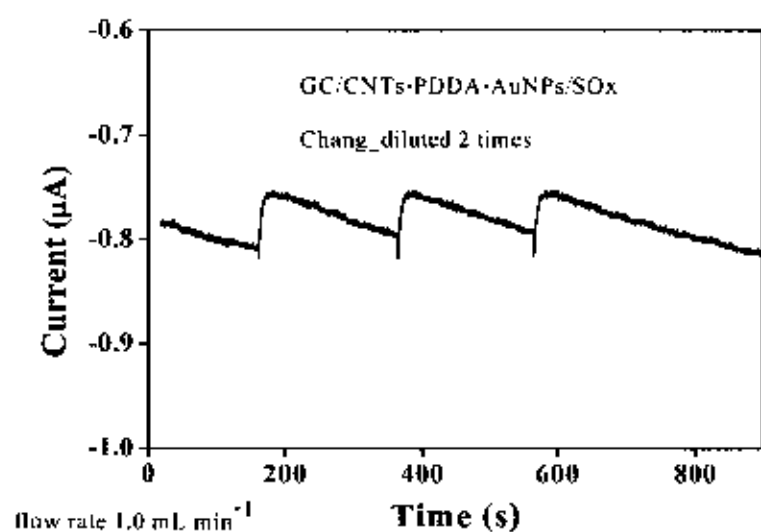
Interference study (raw data for Table 4.1) (Continued)



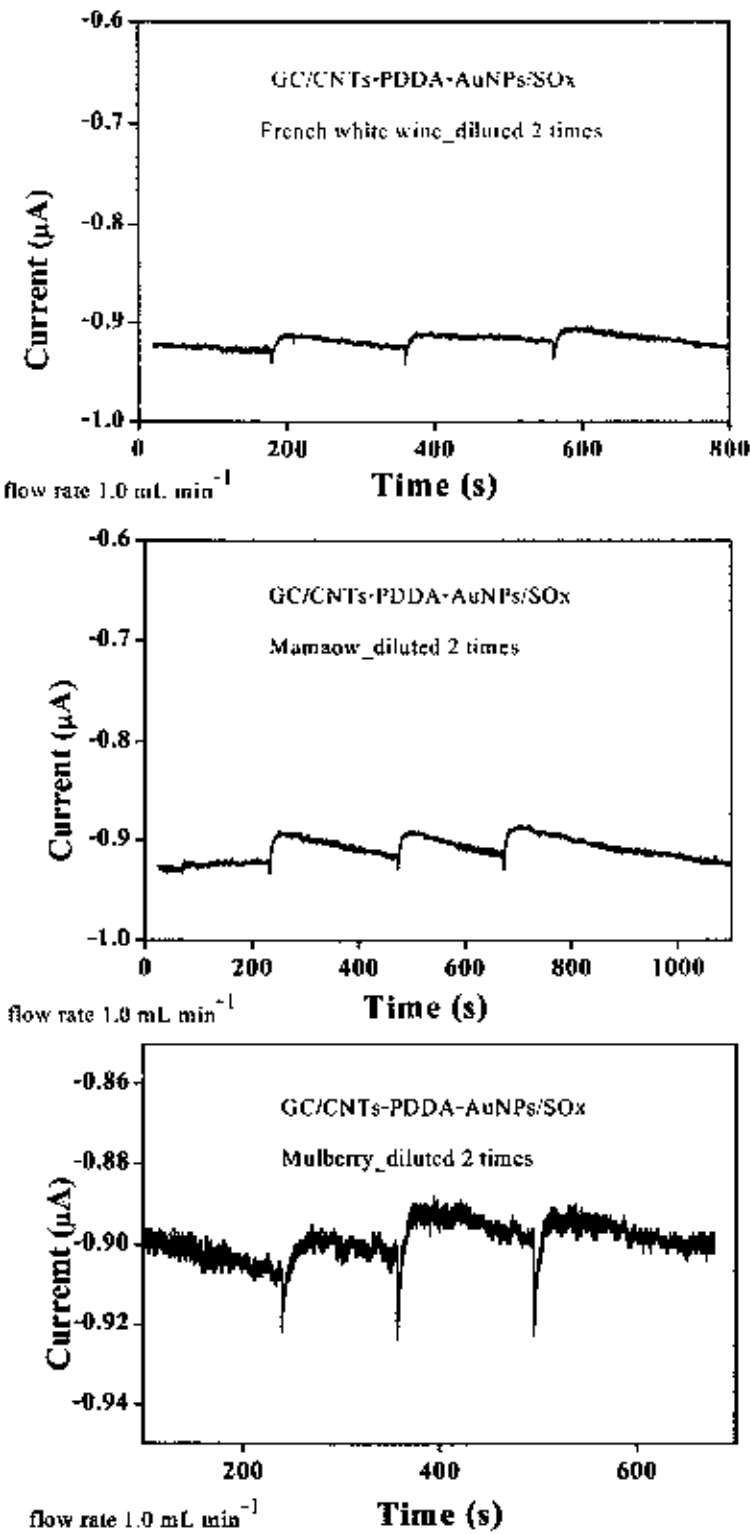
Interference study (raw data for Table 4.1) (Continued)

**Figure A.9** FIA grams of the interference on the sulfite biosensor

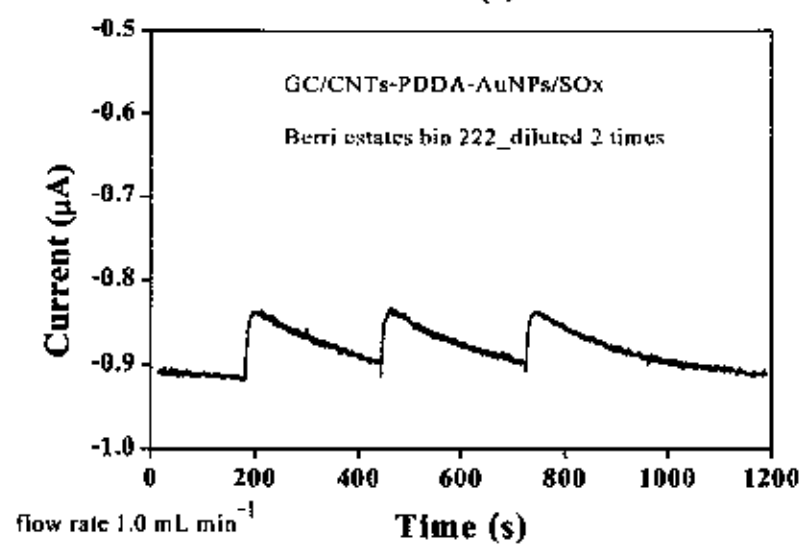
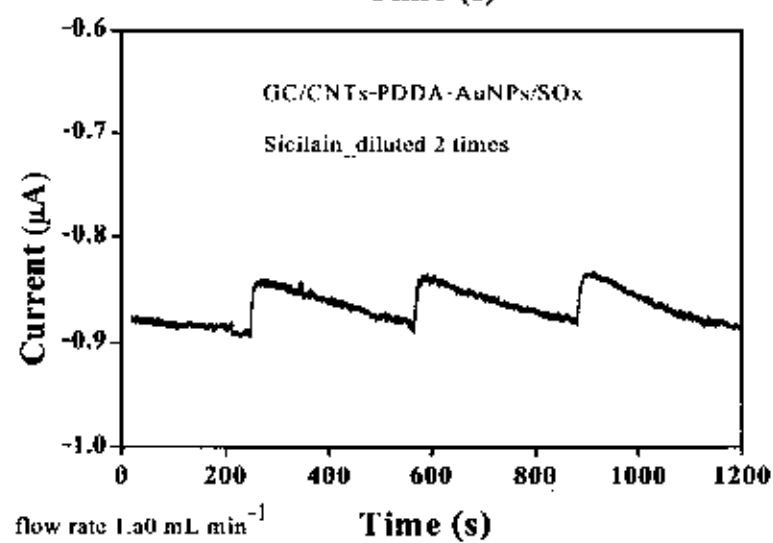
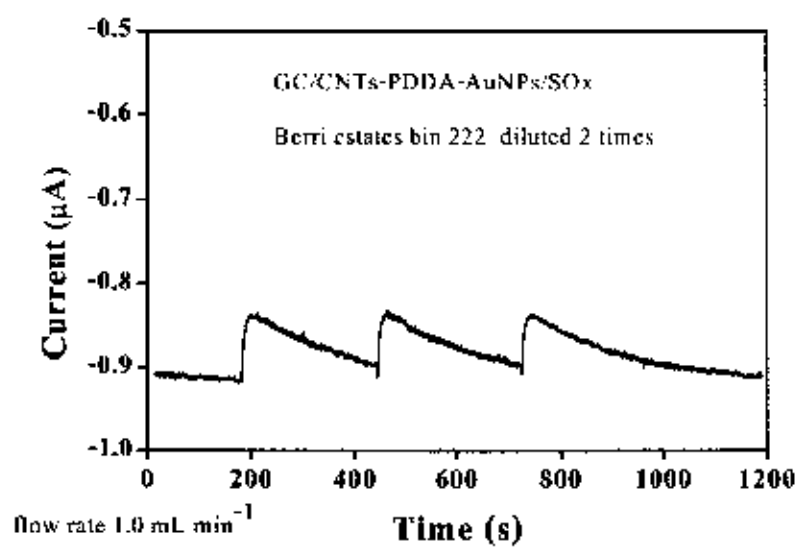
Sample: Beer (raw data for Figure 4.15)



Sample: Wine (raw data for Figure 4.15) (Continued)



Sample: Wine (raw data for Figure 4.15) (Continued)



Sample: Wine (raw data for Figure 4.15) (Continued)

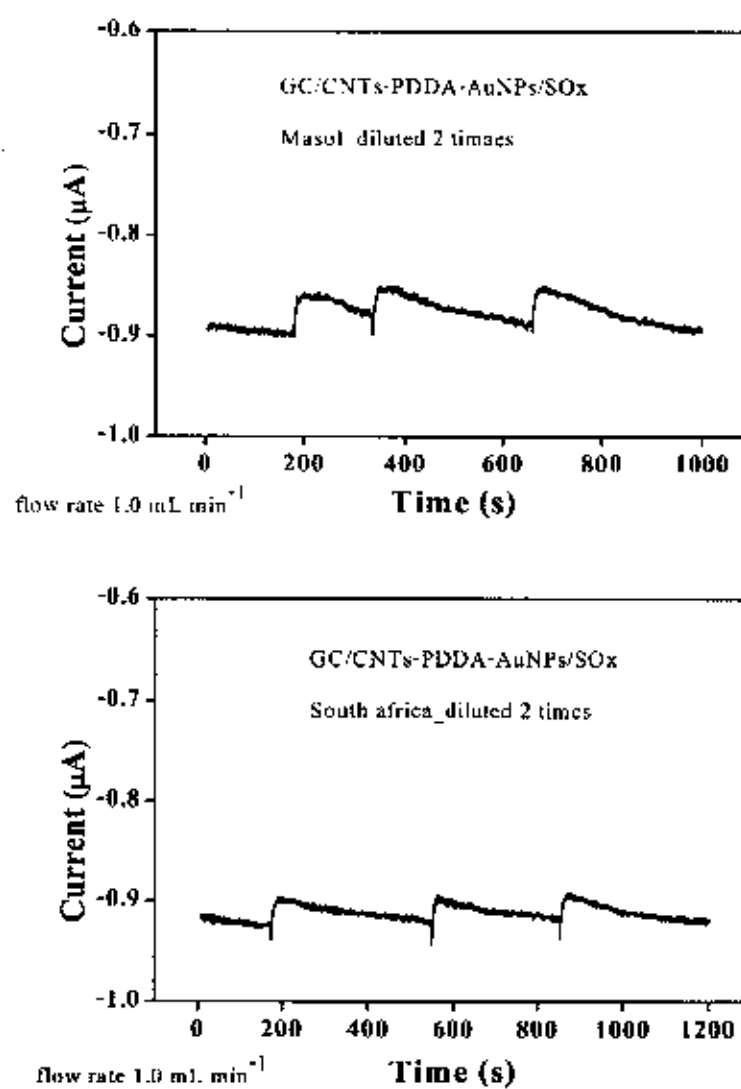


Figure A.10 FIA grams of the sample on the sulfite biosensor

APPENDIX B

Indirect method for detection of sulfite

Optimum potential for H_2O_2 detection (raw data for Figure 4.17)

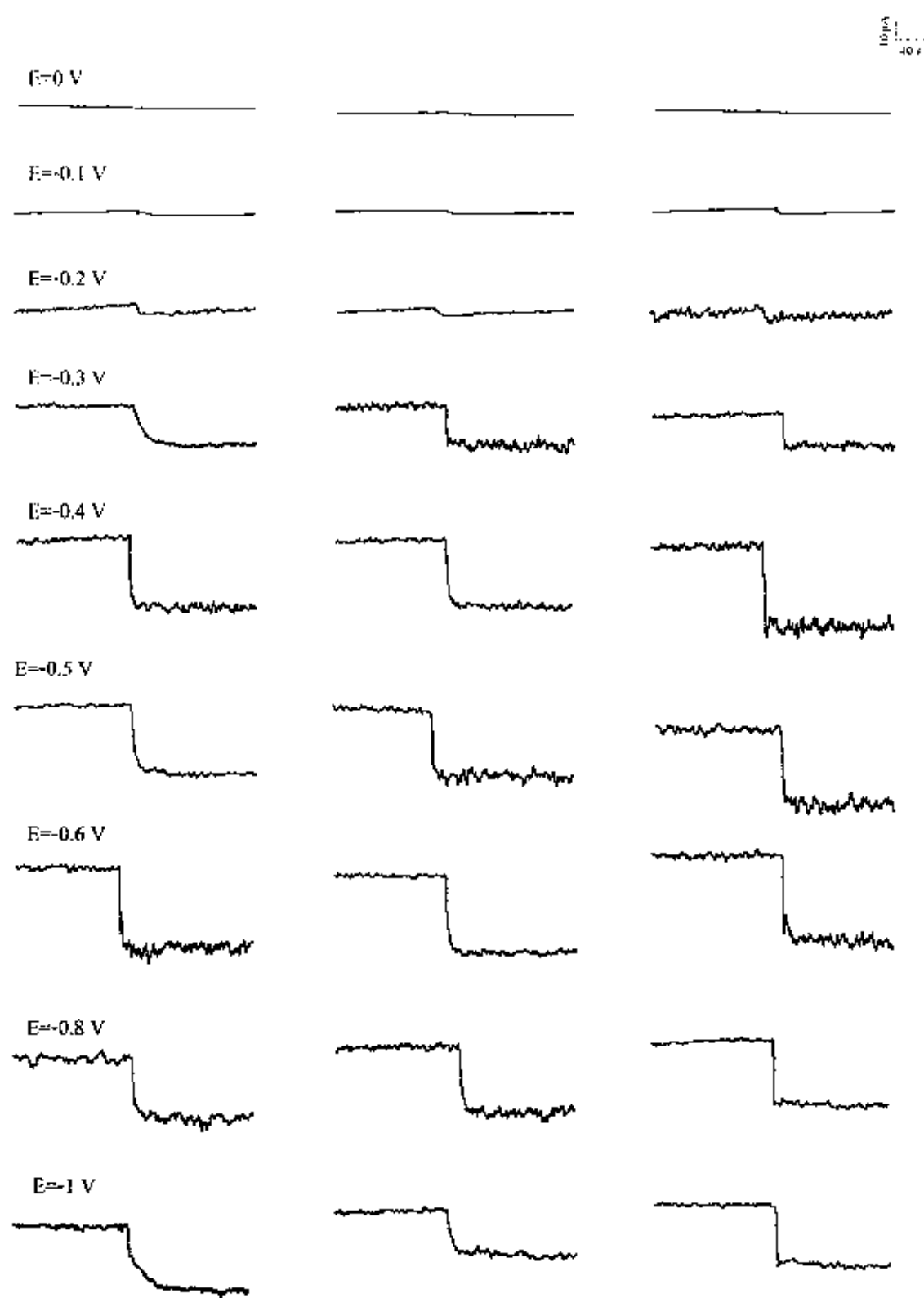


Figure B.1 Amperogram of potential using 0.5 mM H_2O_2 at sulfite biosensor

APPENDIX C

Characterization of the nanocomposites

Scanning Electron microscopy (SEM)

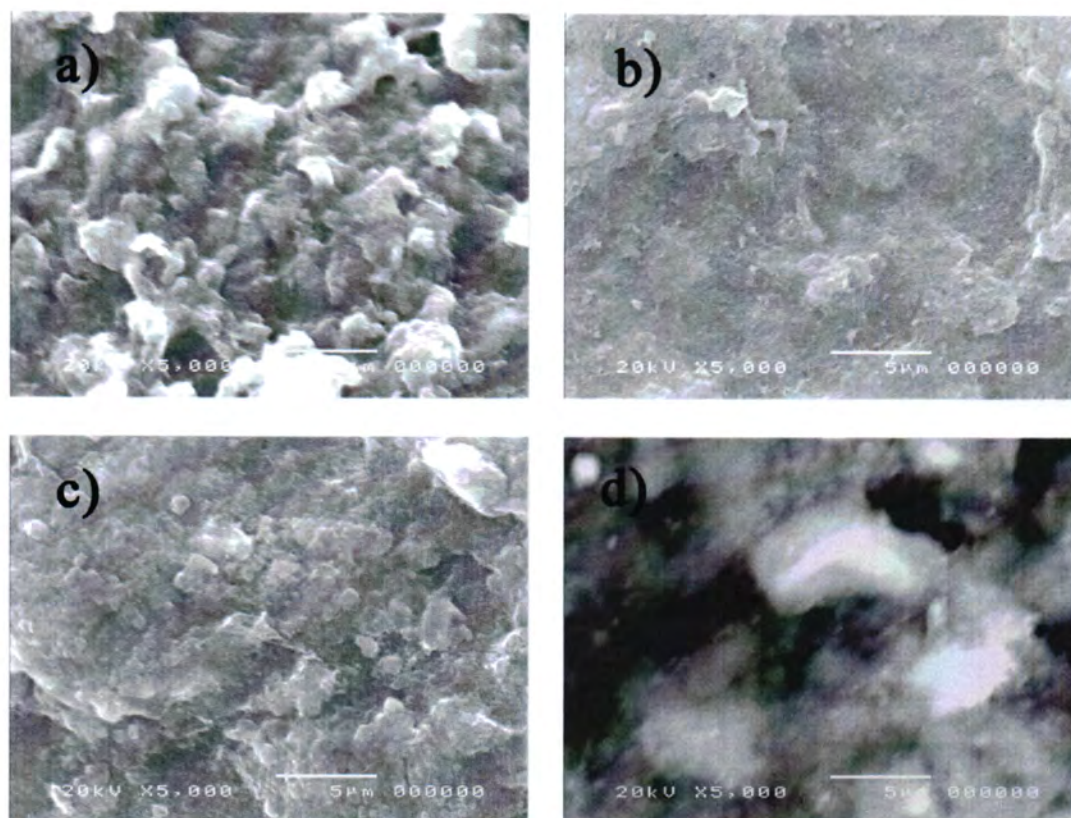


Figure C.1 SEM images of a) CNT-COOH, b) CNTs-PDDA, c) CNTs-PDDA-AuNPs, d) CNTs-PDDA-AuNPs-SOx-glu, e) CNTs-PDDA-AuNPs-SOx at 5000x

Atomic force microscopy (AFM)

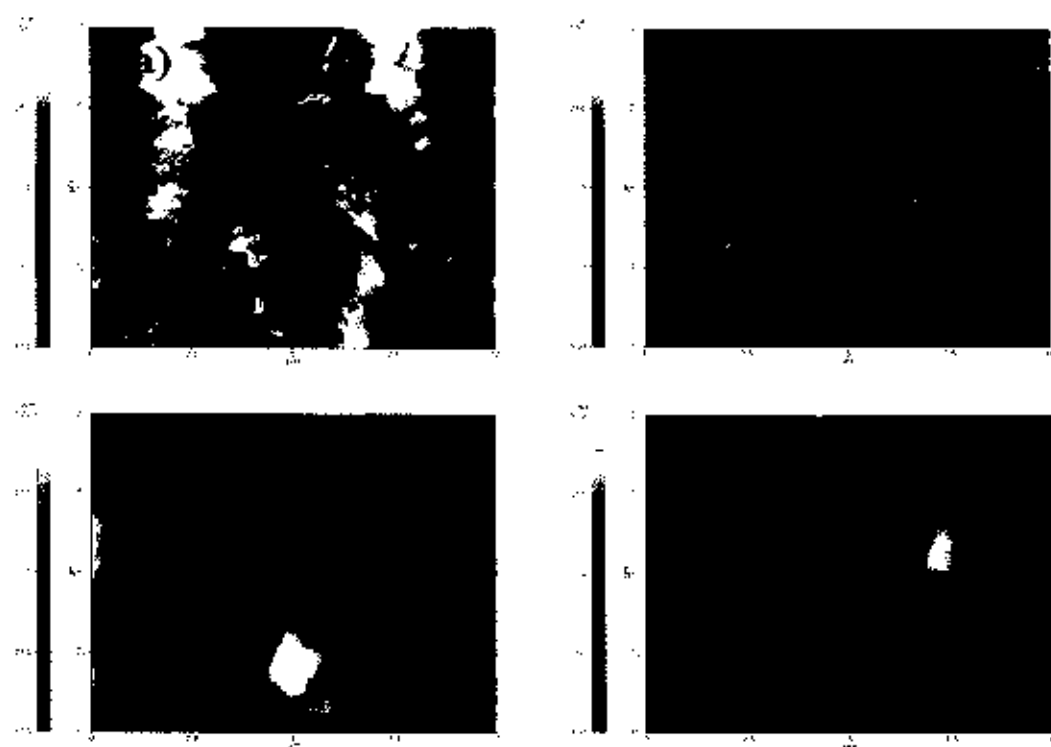


Figure C.2 AFM images of a) CNT-COOH, b) CNTs-PDDA, c) CNTs-PDDA-AuNPs, d) CNTs-PDDA-AuNPs-SOx at 10 μm

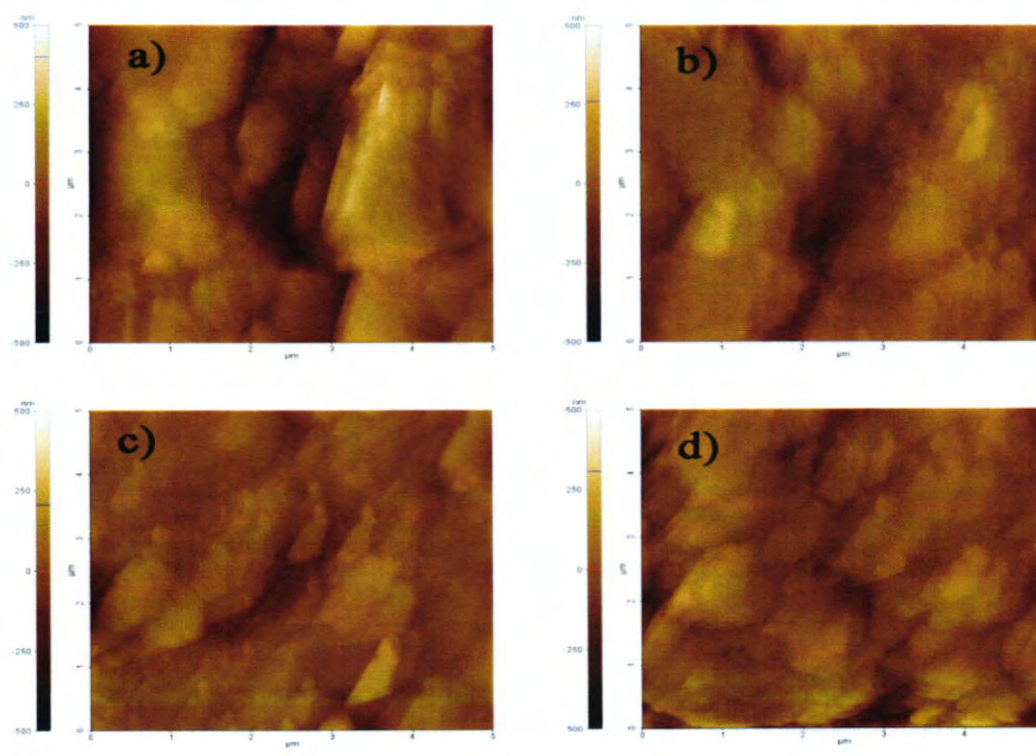


Figure C.3 AFM images of a) CNT-COOH, b) CNTs-PDDA, c) CNTs-PDDA-AuNPs, d) CNTs-PDDA-AuNPs-SOx using scan rate 0.3 Hz

APPENDIX D
CONFERENCES

CONFERENCES

Poster presentation

Wongduan Sroysee and Maliwan Amatatongchai. Amperometric Biosensor for Sulfite Determination Using Glassy Carbon Modified with Hybrid Nano-materials Electrode in Simple Flow Injection System. Pure and Applied Chemistry International Conference 2014 (PACCON 2014), Khon Kaen University, Khon Kaen, Thailand.

Publications

Wongduan Sroysee and Maliwan Amatatongchai. Amperometric Biosensor for Sulfite Determination in Beverages Using Glassy Carbon Modified with Hybrid Nano-materials Electrode in Simple Flow Injection System. Pure and Applied Chemistry International Conference 2014 (PACCON 2014), Khon Kaen University, Khon Kaen, Thailand.



Department of Chemistry,
Faculty of Science
Khon Kaen University,
Khon Kaen, 40002, Thailand

Dear Wongduan Sroysee, Maliwan Amatotongchai

It is our great pleasure to inform you that your paper entitled "Amperometric Biosensor for Sulfite Determination Using Glassy Carbon Modified with Hybrid Nano-materials Electrode in Simple Flow Injection System" has been accepted for publication in PACCON2014 proceedings book.

Thank you for your contribution to the success of the PACCON2014 conference.

Yours sincerely,

Somdej Kanokmedhakul
Chairperson, PACCON2014 Academic Committee
Department of Chemistry,
Faculty of Science,
Khon Kaen University,
Khon Kaen 40002 Thailand

AMPEROMETRIC BIOSENSOR FOR SULFITE DETERMINATION USING GLASSY CARBON MODIFIED WITH HYBRID NANO-MATERIALS ELECTRODE IN SIMPLE FLOW INJECTION SYSTEM

Wongduan Sroysee, Maliwan Amatongchai*

Department of Chemistry and Center of Excellence for Innovation in Chemistry, Faculty of Science, Ubon Ratchathani University, Ubon Ratchathani, 34190, Thailand

*E-Mail: amaliwan@gmail.com, Tel. +66 4535 3401 ext. 4576, Fax. +66 45 288379

Abstract: A simple flow injection system with amperometric detection on a sulfite biosensor was developed for sensitive and rapid measurement of sulfite. The biosensor was developed based on the hybrid materials, composed of carboxylic functionalized carbon nanotubes, poly(diallyldimethylammoniumchloride) and gold nanoparticle (CNTs-PDDA-AuNPs) coated on a glassy carbon (GC) electrode, which constructed an effective immobilization matrix and made the immobilized components hold high stability and bioactivity. Sulfite oxidase (SOx) was immobilized to CNTs-PDDA-AuNPs and cytochrome C composites film by using glutaraldehyde (Glu). Electrochemical oxidation of sulfite was studied at the developed biosensor (GC/CNTs-PDDA-AuNPs/SOx) in 0.1 M phosphate buffer pH 7.0 using cyclic voltammetry. The biosensor displayed good electrocatalytic activity towards the oxidation of sulfite. The estimated apparent Michaelis-Menten constant was 0.49 mM. The developed biosensor was applied in the flow injection system for amperometric detection of sulfite using solution of 0.1 M phosphate buffer (pH 8.0) as a carrier and applying a potential of +0.3 V at the working electrode. The proposed sulfite biosensor exhibits linear calibration over the range of 2-200 mg L⁻¹ of sulfite with slope of 204.66 nA mg⁻¹.L and correlation coefficient of 0.9991. The detection limit (3 S/N of blank) was 1.3 mg L⁻¹ and the estimated precision of 3.8%.

1. Introduction

Sulfiting agent in various forms (sulfite, sulfur dioxide, hydrogen sulfite, metabisulfite) are commonly used as preservatives in food, beverages and several product such as dried fruits and vegetable to prevent microbiological growth, to control browning reaction and to assist in preserving vitamin C [1-3]. However, the level of sulfite in food has been the subject of legislation since it was discovered that certain concentration level causes allergic reactions in some individuals [4, 5]. The United States Food and Drug Administration (FDA) have required labeling of products containing more than 10 µg mL⁻¹ of sulfite in food or beverages [6]. Therefore, it is essential to have accurate and precise methods available to determine the sulfite content in these products. Many analytical methods for the sulfite assays such as high-performance liquid chromatography [7], spectrophotometry [8] and electrochemical methods [9] have been reported. Among these methods, electrochemical detection is more attractive because of its simplicity, high sensitivity, fast response and cheap equipment.

In this work, a simple flow injection system, which employs an amperometric detection on a novel sulfite biosensor, was proposed. The biosensor was fabricated using CNTs-PDDA-AuNPs composites as an effective matrix to immobilized sulfite oxidase (SOx). The nanocomposite materials were formed by coating negatively charged carboxylated CNTs with positively charged PDDA followed by capping with negatively charged AuNPs via electrostatic interaction. The CNTs-PDDA-AuNPs nanocomposite is used to construct a sulfite biosensor by drop coating on the surface of the glassy carbon (GC) electrode. The developed biosensor (GC/CNTs-PDDA-AuNPs/SOx) exhibits many good characteristics including high activity, excellent sensitivity and selectivity in detection of sulfite.

2. Materials and Methods

2.1 Apparatus

Voltammetric and amperometric measurements were performed with an e-DAQ potentiostat (model EA 161, Australia) equipped with e-corder. Three electrode systems were employed in this study. The active surface area of the GC electrode in voltammetry was approximately 0.07 cm². The FI system for amperometric detection at the developed sulfite biosensor comprised of a Shimadzu pump (model LC-10 AD, Japan), Rheodyne injector (model 7725, USA) fitted with 20 µL sample loop and detection system. The electrode area of thin layer flow cell was utilized at 0.06 cm².

2.2 Chemical

Multiwall carbon nanotubes (CNTs, diameter: 30±15 nm, length: 1-5 micron, purity: > 95%) were purchased from Nanolab inc. (MA, USA). Sodium sulfite (Na₂SO₃) and poly (diallyldimethylammonium chloride) (PDDA, MW: 100,000-200,000, 20% w/w) were purchased from Sigma-Aldrich (St. Louis, USA). Hydrogen tetrachloroaurate (III) trihydrate (HAuCl₄.3H₂O, Au > 48%) and cytochrome C (Cyt C, 90% from horse heart) were purchased from Acros Organic (Geel, Belgium). Sulfite oxidase (SOx, 30-70 U mg⁻¹) was purchased from ProNique Scientific, Inc. (Castle Rock, USA). All solutions were prepared in deionized-distilled water (Water Pro PS, USA).

2.3 Procedures

2.3.1 Preparation of CNTs-PDDA

CNTs was chemically shortened and carboxylated by acid treatment mixture of HNO_3 and H_2SO_4 (3:1, v/v) under ultra sonic stirring for 5 h. After that, the suspension was centrifuged at 10,000 rpm and washed repeatedly with deionized water until the pH of washing was 7. The resulting product was then dried at 110°C . The CNTs-COOH was then functionalized with PDDA (CNTs-PDDA) using the method adopted from Cui *et al.* [10, 11]. Briefly, 10 mg of CNTs-COOH were dispersed in 20 mL of a 0.25% PDDA aqueous solution containing 0.5 M NaCl and ultrasonic stirring for 30 min. The resulting dispersion was centrifuged and washed with water for three times to remove residual PDDA. Finally, 4 mg of the collected product was dispersed in 1 mL water and the resulting solution was sonicated for 30 min before use.

2.3.2 Preparation of sulfite biosensor (GC/CNTs-PDDA-AuNPs/SOx)

The sulfite biosensor was prepared by casting 40 μL of the CNTs-PDDA dispersion on the surface of the well-polished glassy carbon (GC) electrode, and then dried at ambient temperature. The surface of the electrode was further coated with 40 μL of 0.02% AuNPs solution. After that, immobilization of SOx was carried out by dropping 15 μL of solution containing of SOx (0.1 U mg^{-1}) and Cyt C (4 mg mL^{-1}) onto the modified electrode. Finally, 15 μL of 0.01 % glutaraldehyde was dropped on the modified electrode and dried at room temperature.

3. Results and Discussion

3.1 Cyclic voltammetry of sulfite

The electrochemical behavior of sulfite at sulfite biosensor (GC/CNTs-PDDA-AuNPs/SOx) was studied using cyclic voltammetry. Figure 1 compared the response of the bare GC and sulfite biosensor toward the electro-oxidation of sulfite at pH 8. Sulfite oxidation is an electrochemically irreversible process. Bare GC electrode results in a peak shape signal at about 0.85 V versus Ag/AgCl, whereas the sulfite biosensor provides the oxidation peak at 0.30 V. These results show that sulfite oxidase (SOx) immobilized on the CNTs-PDDA-AuNPs composite reduces the overpotential of sulfite oxidation and in fact imparts electrocatalytic activity for sulfite oxidation. Enzyme SOx was effectively immobilized on the biocompatibility matrix of CNTs-PDDA-AuNPs and cytochrome C (Cyt C). Then SOx catalyzes a $2e^-$ oxidation of sulfite to sulfate as described in Eq.1.

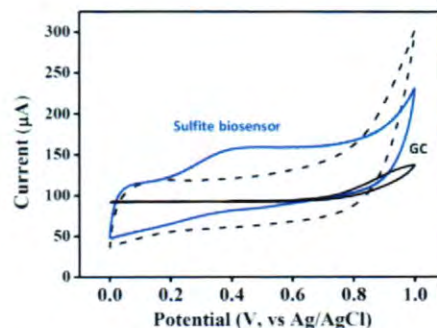
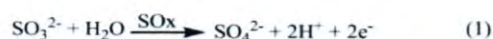


Figure 1. Cyclic voltammograms of 4 mM sulfite (solid line) at bare GC and sulfite biosensor (GC/CNTs-PDDA/SOx) in 0.1 M phosphate buffer (pH 7). Background voltammograms (0.1 M phosphate buffer) is also shown at dotted line for the sulfite biosensor. The scan rate was fixed at 50 mV s^{-1} .

It was observed that the values of peak potential shifted slightly towards less positive values (Figure 2b) when the pH increased. Figure 2c shows that the maximum peak current was observed at pH 8. Therefore, pH 8 was selected as the optimum pH for amperometric detection of sulfite. This result was consistent with the previous report [12] that enzyme SOx provides the best catalytic activity at pH 8.

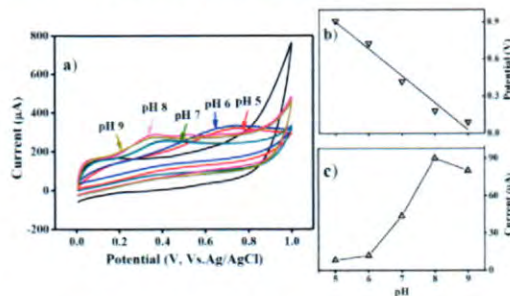


Figure 2. (a) Cyclic voltammetric responses of 2 mM sulfite at various buffer pHs and the dependence of buffer pH on the (b) peak potential (c) peak current obtained from the biosensor, scan rate 50 mVs^{-1} .

3.2 Michaelis-Menten constant

The apparent Michaelis-Menten constant (K_m^{app}), which gave an indication of enzyme-substrate kinetics, could be estimated from the electrochemical version of the Lineweaver-Burk equation (2) [12].

$$\frac{1}{I_{ss}} = \frac{1}{I_{\text{max}}} + \frac{K_m^{\text{app}}}{I_{\text{max}}c} \quad (2)$$

Where c is a substrate concentration in a bulk solution, I_{ss} the steady-state current after the addition of substrate and I_{max} is the maximum current measured under saturated substrate conditions. Figure 3 shows the Lineweaver-Burk plot of SOx

immobilized on the modified electrode in the presence of different concentration of sulfite and the calculated K_m^{app} of 0.49 mM. A low K_m^{app} value obtained represents a strong substrate binding and demonstrates a high affinity of sulfite for the modified electrode.

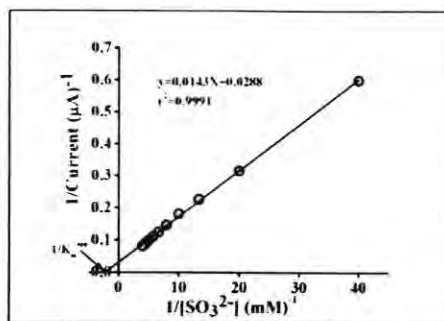


Figure 3. Lineweaver-Bulk plot of sulfite immobilized on the sulfite biosensor.

3.3 Parameters affecting the sulfite biosensor response

Parameters affecting amperometric detection of sulfite at GC/CNTs-PDDA-AuNPs/SOx electrode was examined using the potential of 0.3 V. The effect of CNTs-PDDA concentration on the current signal was studied from 0 to 8 mg mL⁻¹. As shown in Figure 4a the current response increased with increasing CNTs-PDDA loading from 0 to 4 but decreased from 4 to 8 mg mL⁻¹. Therefore, 4 mg mL⁻¹ CNTs-PDDA was chosen for modified electrode and for further experiments.

Figure 4b shows the effect of AuNPs loading on the oxidation current of sulfite. The current increased with increasing amount of AuNPs from 0 to 0.02 and reached the maximum when 0.02 % AuNPs was casted. Therefore, this condition was selected for the biosensor fabrication.

As seen in Figure 4c, the current responses increased with the increase of Cyt c concentration from 0 to 4 and then decreased from 4 to 16 mg mL⁻¹. Thus, to make a sensitive biosensor, 4 mg mL⁻¹ of Cyt c concentration was selected for further investigations.

The effect of SOx concentration on the biosensor response was studied and the results illustrated in Figure 4d. It was found that the current responses increased with increasing the SOx concentration to maximum value at 0.1 U mL⁻¹, and then tended to decrease with further increase in the SOx concentration. This behavior is typical of the enzyme-based biosensors [13]. Thus, 0.1 U mL⁻¹ SOx was chosen for subsequent experiments.

3.4 Effect the potential

In order to obtain the optimal potential for amperometric detection in FIA, hydrodynamic

voltammetric behavior of sulfite was investigated at various potential from 0.0 to 1.0 V. As shown in Figure 5, the peak area reached a maximum value at 0.3 V. Thus, this potential was selected for for amperometric detection in FIA system.

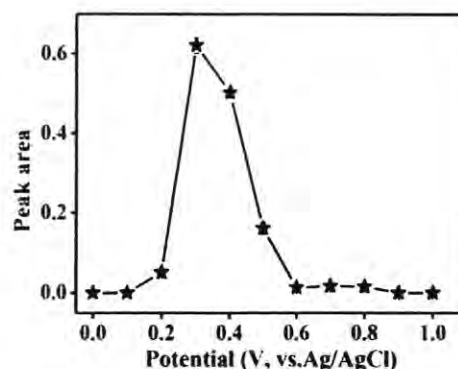


Figure 5. Influence of the applied potential on the biosensor response for 10 mg L⁻¹ sulfite.

3.5 Analytical feature

Representative signal profiles for multiple injections and calibration plot are depicted in Figure 6. Calibration curve is linear in the range of 2 to 200 mg L⁻¹. The detection limit (3 S/N) is ~1.3 mg L⁻¹. The system provides an impressively good precision (%R.S.D = 3.8) for 20 μL injections (n = 20) of 5 mg L⁻¹ sulfite. Throughput of sample is 57 samples h⁻¹.

4. Conclusions

A simple flow injection system with amperometric detection on a novel sulfite biosensor was developed. The biosensor was fabricated using CNTs-PDDA-AuNPs composites as an effective matrix to immobilized sulfite oxidase (SOx). The developed biosensor (GC/CNTs-PDDA-AuNPs/SOx) exhibits good electrocatalytic activity, high sensitivity and selectivity in detection of sulfite.

Acknowledgements

Financial supports from the National Research Council of Thailand (NRCT, 2557 A11702006) and the Center of Excellence for Innovation in Chemistry (PERCH-CIC) are gratefully acknowledged. W.S. would like to thank the scholarship from Science Achievement Scholarship of Thailand (SAST).

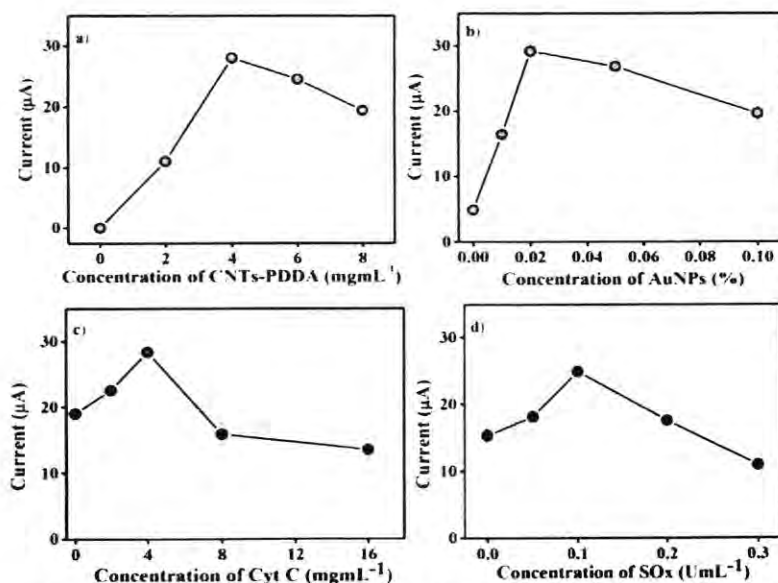


Figure 4. Dependence of current response to 0.5 mM sulfite in 0.1 M phosphate buffer at GC/CNT-PDDA-AuNPs/SOx: a) concentration of CNTs-PDDA, b) concentration of AuNPs, c) concentration of Cyt C and d) concentration of SOx.

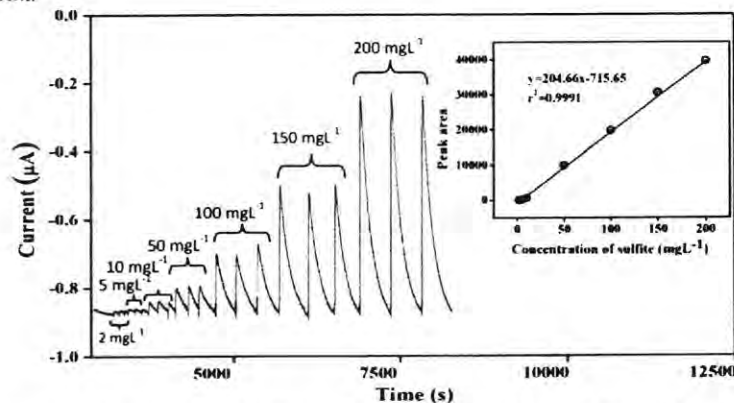


Figure 6. FIA grams obtain for injections of sulfite standards. The inset shows the linear relationship between the signal of sulfite and the concentration.

References

- [1] S. S. M. Hassan, M. S. A. Hamza, A. H. K. Mohamed, *Anal. Chim. Acta* **570** (2006) 232-239.
- [2] S. M. Oliveira, T. I. M. S. Lopes, I. V. Tóth, A. n. O. S. S. Rangel, *J. Agric. Food Chem.* **57** (2009) 3415-3422.
- [3] S. Satiaperakul, P. Phongdong, S. Liawruangrath, *Food Chem.* **121** (2010) 893-898.
- [4] S. Theisen, R. Hänsch, L. Kothe, U. Leist, R. Galensa, *Biosens Bioelec.* **26** (2010) 175-181.
- [5] Ü. T. Yilmaz, G. Somer, *Anal. Chim. Acta* **603** (2007) 30-35.
- [6] B. Bahmani, F. Moztarzadeh, M. Rabiee, M. Tahriri, *Synthetic Metals* **160** (2010) 2653-2657.
- [7] R. F. Mcfeeters, A. O. Barish, *J. Agric. Food Chem.* **51** (2003) 1513-1517.
- [8] S. S. M. Hassan, M. S. A. Hamza, A. H. K. Mohamed, *Anal. Chim. Acta* **570** (2006) 232-239.
- [9] R. Spricigo, R. Dronov, F. Lisdat, S. Leimkühler, F. Scheller and U. Wollenberger, *Anal. Bioanal. Chem.* **393** (2009) 225-233.
- [10] R. Cui, H. Huang, Z. Yin, D. Gao and J.-J. Zhu, *Biosens Bioelec.* **23** (2008) 1666-1673.
- [11] M. Eguílaz, R. Villalonga, L. Agüí, P. Yáñez-Sedeño and J. M. Pingarrón, *J. Electroanal. Chem.* **661** (2011) 171-178.
- [12] J. Hong, A. A. Moosavi-Movahedi, H. Ghourchian, A. M. Rad and S. Rezaei-Zarchi, *Electrochim. Acta* **52** (2007) 6261-6267.
- [13] R. Rawal, S. Chawla, T. Dahiya and C. Pundir, *Anal. Bioanal. Chem.* **401** (2011) 2599-2608.